Coastline evolution around African seaports

– An evidence database from space

Yongjing Mao

TUDelft

Deltares
Enabling Delta Life

ERASMUS +: ERASMUS MUNDUS MOBILITY PROGRAMME

Master of Science in

COASTAL AND MARINE ENGINEERING AND MANAGEMENT

CoMEM

**COASTLINE EVOLUTION AROUND AFRICAN SEAPORTS
– AN EVIDENCE DATABASE FROM SPACE**

Delft University of Technology
July 10, 2018

Yongjing Mao

The Erasmus+: Erasmus Mundus MSc in Coastal and Marine Engineering and Management is an integrated programme including mobility organized by five European partner institutions, coordinated by Norwegian University of Science and Technology (NTNU).

The joint study programme of 120 ECTS credits (two years full-time) has been obtained at two or three of the five CoMEM partner institutions:

- Norges Teknisk- Naturvitenskapelige Universitet (NTNU) Trondheim, Norway
- Technische Universiteit (TU) Delft, The Netherlands
- Universitat Politècnica de Catalunya (UPC). BarcelonaTech. Barcelona, Spain
- University of Southampton, Southampton, Great Britain
- City, University London, London, Great Britain

During the first three semesters of the programme, students study at two or three different universities depending on their track of study. In the fourth and final semester an MSc project and thesis has to be completed. The two-year CoMEM programme leads to a multiple set of officially recognized MSc diploma certificates. These will be issued by the universities that have been attended by the student. The transcripts issued with the MSc Diploma Certificate of each university include grades/marks and credits for each subject.

Information regarding the CoMEM programme can be obtained from the programme coordinator:

Øivind A. Arntsen, Dr.ing.
Associate professor in Marine Civil Engineering
Department of Civil and Transport Engineering
NTNU Norway
Telephone: +4773594625 Cell: +4792650455 Fax: + 4773597021
Email: oivind.arntsen@ntnu.no

CoMEM URL: https://www.ntnu.edu/studies/mscomem

CoMEM Master Thesis

This thesis was completed by:
Yongjing Mao

Under supervision of:

Prof. ir. T. Vellinga, Delft University of Technology
ir. W.P. de Boer, Delft University of Technology, Deltares
Dr. ir. S. de Vries, Delft University of Technology
ir. G.S. Hagenaars, Deltares

As a requirement to attend the degree of
Erasmus+: Erasmus Mundus Master in Coastal and Marine Engineering and Management
(CoMEM)

Taught at the following educational institutions:

Norges Teknisk- Naturvitenskapelige Universitet (NTNU)
Trondheim, Norway

Technische Universiteit (TU) Delft
Delft, The Netherlands

University of Southampton,
Southampton, Great Britain

At which the student has studied from August 2016 to July 2018.

Coastline evolution around African seaports
– An evidence database from space

By

Yongjing Mao

in partial fulfilment of the requirements for the degree of
Master of Science
in Civil Engineering and Geosciences
at the Delft University of Technology,
to be defended publicly on Wednesday, July 18, 2018, at 13:00 PM.

Thesis committee:	Prof. ir. T. Vellinga,	Delft University of Technology
	ir. W.P. de Boer,	Delft University of Technology, Deltares
	Dr. ir. S. de Vries,	Delft University of Technology
	ir. G.S. Hagenaars,	Deltares

This thesis is confidential and cannot be made public until July 1, 2019.

Cover page: USGS Landsat 8 Satellite Image - The Port of Nouakchott, Mauritania

T̃U Delft

Preface

With this thesis, I conclude my two-year MSc study in CoMEM programme. During my master program, I had the opportunity to gain knowledge in interesting fields of coastal engineering from different universities in different countries. In my first semester in Norges Teknisk- Naturvitenskapelige Universitet (NTNU), I worked on a project which aimed at detecting ice thickness from photos of the ship-borne camera. It is my first contact with remote sensing and image processing, inspiring me to explore this field of science. The content of this thesis embodies both this passion for remote sensing and my knowledge in coastal engineering.

The thesis was conducted at the Deltares research institute in Delft. I would like to thank my supervisors for their help and opportunity to work on my thesis at Deltares. Special thanks go to my daily supervisor Wiebe de Boer. Besides our meaningful meetings and his brilliant ideas on this topic, I would like to thank him for the effort he put in proofreading drafts and structuring the content of this thesis. Also, I appreciate the opportunity he offered to work on this subject after graduation. I would like to thank Gerben Hagenaars. His algorithm for Satellite derived shoreline (SDS) lays a solid foundation for this research. Also, his experience on the Google Earth Engine and remote sensing help me to get familiar with these fields. I would like to thank Sierd de Vries for his intention to contact me about the start of this thesis, his insights into interpreting results and enthusiasm that kept me going through the process. Last but certainly not least I would like to thank my professor Tiedo Vellinga for charging my committee and his feedback during meetings. Having my graduation supported by a committee with this expertise was certainly a privilege.

For their support during my studies and time abroad, I would like to thank my family and friends, without whom support I certainly was not able to achieve this result.

Yongjing Mao

Delft, July 2018

Executive Summary

Seaports are important maritime commercial facilities and key hubs for national and global trades. There is a growing need for seaborne transport and, hence, seaport facilities, especially in emerging economies due to economic and population growth, such as in Africa. In sedimentary environments, port construction may induce coastal impacts regarding up-drift accretion and down-drift erosion. These coastal impacts potentially increase risks such as harbour siltation and coastal area erosion. To mitigate or even avoid these risks in the pre-construction stage, coastline evolution around ports needs to be well-understood. Analysis of long-term shoreline position data around existing ports can provide this understanding.

Long-term in-situ shoreline position data around ports are often unavailable or inaccessible, especially in emerging economies which are often data poor. Nevertheless, nowadays a growing database of satellite images provides these data on a global scale for the last decades. Furthermore, the launch of Google Earth Engine cloud computing platform in 2016 enabled accessibility and efficient processing of these satellite images. This development allows building an evidence database for shoreline positions even in data-poor environments such as Africa. With this database, coastline evolution trends around all African seaports can be analysed, inter-compared and related to environmental and port characteristics to derive lessons for future port development.

In this thesis, according to the World Port Index, 165 African seaports (after excluding river ports, offshore platforms and anchorages from 266 African ports) are identified. Only 125 ports at sandy coastlines, where SDS detection has been validated, are focused in this research. Environmental and port characteristics including gross longshore wave power, the presence of nearby rivers and inlets, natural shelter conditions, port breakwater length and the presence of other nearby structures are researched. To build a shoreline evolution evidence database, we apply an automated Satellite Derived Shoreline (SDS) detection method to calculate cumulative magnitudes and present rates of coastal area erosion/accretion and shoreline advance at the up-drift boundary of the port.

Regarding historical coastline evolution, the sum of accretion and erosion area over all 125 African seaports at sandy coastlines is found to be 55 km^2 including 29 km^2 accretion and 26 km^2 erosion since 1984. The 55 km^2 coastal area change is distributed along the 2600km coastline, indicating an average shoreline change of 21m. Compared with the 30m satellite image resolution, the coastline evolution is not significant from a continental perspective. This situation is due to that most ports are located at Afro-trailing coastlines, where a small quantity of sediment is available for longshore sediment transport (LST) and coastline evolution. However, when looking at hotspots, the top 10% of ports is responsible for 50% (27 km^2) of the total coastal area change. The gross coastal area change around a single port (Port of Nouakchott) can be up to 7 km^2 including 4.5 km^2 erosion. With the population density of 960/km^2 for the corresponding port city, about 4,000 people can be directly affected by the coastal area erosion. If the increased flood risk due to shoreline erosion is considered, the number of people under influence can be even larger. Regarding present coastline evolution rates, 125 African seaports at sandy coasts are classified concerning coastline stability. 90 ports are found to be located at dynamic coastlines where coastal area erosion (45 ports) or accretion rate (68 ports) is larger than SDS detection accuracy. This means the majority of African ports still have erosion and siltation risks in the future. Both hindcast and forecast indicators suggest that accretion is more prominent than erosion for African seaports, which can be due to the restriction of rocky substratum on coastal area erosion and human activities to stimulate accretion.

By relating coastline evolution indicators to environmental parameters, common characteristics of ports with significant and limited coastline evolutions are identified respectively. Ports with significant coastline evolution are found to be mainly located at open coasts with large longshore wave power, especially when rivers and/or inlets are nearby. On the contrary, most ports with limited coastline evolution are located at sheltered coasts with small longshore wave power and low sediment supply. After relating coastline evolution indicators to ports characteristics and human interventions, it is found that ports constructed more recently tend to have more substantial present coastline evolution rates. Regarding human interventions, breakwater length positively correlates to present erosion/accretion rates. Shore protection structures are found to reduce coastal area erosion significantly within the monitoring period, while longshore sediment transport interruption structures such as groynes increase the erosion hazards as it stimulates accretion.

After analysing coastline evolution indicators from the continental perspective, hotspots are focused. 27 ports are identified to have prominent erosion and/or siltation hazards, which rank top 10% either for the erosion indicators or the siltation indicators. Some of these high-hazard ports also have large port city population, resulting in larger coastline erosion impacts. Different from statistics of coastline evolution from the continental perspective, erosion instead of accretion appears to dominate coastal area change for these identified ports. This difference can be due to less limitation on down-drift erosion since these identified ports are mostly located at sediment-rich environments and less restricted by rocky substratum. The net erosion area is then caused by sediment deposition at harbour basins and channels. Amongst these hotspots, ports with larger longshore wave power are more likely to show equilibrium trends, but the majority of them have erosion rates that are currently still high. These high-hazard African seaports are found to be mainly located in five regions, which are North West Africa, West Africa, East coast of South Africa, Nile River Delta and West Mediterranean Sea. The by-pass technique has been implemented for ports in East coast of South Africa including Port of Durban, Richards Bay, East London and Ngqura. Ports with by-pass technique have less coastline evolution, compared with ports which have the same order of LST in West and North West Africa.

Effects of environmental and port characteristics on the coastline evolution are used to derive lessons for future port design. Firstly, regarding site selection and breakwater design, ports with massive river sediment supply and/or ports at open coasts are under larger negative coastal impacts concerning port siltation and down-drift erosion. For coasts with river sediment supply, it is better to construct ports at the up-drift side of the river mouth to avoid interruption of river supplied sediment transport, which is found helpful for ports around West Mediterranean Sea. Shoreline management plan should be coupled with methods to maintain or increase river sediment supply, which can be learnt from shoreline retreating around ports in West Africa. Furthermore, to reduce coastal impacts around ports, port breakwaters at open coasts should be carefully designed regarding length and orientation to achieve a smaller shore-normal projected length, especially when the gross longshore wave power is massive. Regarding mitigation methods for coastline evolution impacts, shoreline protection structures are effective in reducing erosion hazards in the time scale of 30 years. Extension of the port breakwater (s) can be a temporary solution to mitigate the potential siltation problem but to reduce the down-drift erosion problem at the same time, sediment by-pass system, which is proved to be successful in South African ports, should be designed.

Lessons learnt from this research can be applied to present port extensions and new port constructions. The use of SDS can serve to obtain (historical) coastal system understanding and to validate models which aim to predict future impacts. Additionally, with the development of remote sensing and implementation of accuracy assessment for sediment compositions other than sand in the future, this methodology has the potential to be utilised for all seaports on a global scale, supporting engineers and decision makers to understand coastline evolution around ports worldwide.

Contents

1

Introduction

1.1 Background

Seaports are significant maritime commercial facilities and key hubs for national and global trades. In Africa, economic growth is accompanied by a growing need for seaborne trade since the beginning of the 21st century. Correspondingly, ports have become increasingly congested on this continent (African development bank, 2010). Meanwhile, container port-handling growth rates, although remained below the historical trends of the 1980–2016, is predicted to be 3% for Africa in 2018 (UNCTAD, 2017) indicating construction of new ports and expansion of existing ports.

Despite their positive effects on the local and national economy, seaports at coastlines in sedimentary environments are expected to affect the coastline evolution significantly due to the interruption of the littoral drift. An example of such coastline impacts is shown for Port of Nouakchott in Mauritania in Figure 1-1. If not managed properly, the morphological change around seaports can increase the risk for port siltation (due to increased sediment by-pass up-drift of the port) and/or coastal erosion at the down-drift side of the port (Giardino et al., 2017). Mitigation measures for these risks in the form of maintenance dredging and coastal protection measures are potentially expensive. Hence, ideally, these negative effects should be considered in the planning and design stages of ports instead of mitigated afterwards, requiring a good understanding of port's influence on the coastline evolution in the feasibility stages of port developments.
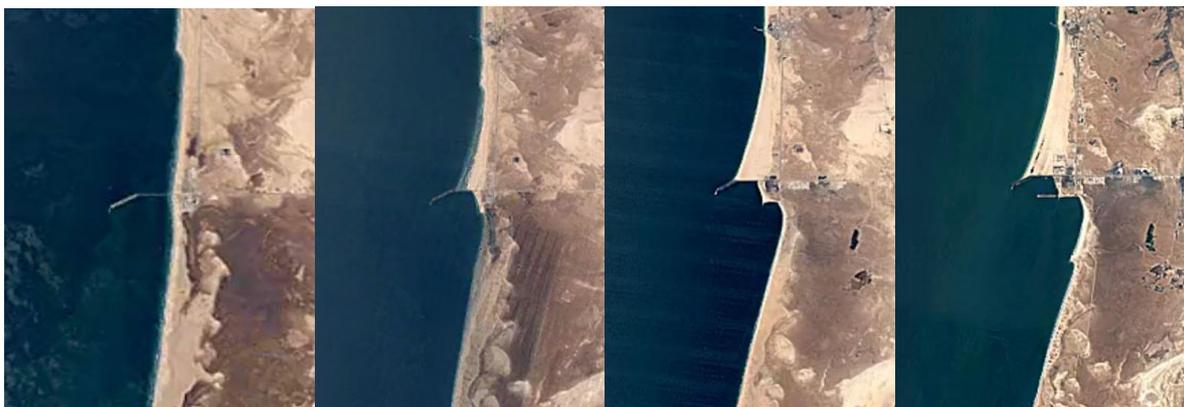

Figure 1-1 Satellite images of coastline evolution around Port of Nouakchott, Mauritania in 1984, 1994, 2004 and 2014 respectively (from left to right).

Coastline evolution is affected by a variety of both natural and human-induced factors, such as waves, tide, storm surge, relative sea-level changes, sediment loads from rivers and human interventions. Often empirical

formulas and numerical models are used to understand the relative importance of these factors and predict the coastline evolution around ports beforehand. However, the accuracy of these methods is affected by uncertainties in bathymetry and hydrodynamics. These uncertainties can be extraordinarily high in data poor environments. Hence, model results need to be validated against shoreline position measurements (Stive et al., 2002).

Although the post-construction shoreline monitoring using ground surveys has been implemented for a large number of seaports, the high cost of this data collection method reduces public data accessibility and restricts the promotion of post construction monitoring in developing countries (Appeaning Addo et al., 2008). Data unavailability and/or inaccessibility hamper the integral assessment of coastline evolution around seaports on continental or global scales.

Development of technology provides an opportunity to monitor shoreline from space. With the availability of a growing database of satellite imagery, tools such as the Google Earth Engine (GEE) (Gorelick et al., 2017) enable engineers and scientists to analyse these data efficiently, and shoreline positions can now be studied worldwide for over 30 years (Luijendijk et al., 2018). These developments make it possible to perform an integral study of the coastline evolution of seaports worldwide, also in data poor environments. In this thesis, these new techniques of Satellite Derived Shorelines (SDS, Hagenaars et al., 2018) are applied to study the coastline evolution around existing seaports in Africa. Based on this evidence database of shoreline data, lessons can be learnt from past port construction to inform decision making for future port developments.

1.2   Objectives and research questions

With the help of a GEE based SDS detection method, this thesis aims to create an evidence database, combining coastline evolution trends around existing African seaports with environmental and human intervention characteristics. This database can be used to study the coastline evolution around existing African seaports and learn lessons for both existing and future port developments. This objective leads to the main research question:

What lessons can be learnt from the historic coastline evolution around African seaports over the past 34 years to inform decision making for both existing and future port developments?

The main research question can be approached by the following steps. Firstly, coastline evolution around seaports cannot be analysed solely without describing the surrounding environment and the port characteristics. Moreover, the SDS detection algorithm cannot be applied without a satisfying accuracy, which is also related to the local environment. For these reasons a systematic overview of the environmental conditions and human activities around African ports is necessary. Secondly, to derive lessons from the coastline evolution trends around existing ports and allow for inter-comparison across these ports, meaningful indicators are identified to describe the morphological change both down-drift and up-drift of the ports. Thirdly, to understand whether coastline evolution is a problem and how significant it is for African seaports, statistics of indicators are analysed from the continental perspective. Fourthly, from the historic coastline evolution around existing African seaports in relation to their environmental and port characteristics, causes for coastal morphological change around ports are identified. Finally, instead of analysing coastline evolution from the continental perspective, hotspots of African seaports are focused and common characteristic of them are summarized. Based on the above steps, lessons are derived for both existing and future port development

and the main research question can be answered. The following sub-questions are therefore defined to guide the research:

1. What are relevant environmental and port parameters that affect the coastline evolution around existing African seaports?

2. What are meaningful coastline evolution indicators to describe and cross-compare coastline evolution trends around African seaports?

3. What are the coastline evolution statistics of existing African seaports based on the above indicators?

4. What are the effects of environmental and port characteristics on the coastline evolution around African seaports?

5. Which ports have prominent coastline evolution related hazards and what are the common characteristics of these ports?

1.3   Thesis outline

To address the main research question, sub-question 1 and 2 are firstly answered by a thorough literature review in Chapter 2, where environmental/port parameters and coastline evolution indicators are identified. Then methodology to quantify and analyse coastline evolutions is introduced in Chapter 3. Following the methodology, environmental/port parameters and coastline evolution indicators are prepared. These indicators and parameters are then analysed in Chapter 4, aiming at answering sub-question 3, 4, 5 and the main research question. Chapter 5 and 6 provide the synthesis of the previous chapters, answering the main question and presenting recommendations for future studies. Appendices A and B provide additional information on optimising indicator calculation process. The links between successive chapters are shown in Figure 1-2.
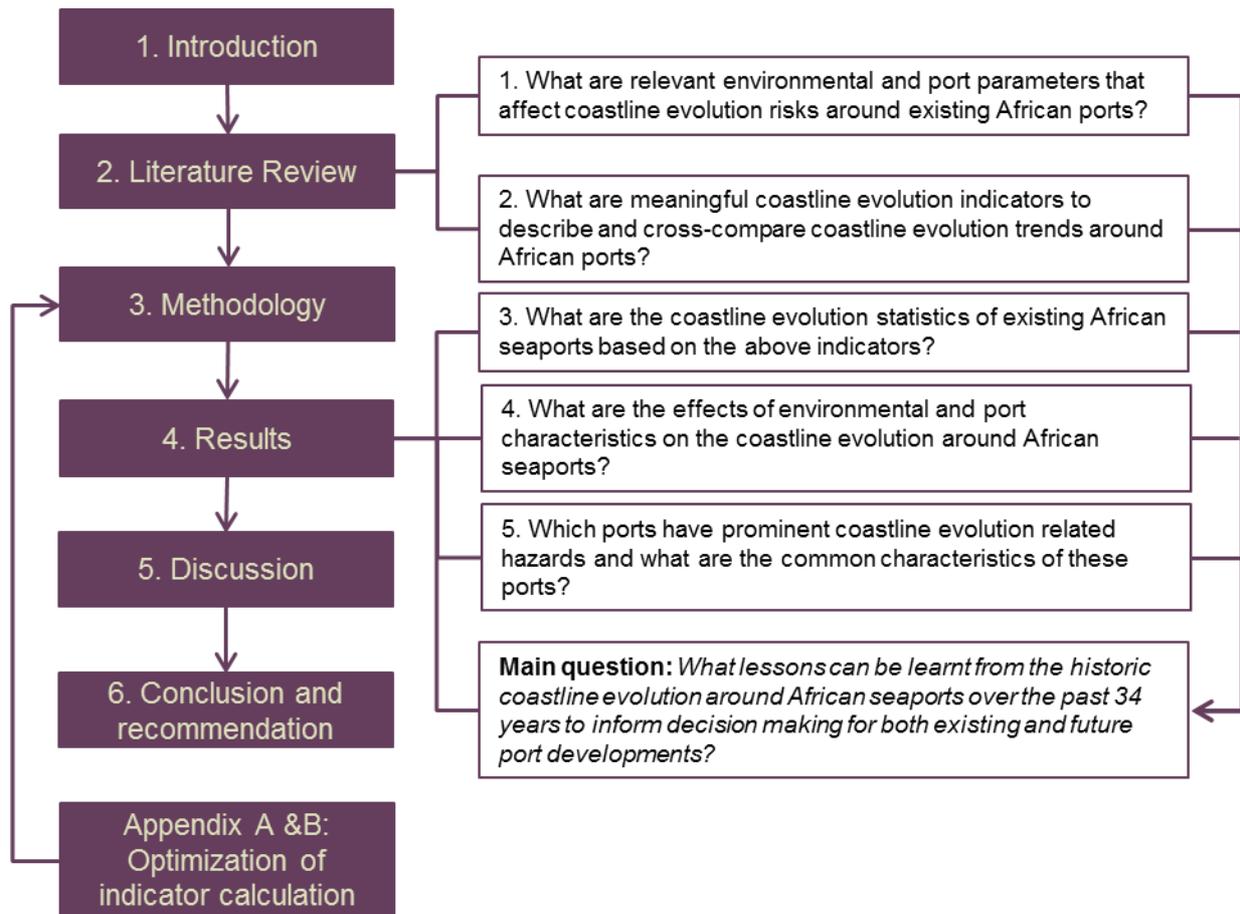
Figure 1-2 Thesis outline

<div align="right">

2

</div>

Literature Review

To answer the main research question and sub-questions, a thorough literature review is essential. Firstly, to find possible parameters affecting the coastline evolution, previous research on coastal morphological changes are reviewed in Section 2.1. Furthermore, meaningful indicators used in literature to describe and inter-compare coastline evolution trends are described in Section 2.2.

2.1   Drivers for coastline change

The main principles behind coastline changes have been indicated by Bosboom and Stive (2015). Coastline changes occur where there are spatial sediment transport gradients and/or sediment sources or sinks. This can be explained using a coastal sediment budget analysis technique (Jarrett, 1991). It firstly divides the coastline into several cells, extending from the coastline to the depth of closure where bathymetry change is smaller than the accuracy of measurement. Then after including all sediment inputs into and outputs from this cell, a residual sediment volume can be calculated. If the residual value is zero, the shoreline is stable. However, if the residual sediment volume is negative, shoreline erosion is expected. Alternatively, if the residual value is positive, shoreline accretion is expected. The sketch of a coastal cell and the typical coastline evolution around the port is shown in Figure 2-1, which includes both natural and human-induced sediment sources and sinks that can be relevant for the sediment budget in a coastal cell. Environmental parameters affecting LST are discussed in Section 2.1.1. Then Section 2.1.2 focuses on sources and sinks. Finally, human interventions, which can change the LST gradient or add new sources/sinks to a coastal cell, are introduced in Section 2.1.3.
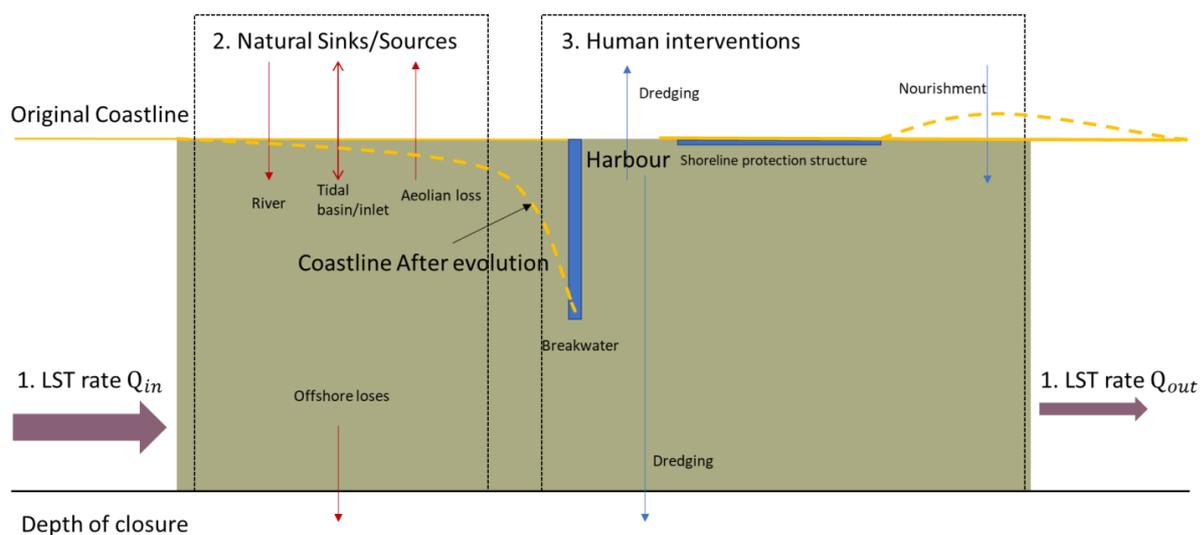

Figure 2-1 Schematic diagram of a coastal cell around a port with possible human intervention and natural sources/sinks

2.1.1   Natural processes affecting Longshore Sediment Transport (LST)

In this Section, element 1 in Figure 2-1 is reviewed. A thorough understanding of sediment transport requires knowledge of both sediment properties and physical forcing. Currently, the underlying physics of how water moves sediment are not well understood, and prediction of transport rate relies on empirical formulas based on fluid properties, flow conditions and sediment properties. Choices on suitable empirical formulas firstly depend on sediment types. The SDS detection method applied in this research has only been validated for sandy coasts and SDS accuracies of other types of coasts have not been assessed yet. To make conclusions more reliable, this thesis should be based on validated methods. Although Shoreline positions of coasts with other sediment type are also collected, their corresponding coastline evolution trends are not the focus of this thesis. Hence only LST formulas for sandy coasts are reviewed in the following Sections.

Dominant environmental forces for LST

For a sandy coastline, the sediment transport rate is dependent on current velocity. In a coastal region, the flow condition is complicated. Kaji et al. (2014) applied numerical models to investigate effects of different environmental forcing processes on LST at a sandy section along the Holland coast. They found that, without wave force, wind and tide can hardly induce any sediment transport, and LST corresponding to wave force has larger magnitudes than wind and tide. Hence, although tide and wind-driven currents can be relevant, in sandy environments, LST in the nearshore is often dominated by wave-driven currents.

Significant parameters for wave-dominated the environment

For the wave-dominated environment, different empirical formulas have been proposed to calculate LST based on wave parameters, CERC formula (SP Manual, 1984) and Kamphuis (1991) are the two popular ones. Regarding nearshore wave parameters, both of these two methods address the significance of wave height and wave angle for LST, while Kamphuis (1991) also considers the effect of wave period, which affects wave breaking pattern. Regarding beach profile, Kamphuis (1991) addresses the effect of grain diameter and beach slope at on LST, and these two parameters are also included in K coefficient in Cthe ERC formula. However, in general, grain size and nearshore bathymetry data are less available in Africa and only wave parameters are applied to indicate the effect of LST on shoreline change.

Difference between nearshore and offshore wave data

Both CERC formula and Kamphuis (1991)'s formula require wave data at the point of wave breaking, but this data is not always available for African seaports. Wave hindcast with numerical models are more widely applied in the data poor environment (Kumar and Naseef, 2015). Theoretically, due to nearshore wave process such as shoaling, refraction, diffraction, wave data from global scale hindcast cannot be applied to nearshore coastal research without validation by local measurements. However, a shortage of buoy data and the scale of this research make it difficult to implement such data validation for all African seaports. The difference between nearshore and offshore wave data is affected by natural shelters, which determines types and effects of nearshore wave process.

In summary, for a sandy coast, parameters including offshore wave height, wave angle, wave period as well as natural shelters around ports are critical to describe LST. To derive the wave angle concerning the shore-normal direction, the coastline orientation is also required.

2.1.2   Natural and human-induced sediment sources and sinks

In this Section, element 2 in Figure 2-1 are discussed. The US Army Corps of Engineer list possible types of sources and sinks for coasts (UACOE, 2002). Sources include cliff, dune, rivers, aeolian sources, landward wave transport, biogenic formation and authigenic precipitation. Sinks include dune, offshore wind transport, inlets, lagoons and barrier islands, seaward storm transport, offshore canyons, mining and dredging. To analyse coastline evolution around ports, the existence of sources and sinks need to be determined.

2.1.3   Other human interventions affecting the coastline evolution

In this Section, the element 3 in Figure 2-1 are discussed. Human interventions discussed in this thesis include but are not restricted to ports. Other hard or soft measures, aiming at protecting coasts around ports are also considered. Influence of different human interventions is elaborated by Bosboom and Stive (2015). They firstly separate beach nourishment, which is a 'soft solution', from other interventions in forms of hard structures. Although nourishment affects coastline change by adding a source, it is not included in this research, because the influence of this method lasts only several years (Bosboom and Stive, 2015), having less effect on long-term coastline evolution. Regarding hard structures, human interventions are further classified into three categories based on their primary aims.

Port breakwaters

Breakwaters of ports not only shelter the harbour basin from wave and wind effects but also affect LST. These structures change LST gradient directly by blocking sediment transport and indirectly by affecting local wave and flow conditions such as generating eddies, diffracting waves, inducing residual currents. Their ability to block sediment depends on their length, while the lee-side wave and flow conditions are influenced by the length and orientation of these structures.

Other structures interrupting the LST

These human interventions include jetties, groynes, and shore-parallel breakwaters. These structures have similar effects as port breakwaters, but their original aim is to adjust the LST rate to enhance local accretion in specific areas instead of protecting the harbour basin from wave penetration.

Shore protection structures

These human interventions include seawalls, revetments and sea-dikes. Although these structures are designed to prevent cross-shore sediment transport with no or limited influence on the LST gradient, they affect the coastline evolution by locally stopping the LST induced coastline retreat. Additionally, the re-orientation of the coastline around these structures can affect the LST gradient in the vicinity of those structures.

In summary, for human interventions, parameters including the existence of different types of structures are firstly included. Additionally, since breakwaters of ports are the main artificial structures accompanied by ports construction, their influence on coastline evolution is more important than other structures.

2.2 Coastline evolution indicators

In the Digital Shoreline Analysis System (DSAS) developed by the United States Geological Survey (USGS) (Thieler et al., 2009), coastline evolution trends are described as erosion/accretion rates at shore-normal transects along the coastline, which are widely applied in coastline monitoring research such as Archetti (2009), Jonah et al. (2016) and Hagenaars et al. (2018). These indicators are useful to analyse accretion/erosion rates along the coastline at a single site, but a large number of transects makes it difficult to conclude and compare aggregated accretion/erosion trends among different sites. Hence, for the cross-comparison of different sites, aggregation and adjustment of these indicators are necessary.

Coastline evolution indicators consist of a spatial component (shoreline position change at shore-normal transects) and a temporal component (average rate). Both are discussed in the subsequent sections.

Spatial indicators

This thesis focuses on harbour siltation and coastal area erosion hazards. Regarding harbour siltation, Wu (2007) found that transects close to the port up-drift boundary have higher accretion rate than those distant from the port. Hence shoreline position at up-drift boundary can be used to analyse siltation hazard around a port. Regarding erosion, Giardino et al. (2017) used area instead of shoreline position to represent this hazard. As a more aggregated parameter, erosion area is used as the indicator in this research. Besides the above two indicators, accretion area is also identified and applied to calculate gross and net coastal area change, which is helpful to reflect the magnitude of coastline evolution. Sketch of spatial indicators is shown in Figure 3-4.

Temporal indicators

DSAS uses the average rate as the indicator for the time series of spatial parameters, which is suitable for a nature coast where coastline evolution shows a linear trend. However, its applicability to shorelines where inlets or human intervention exist is doubted (Galgano and Douglas, 2000). For morphological change around ports, which is due to an abrupt distribution of the original system, the evolution rate is fast at the beginning and declares when the new equilibrium situation is approached (Bosboom and Stive, 2015). Hence instead of using the average rate, the present coastline evolution rate is more accurate.

Besides forecast indicators such as coastline evolution rates, hindcast indicators such as cumulative erosion/accretion area and shoreline advance can give intuitive feelings of port effect in the history on coastal morphology. Hence in addition to forecast indicators, cumulative magnitudes of morphological change after ports construction are also included in the database.

In summary, this research will investigate the coastline evolution in terms of three forecast indicators (i.e. present shoreline advance rate at up-drift of the port in m/yr, present coastal erosion and accretion area rates in km^2/yr) and three hindcast indicators (i.e. cumulative shoreline advance at up-drift of port in m, cumulative coastal erosion and accretion area in km^2).

2.3 Summary of parameters and indicators to be included in the database

Besides environmental and human intervention parameters, information about ports themselves is also crucial for coastline evolution. Port location decides where to perform coastline evolution analysis; port construction

date indicates the duration of ports influence on coastline change, while port city size relates to risks of port induced erosion.

Parameters and indicators identified in the literature review are summarized in Table 2-1:

Table 2-1 Summary of parameters and indicators identified by Literature Review

Parameters	
Ports information	Port location
	Port construction date
	Port city size
LST	Wave climate (H_s, T_p, α)
	Shoreline orientation
	Natural shelters
Sources/Sinks	The presence of sources/sinks
Human intervention	Length of the port breakwater (s)
	The presence of LST interruption structure
	The presence of shore protection structure
Indicators	
Coastline evolution trends	Shoreline position advance rate at up-drift breakwater
	Coastal area erosion rate around ports
	Coastal area accretion rate around ports
	Cumulative shoreline position advance at up-drift breakwater
	Cumulative coastal area erosion around ports
	Cumulative coastal area accretion around ports

<div align="right">

3

</div>

Methodology

In this chapter, the method for each research step is described. Section 3.1 focuses on the methodology and limitation for the SDS detection. Then based on the detected shoreline vectors, methods to calculate coastline evolution indicators are described in Section 3.2. The selection of African seaports incorporated in the shoreline evolution analysis is discussed in Section 3.3. Finally, the methodology to analyse coastline evolution data in relation to environmental and port characteristics is presented in Section 3.4.

3.1   Methodology and limitations of SDS detection method

The shoreline position is import to coastal managers, scientists and engineers. Traditionally, the location of shoreline is derived from aerial photography or video imagery (Pianca et al., 2015) or in-situ measurements of the beach topography ((Ruggiero et al., 2005) and (de Schipper et al., 2016)). These traditional shoreline datasets are often expensive and constrained in time and/or space, while satellite imagery is publicly available for the past 34 years. Also, recently launched Google Earth Engine platform and development of image processing techniques allow deriving a so-called Satellite Derived Shoreline (SDS) position from satellite imagery (García-Rubio et al., 2015) on large temporal and spatial scales. Hagenaars et al. (2018) validated SDS detection results for sandy coasts and pointed out limitations of this technique. In this section, the research of Hagenaars et al. (2018) is reviewed and parameters in SDS detection are determined.

3.1.1   Image Processing

Different from common images, optical satellite images contain information about the actual earth radiance light spectrum ranging from visible light to infrared, which is appreciated by image processing because different features of the earth's surface have different sunlight reflections. This difference helps to distinguish between features such as land and water. In Google Earth Engine, four satellite missions containing optical sensors and moderate spatial resolutions are focused, and an overview of them is shown in Table 3-1.

Table 3-1 Overview of satellite missions available in GEE platform

Mission	Spatial resolution (m)	Revisit time (days)	Available Period
NASA Landsat 5	30×30	16	01/01/1984~05/05/2012
NASA Landsat 7	30×30	16	01/01/1999~07/02/2017*
NASA Landsat 8	30×30	16	11/04/2013~present
ESA Sentinel 2	10×10	5	23/06/2015~present

* For NASA Landsat 7, satellite imagery after 31/05/2003 is affected by the redundancy of Scan Line Corrector (SLC) on the satellite, causing large gaps in the data.

SDS is defined as the line that runs between pixels classified as either sea or land (García-Rubio et al., 2015). The general steps to detect this line with GEE are described by Hagenaars et al. (2018) as Figure 3-1.
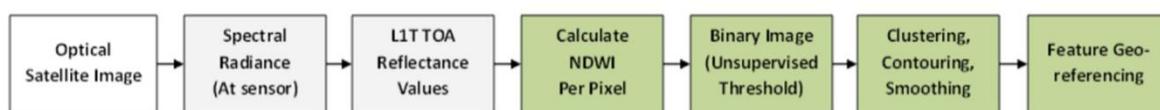

Figure 3-1 Satellite image processing steps. The steps in grey are products by GEE. The steps in green are performed by image processing. Source: Hagenaars et al. (2018)

Firstly, to better distinguish land and water in a single satellite image, the Normalized Difference Water Index (NDWI) was introduced by Gao (1996):

$$NDWI = \frac{\lambda_{NIR} - \lambda_{Green}}{\lambda_{NIR} + \lambda_{Green}}$$

Equation 3-1 Formula to calculate NDWI

Where λ_{NIR} (nm) indicates the Top-Of-Atmosphere (TOA) reflectance value in the Near InfraRed (NIR) band, and λ_{Green} (nm) indicates the TOA reflectance value in the Green band. The NDWI for land is high while it is low for water. Calculating the NDWI for each pixel of an image creates a greyscale image with values ranging from -1 to 1. A threshold needs to be specified to classify pixels in NDWI images. Otsu (1979) introduced an unsupervised threshold determination method to find an optimum value to separate two groups of data. When applying this algorithm to NDWI image, values less than this threshold are classified as water while values larger than the threshold are land. This process creates binary images. Binary image for coast around Port of Lome is shown in Figure 3-2 as an example.
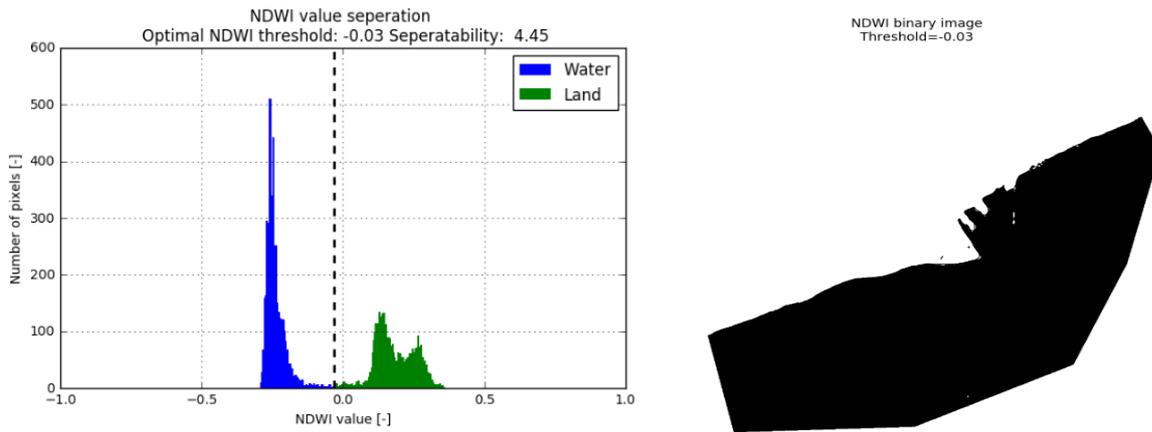
Figure 3-2 NDWI histogram (left) and resulting binary image (right) for a Landsat 5 image acquired on 1985-04-16 around Port of Lome

Thirdly, a region growing algorithm (Kamdi and Krishna, 2012) is applied to the binary image for clustering. It starts with a random water pixel and then searches for adjacent water pixels. This process creates polygons representing water area. SDS vectors are the outer edges of these polygons. However, in most cases, detected shorelines have a sawtooth pattern, because it follows edges of pixels. To overcome these unrealistic sawtooth patterns, clustering is followed by smoothing of coastline vectors using bicubic interpolation of the pixel values. The detected around Port of Lome is shown in Figure 3-3.

Figure 3-3 SDS around Port of Lome acquired on 1985-04-16 around. The derived SDS is plotted in black

Fourthly, satellite images on the GEE platform are georeferenced initially with respect to the first image in a collection. Errors in the first georeferencing lead to offsets between satellite baseline and in-situ data. However, in this research, as SDS data are not compared with in-situ data and all SDS vectors themselves from Landsat images have the same georeference, this step is not necessary.

3.1.2   Accuracy and its determinants

The accuracy of SDS detection method introduced above has been validated for a sandy shoreline in the Netherlands by Hagenaars et al. (2018). Hence, the detection algorithm has demonstrated a skill for sandy environments. Nevertheless, Hagenaars et al. (2018) indicated environmental and satellite related drivers of inaccuracy in the SDS:

Hagenaars et al. (2018) distinguish environmental drivers of inaccuracy include cloud cover, waves (surface roughness and foam) and soil moisture. Amongst these parameters, waves (surface roughness and foam) are hard to be quantified without nearshore wave and bathymetry data, which are hard to obtain in data-poor environments, such as in Africa. Similarly, soil moisture cannot be described due to the deficiency of soil data. Regarding satellite related drivers, sensor corrector failure, georeferencing errors and image pixel resolution are distinguished. However, as it is described in Section 3.1.1, georeferencing is not a problem for this research as no comparison with in-situ data is required and only Landsat images are used which have the same georeferenced (Section 3.1.3). As same satellite missions are applied to all sites, pixel resolution and satellite instrument do not vary among ports.

Hagenaars et al. (2018) also applied the image composite technique (Donchyts et al., 2016) to minimise errors due to environmental drivers. This technique uses a sequence of satellite images to obtain a single composite image. Each pixel in the composite image is obtained from the clear concurrent pixel within a sequence of individual images. This method was found to reduce offsets efficiently down to 10~30m. However, the effect of image composite technique relies on the number of satellite imagery in the composite window. Although the quantitative relationship between these two parameters has not been researched, image composite window with more images is found to have a better description of the shoreline position.

In summary, since SDS validation research has not been conducted for other types of coasts, sediment type is the first parameter affecting the reliability of SDS detection. Additionally, cloud coverage and the number of satellite imagery in the composite window are the other two parameters to be included in the database regarding SDS detection reliability.

3.1.3   Parameter determination

For each African seaport, a merged satellite image collection of Landsat 5, 7 and 8 is applied to SDS detection, covering the period from 1984-01-01 to 2018-01-01. The inclusion of ESA Sentinel 2 images will increase the computational time of SDS detection for each port significantly, considering the continental research scale of this thesis. As a result, Sentinel 2 images are not included. Then in this merged image collection, images with cloud cover larger than 30% are filtered out from image processing because for these images, a significant portion of shorelines are sheltered by cloud and cannot be adequately detected.

Then satellite images are clipped to the Area of Interest (AOI) with a user-defined polygon that centres a port of interest. The longshore stretch of the polygon is determined based on coastline evolution scales. The spatial scale is estimated to have a linear relationship with the temporal scale (Stive et al., 2002), corresponding to 30 years monitoring, coastline evolution in the order of 10km is expected. In this thesis, the 30km longshore stretch is selected and applied to all African seaports. This polygon then extends 15km to both up-drift and down-drift of ports at open coasts. For ports with natural shelters, this polygon ends at morphological features such as headlands, which separate coastal cells. Although coastline evolution around ports is possible to

extend larger than 30km, which has been reported in the literature (Bruun, 1995), due to efficiency reason, larger polygons are used only if 30km AOI is found to be insufficient. Uncertainties caused by the above two efficiency related simplifications are discussed in Chapter 5.4 and 5.5.

Besides the above two parameters, composite window length is set to 360 days and SLC-off images are included in the research. These two parameters are determined by a case study on Port of Lome, details of which are introduced in Appendix A.

3.2   Methodology for calculation of coastline evolution indicators

In this section methods to calculate coastline evolution indicators are introduced. Firstly, in Section 3.2.1, methods for spatial aggregation are summarized to calculate spatial parameters. Then, to calculate forecast and hindcast indicators, curve fitting formulas and methods are determined in Section 3.2.2.

3.2.1   Spatial aggregation

For each African seaport, after applying SDS detection, a sequence of SDS vectors with different acquisition dates is obtained. To derive identified spatial parameters from these vectors, spatial aggregation is necessary. Firstly, a baseline is defined as the shoreline vector detected from the first available satellite image after ports construction. Then vectors collected in other dates are compared with this baseline to derive identified spatial parameters. Sketch of spatial parameters is shown in Figure 3-4. Gross and net coastal area changes are defined as the sum of and difference between the absolute value of accretion and erosion areas.
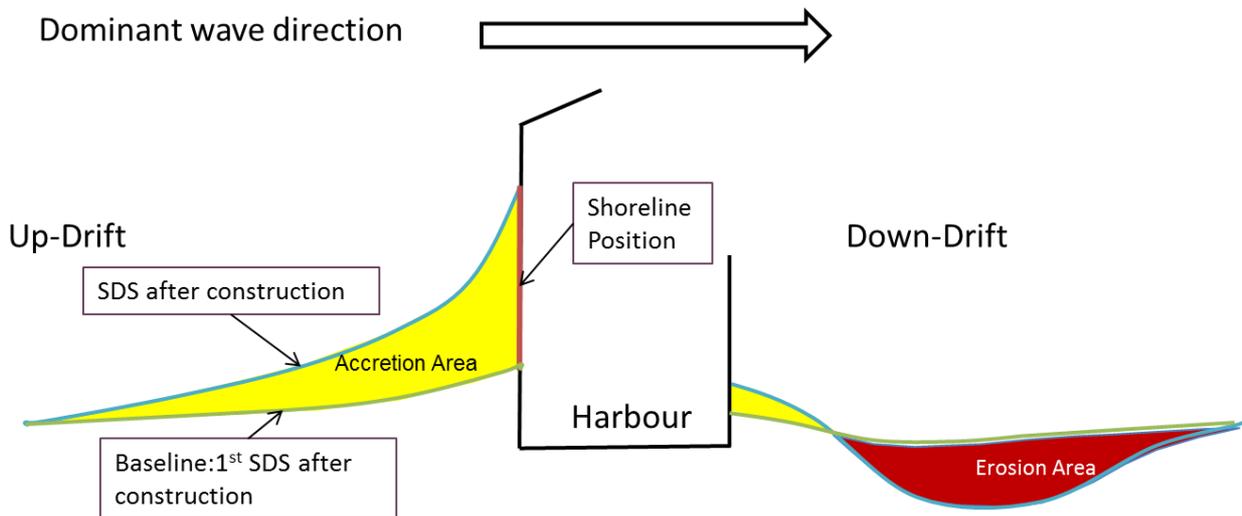

Figure 3-4 Schematic sketch of spatial indicators

Shoreline position at the up-drift boundary of port

The vector at the up-drift boundary is detected along up-drift breakwater or up-drift boundary of berthing structure (for ports without breakwater) manually from the most recent aerial and satellite imagery provided by Google Earth. The intersection between this transect and baseline is defined as the origin point. Then such intersection point is calculated for each SDS vector, and its distance to the origin point is defined as shoreline position at up-drift boundary.

Accretion/Erosion area around the port

The shore-normal transect at the up-drift and down-drift boundaries are collected manually from aerial or satellite imagery provided by Google Earth. Then for each shoreline vector, its joint points with the baseline vector and ports boundary vectors can be found. These points divide the baselines and SDS into segments. Then polygons bounded by these segments are identified, and the areas of polygons are calculated with the Shapely Library in Python. Since SDS vectors represent the whole boundary of the water body in research area due to the region growing algorithm, the original area of the sea can be derived from baseline vector which is defined as the base polygon (Figure 3-5 d). If the identified polygon is within the base polygon, it is accretion area. Otherwise, it is erosion area. Finally, areas of accretion polygons and erosion polygons are summed up respectively to obtain accretion and erosion area for each SDS. An example of accretion/erosion area calculation for an SDS of Nouakchott coast is shown in Figure 3-5.
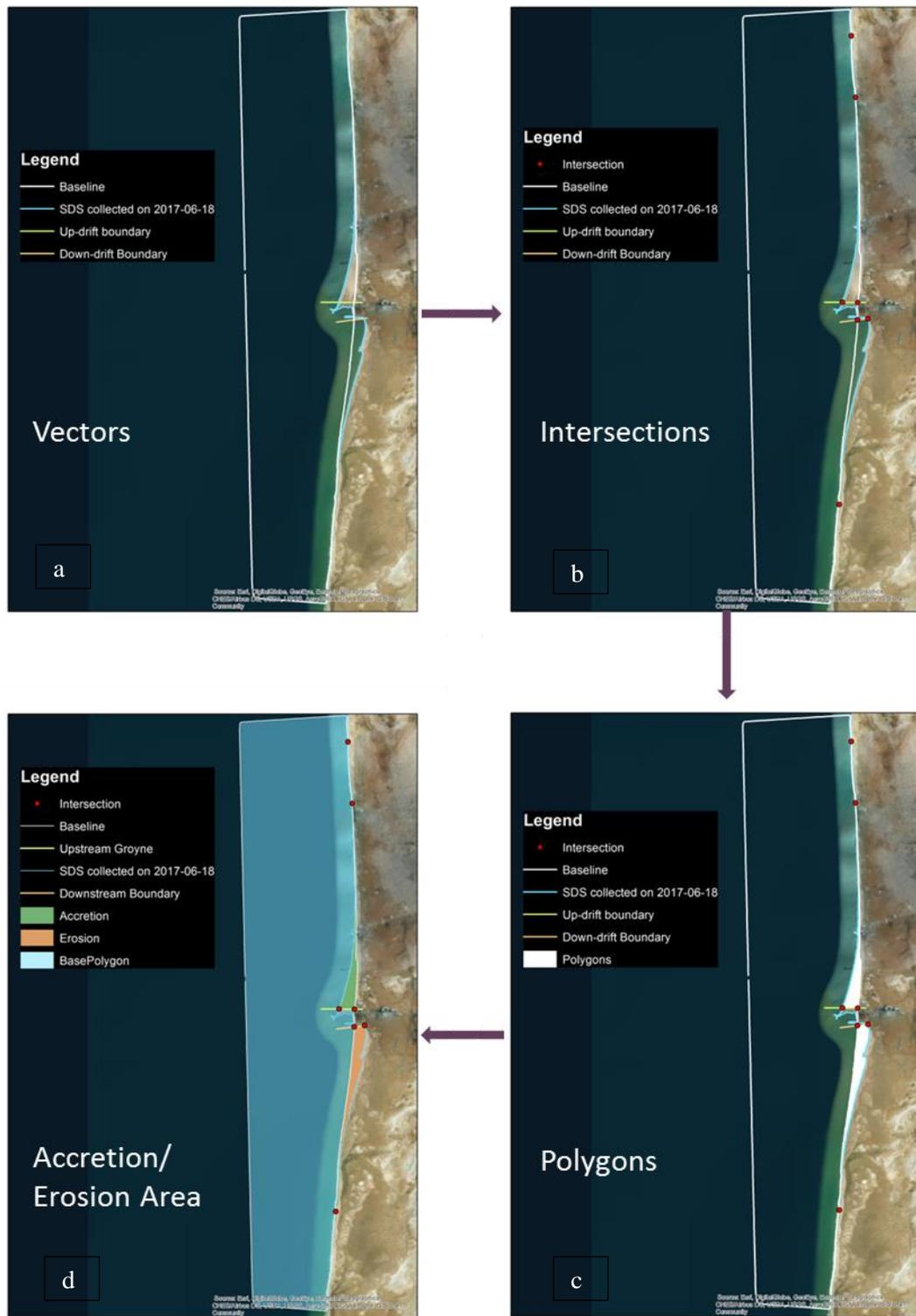
Figure 3-5 Erosion/Accretion area calculation for SDS acquired on 2017-06-18 around Port of Nouakchott

3.2.2   Time series curve fitting

For an African seaport, after applying spatial aggregation to a sequence of SDS vectors, time series of shoreline position at up-drift boundary, erosion area and accretion area can be obtained respectively. Then curve fittings are applied to derive hindcast and forecast indicators.

Curve fitting formulas

In this thesis, linear and exponential curves are applied to fit scattered points of each spatial parameter for every African seaport.

1. Linear fitting: Linear curve is widely applied to describe the change of shoreline position and has been proved representative for most cases. Ordinary Least Squares (OLS) is applied to fit through the spatially aggregated data after ports construction with a linear equation:

$$y_1(t) = a_1 t + b_1$$

Equation 3-2 Formula of the linear curve

Where $y_1(t)$ can be the shoreline position or erosion/accretion area at time instance t and a_1 is an indicator for the structural rate of change.

2. Exponential fitting: As it is described in the literature review, the evolution rate is fast at the beginning and declares when the new equilibrium situation is approached. Such a process can be expressed exponentially. Hence instead of using a linear equation, an exponential curve is applied to fit through the time series data after ports construction:

$$y_2(t) = a_2 \left(1 - e^{-\frac{t}{b_2}} \right) + c_2$$

$$b_2 = \frac{a_2}{(dy/dt)_{t=0}}$$

Equation 3-3 Formula of the exponential curve

Where a_2 is the equilibrium states for a spatially aggregated parameter, b_2 is the morphological timescale. With this method, the present rate can be calculated from the derivative of the above formula at the point of 2018.

Curve fitting improvements

To improve curve-fittings, the following two methods are applied. Design and test of these methods are shown in Appendix B.

1) Weighted fitting: The quantity of images in a composite window determines the reliability of the SDS detection and then spatial aggregation. In other words, uncertainties of scattered points vary according to the number of images involved. The assumption of constant variance of errors is violated and Weighted Least Square (WLS) fit can be performed. In the weighted fitting, less weight is given to less precise measurements and more weight to more precise measurements (Croarkin et al., 2002). If the image quantity in a composite

window is larger than 20, corresponding points are assigned a weight of 1. Otherwise, weights are normalised between 0 and 1 based on image quantity.

2) Outliner Detection: While weighted fitting is only able to reduce image quantity related errors, outlier detection targets on all kinds of deviations. Scattered points with 10% largest variations are detected and removed from fitting.

Curve fitting assessment

The coefficient of determination R-squared (Devore, 2011) is used to judge the quality of each fitting curve. This coefficient compares fitting models with the method of a simple average. For a dataset of n values of y_i, and each associated with a predicted value f_i, R-squared can be defined as:

$$R^2 \equiv 1 - \frac{SS_{res}}{SS_{tot}}$$

$$SS_{tot} = \sum_i (y_i - \bar{y})^2$$

$$SS_{res} = \sum_i (y_i - f_i)^2$$

Equation 3-4 Formulas to calculate the coefficient of determination

Where R^2 is the coefficient of determination, SS_{tot} is the total sum of squares and SS_{res} is the residual sum of squares.

Indicator determination

Derivative at the year of 2018 and vertical span of curves with the largest R-squared are defined as present evolution rate and cumulative evolution magnitude respectively. A sketch of temporal indicators is shown in Figure 3-6. The process to calculate erosion indicators are shown in Figure 3-7. The same process is also applied to accretion area and shoreline position at the up-drift boundary of a port.
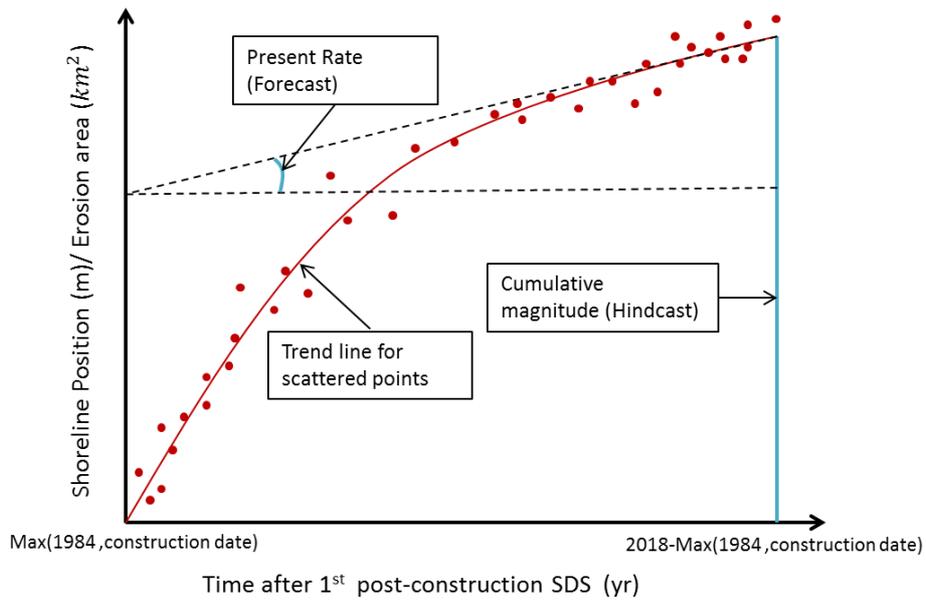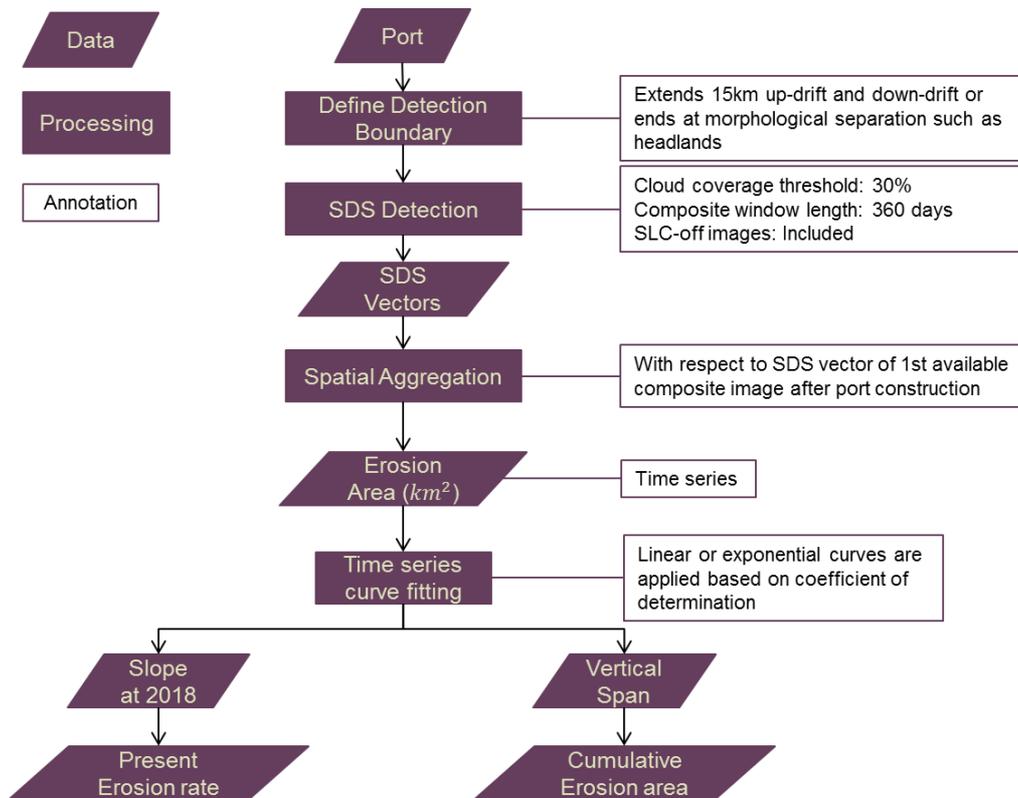
Figure 3-6 Schematic sketch of temporal indicators

Figure 3-7 Steps to calculate coastal area erosion indicators.

3.3   African seaports scoping

In this section, sources of data to define African seaports are introduced in Section 3.3.1. Then these ports are filtered with respect to research objectives and applicability of SDS detection. Steps and criteria to filter ports are shown in Section 3.3.2.

3.3.1   African seaports definition

Seaports are defined as maritime facilities providing access to seagoing ships (Dictionary, 2002). Based on this definition, places where ships dock can be called ports. By analysing sailing charts and recording vessel positions, US National Geospatial-Intelligence (2017) listed thousands of ports throughout the world and produced the World Port Index (WPI) report. Coordinates of these ports are included in WPI, based on which, 266 ports are found in Africa. However, 42 of these ports are located at rivers, canals and lakes, which are unaffected by coastal processes. For the remaining 224 ports, 59 of them are either offshore platforms or anchorages, where port structures cannot be found from satellite imagery. Since this group of so-called ports do not have coastal structures, their potential influence on coast, if any, is difficult to locate. This group of ports are also scoped out from this research and finally, 165 ports are defined as African seaports.

3.3.2   African seaports filtration

Criteria for filtration are first introduced, followed by description of method and source to collect data required for filtration. Finally, results of filtration are plotted.

Criteria for filtration

As it is described in Section 3.1.2, SDS detection methods have only been validated for the sandy coast. Hence, in this research, the applicability of SDS detection to muddy and rocky coasts is firstly checked. Luijendijk et al., (2018) mentioned that the dark colour of the muddy flat makes it difficult to be distinguished from the sea. Regarding the rocky coast, the shadow of the cliff also has a dark colour, which can lead to the similar problem experienced by muddy flats. In addition to SDS detection accuracy, processes of sediment transport and morphological change of muddy and rocky coasts are more complicated than sandy ones, more data about fluid and flow conditions are required, which are not available for most African ports. Hence ports on muddy and rocky coasts are filtered out from this research.

Sediment type definition

Three types of coasts are defined regarding sediment, including sandy, rocky and muddy coasts. Coasts with sandy beach, even on rocky substratum are also defined as sandy coasts. Coasts with rock/reef/cliff are defined as rocky coasts, while coasts with muddy flats are defined as muddy coasts. These three types of coasts have different sunlight reflection features. Examples of sandy, muddy and rocky coasts are shown in Figure 3-8.
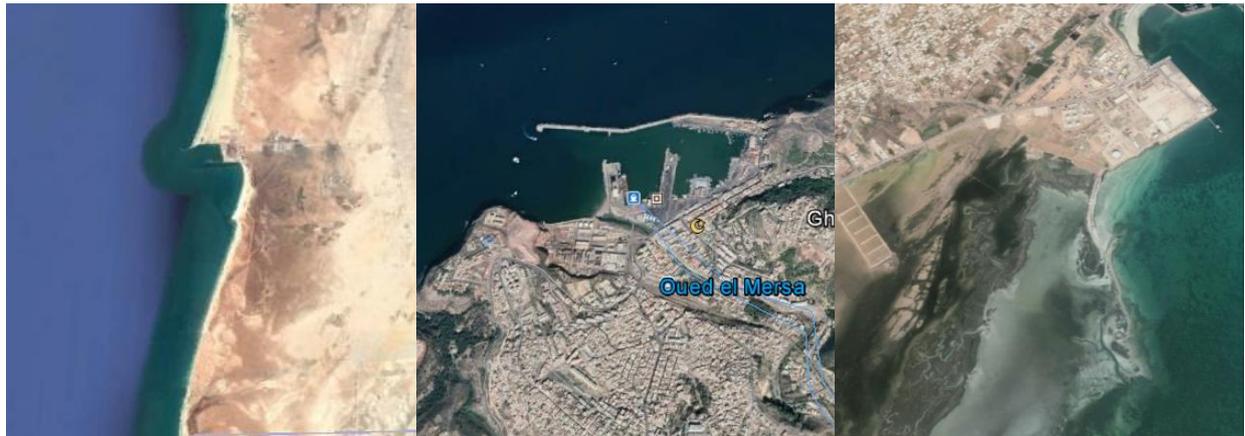
Figure 3-8 Examples of Sandy, Rocky and Muddy coasts. Left: Sandy coast around Port of Nouakchott, Mauritania; Middle: Rocky coast around Port of Ghazaouet, Algeria; Right: Muddy coast around Port of Zarzis, Tunisia

Luijendijk et al. (2018) applied machine learning to judge whether a coast is sandy or not. This database is used to pre-determine sandy coasts. Then research on sedimentation in the inner continental shelf (Mhammdi et al., 2014, Flemming, 1981) and research on the distribution of muddy and rocky coastlines (Flemming, 2002, EDWARD, 2006, Furlani et al., 2014) are used to validate results from the previous step and classify non-sandy coasts into muddy and rocky ones. Finally, classification results are adjusted by manual inspections based on satellite imagery, aerial imagery and snapshots available on Google Earth.

Filtration results

Ports filtered out and examples of SDS detection failure for muddy and rocky coasts are shown in Figure 3-9. It can be seen that rocky coasts are mainly distributed around Mediterranean Sea and south-west coast of South Africa. The existence of cliff shadow (Port of Chazaouet) moves SDS landward. Muddy coasts are located around river month and tidal inlets; the existence of muddy tidal flat (Port of Maputo) moves SDS seaward.

After filtering ports on muddy and rocky coasts, 40 of 165 ports are scoped out from research and distribution of 125 ports remaining for research is shown in Figure 3-10.
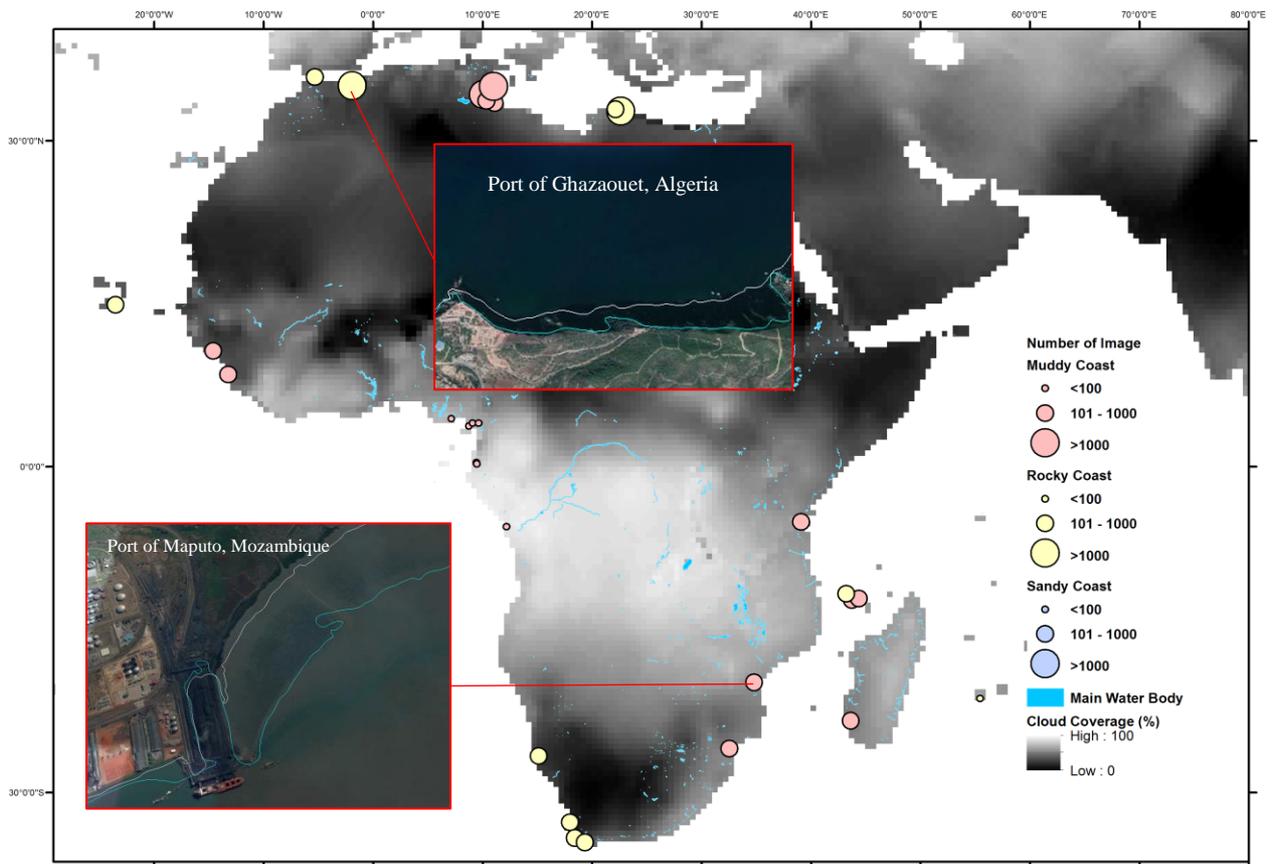
Figure 3-9 Distribution of African seaports which are filtered out. Blue lines in zoomed figures are inaccurate SDS detections while white lines are real shoreline positions.
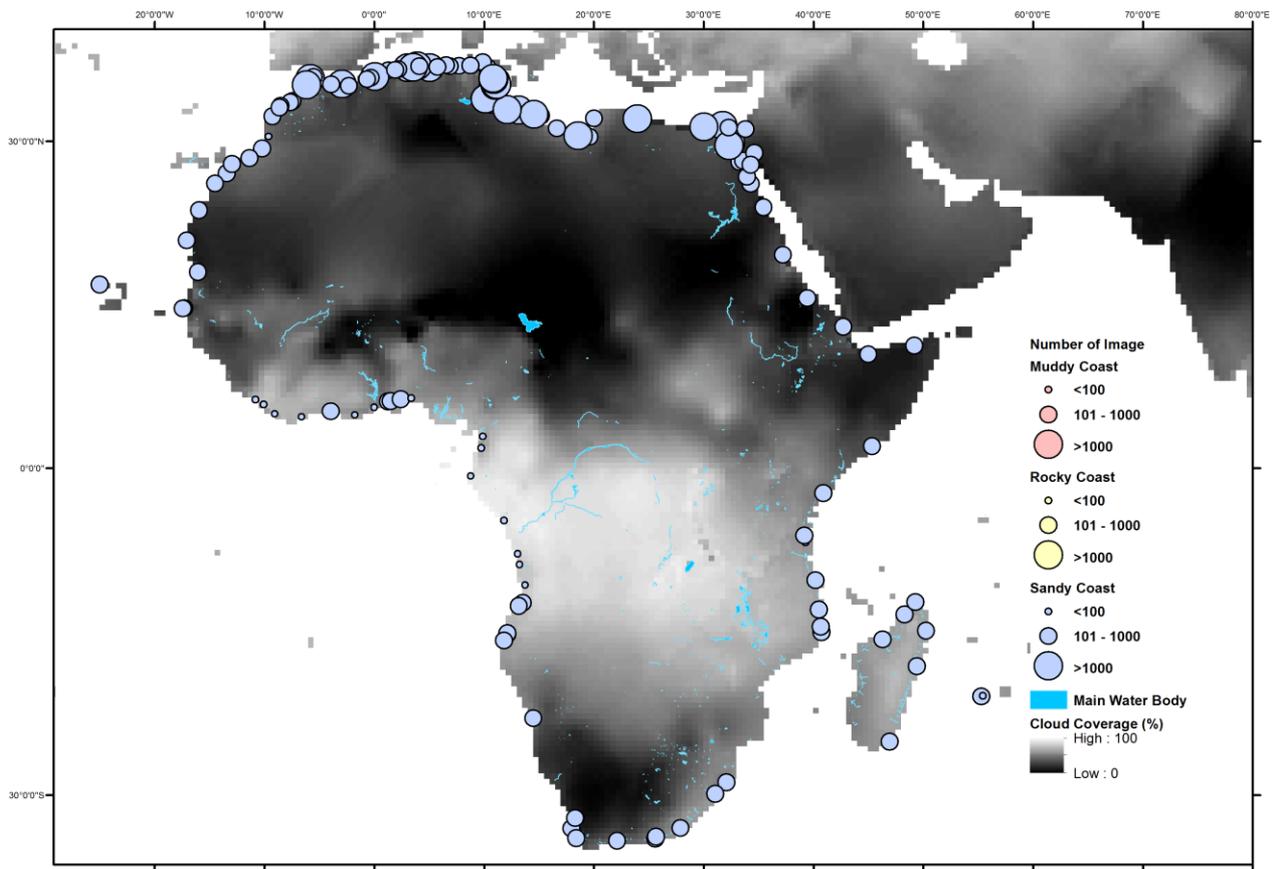
Figure 3-10 African seaports after filtration

3.4 Coastline indicator analysis

Coastline evolution indicators are analysed from three aspects. Firstly, to justify whether coastline evolution is a problem for African seaports, methodology to analyse indicators from the continental perspective is shown in Section 3.4.1. Secondly, to understand the causes to coastline evolution, sources and methods to collect and aggregate data for environmental and port parameters are shown in Section 3.4.2. Methods to investigate influences of different environmental/ports characteristics are introduced in Section 3.4.3. Thirdly, to identify hot spots regarding coastline evolution trends, methodology to identify ports with high erosion and/or accretion hazards is introduced in Section 3.4.4.

3.4.1 Coastline evolution trends analysis from the continental perspective

Coastline evolution indicators are used to analyse probability and magnitude of coastline evolution from the continental perspective. While two hindcast indicators including cumulative erosion and accretion area are used to calculate gross and net coastal area change, which are indicators for coastline evolution magnitude around African seaports, two forecast indicators including present coastal area erosion and accretion rates are used to classify coasts around African seaports into dynamic and stable ones. The portion of dynamic coasts after classification is used as the indicator for the future probability of coastline evolution around ports.

In order to know the portion of ports with dynamic coasts, criteria to define dynamic coasts are important. Regarding shoreline position, Luijendijk et al., (2018) defined the threshold based on the mean offsets of SDS detection. He applied 192 days composite window with the mean offset of 15m. By defining coasts with cumulative shoreline change larger than detection error as dynamic coasts, with a monitoring period of approximately 30 years (33 years), he decided to use 0.5m/yr as the threshold for shoreline advance/retreat rate. Since 360 days instead of 192 days composite window is applied in this research, the mean offset of SDS is reduced significantly to 4.9m based on Hagenaars et al. (2018). Correspondingly, the threshold for shoreline position advance rate reduces to 0.15m/yr. The thresholds for coastal area erosion and accretion rates are defined as the product of the threshold for shoreline position and erosion length l_{ero} and accretion length l_{acc} respectively. Erosion/accretion length is calculated as the sum of baseline length where erosion/accretion polygons are identified. Since these erosion/accretion lengths are varying, thresholds for coastal area erosion/accretion rates to define dynamic coast are also varying from port to port.

With these thresholds for coastal area erosion/accretion rates, dynamic coasts with respect to erosion and accretion can be identified respectively. To be conservative, coasts have either accretion or erosion trends are classified as dynamic coasts. Otherwise, they are classified as stable coasts. The classification process is summarized in Figure 3-11.
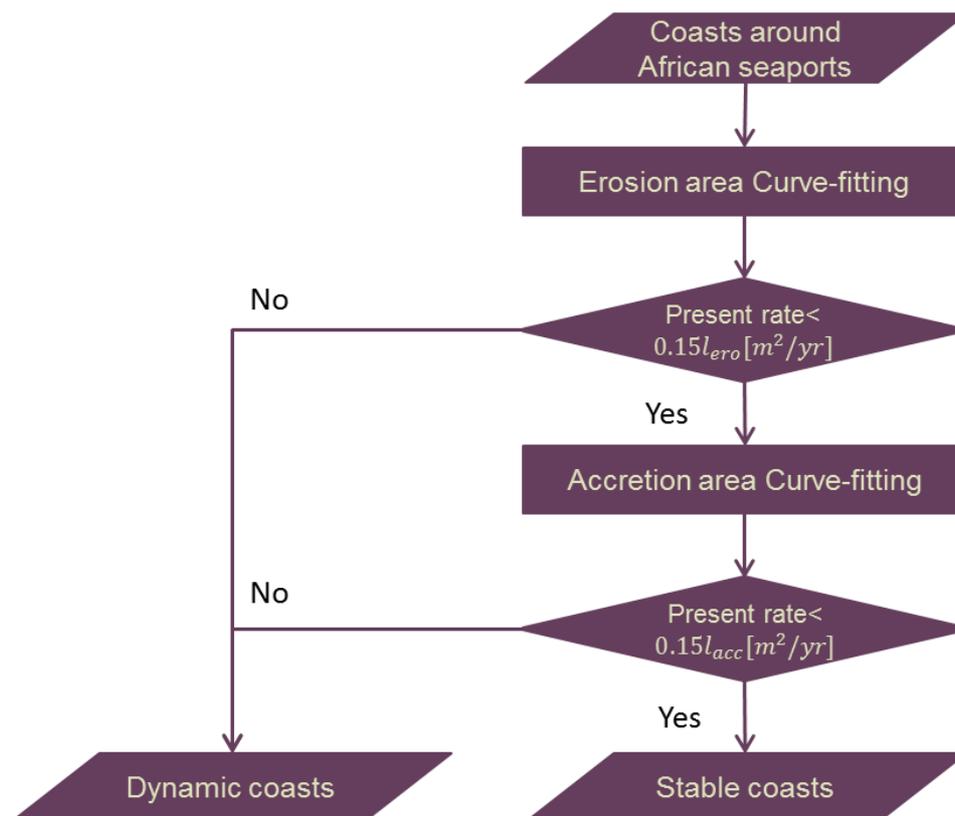

Figure 3-11 Classification criteria for coasts with respect to coast stability

3.4.2   Data collection of environmental/port characteristics on coastline evolution

In this section, sources and methods to collect and aggregate data for parameters in Table 2 are introduced.

Wave climate

Wave climate is essential for LST and coastline evolution. Since wave parameters do not affect LST independently, further aggregation is necessary. The assumption used in CERC formula is applied to achieve this goal. By balancing immersed sediment weight with the longshore component of the wave energy flux (wave power), a relationship between LST and aggregated wave parameters can be obtained:

$$Q_l = K \frac{\rho g^{0.5}}{16\sqrt{\gamma_b}(\rho_s - \rho)(1-p)} H_{sb}^{2.5} sin2\alpha_b$$

Equation 3-5 CERC formula to calculate LST

Q_l (m^3/s) is the volumetric sediment transport rate, γ_b is the breaking index, ρ_s and ρ (kg/m^3) are the density of sediment and water respectively, p is the porosity factor of sediment, $\alpha_b (degree)$ is the wave angle of incidence, H_{sb} (m) is the significant wave height at the breaking point, K is a coefficient related to the sediment grain size. K is difficult to determine without soil properties. Due to the difficulty to obtain accurate wave climate at breaking point, offshore wave angle α and significant wave height H_s are directly applied in this formula, longshore component of wave power indicator $H_s^{2.5} sin2\alpha$ is then used to represent wave effects. Wave angle with respect to shore normal direction α requires also information on the shoreline orientation, which is measured from present shoreline on Google Earth. A straight line is drawn to connect the starting and end points of coastline in AOI with land in the right-hand side. Orientation of this line is used to define shoreline orientation.

In terms of hindcast wave datasets, the ECMWF Re-Analysis-Interim (ERA-I) (Dee et al., 2011) dataset is available for all locations of the globe from 1979. Stopa and Cheung (2014) observed that ERA-I data although generally underestimate wave height, maintain a satisfying accuracy. Hence wave data are collected from this database. Because nearshore bathymetry applied in this hindcast database is not accurate, wave climate in the nearshore zone, although available in some cases, is not accurate. To avoid these nearshore data, a buffer zone is defined around African coast and the width of buffer is determined by the width of nearshore zone. The nearshore depth is found to be 5~15m ((Simm et al., 1996)) and Dean (1977)'s profile $h = Ax^m$ is used to calculate corresponding offshore distance. In this formula, h is water depth, x is the distance from the shoreline, A and m are coefficients describing overall steepness and profile shape. From previous research, A is found to range from 0.075 to 0.107 and m is 0.67 (Cerkowniak et al., 2017). To be conservative, A=0.075 and h=15m are used to estimate the width of nearshore zone, which is calculated to be 2718m and therefore the buffer width is set to 3km.

For each port, among all offshore ERA-I grid points (3km away from the coastline), the one closest to port is used to collect significant wave height and wave direction from 1984 to 2017 with 6 hours timestep. Significant wave height H_s is classified into 11 groups (10 groups ranging from 0 to 5m with 0.5m step and a group larger than 5m). Similarly, wave direction is classified into 24 groups (ranging from 7.5 to 352.5 degrees, with 15 degrees step). After classification, 262 scenarios are defined. Each scenario has a corresponding wave height, wave direction and frequency. Wave data processing results for Nouakchott coast is shown in Figure 3-12 as an example.

Since shoreline orientation is defined to keep land on the right-hand side, it is not difficult to distinguish waves from land and sea. Offshore waves from the land side are filtered out. Then $H_s^{2.5} sin2\alpha$ is applied to all filtered wave scenarios, where α is the angle between shore normal vector and wave direction, ranging from

$0°$ to $45°$. For waves from the right side of shore normal vector, α is set to be negative and $sin2\alpha$ then ranges from -1 to 0. Correspondingly, waves from left side has positive α and $sin2\alpha$ ranges from 0 to 1. By doing so, waves from the right side of shore normal vector result in negative $H_s^{2.5}sin2\alpha$, while waves from the other side have positive value. Finally, $H_s^{2.5}sin2\alpha$ with negative and positive values are summed up respectively as indicators for longshore component of wave power from two opposite directions, noted as P_1 and P_2. The gross longshore wave power indicator $P_{Gross} = |P_1| + |P_2|$, while net longshore wave power indicator $P_{Net} = |P_1 + P_2|$.

After this process, gross longshore wave power indicator for all African seaports on sandy coasts is obtained, which is shown in Figure 3-13. It can be seen that large wave energy does not always correspond to large longshore wave power; coasts with milder wave condition can also have a large magnitude of LST if the waves are unidirectional and have small α. Large longshore wave power is distributed around West Africa, North West Africa, South African coast and East coast of Madagascar. Waves around Red Sea and Mediterranean Sea result in smaller magnitudes of longshore wave power.
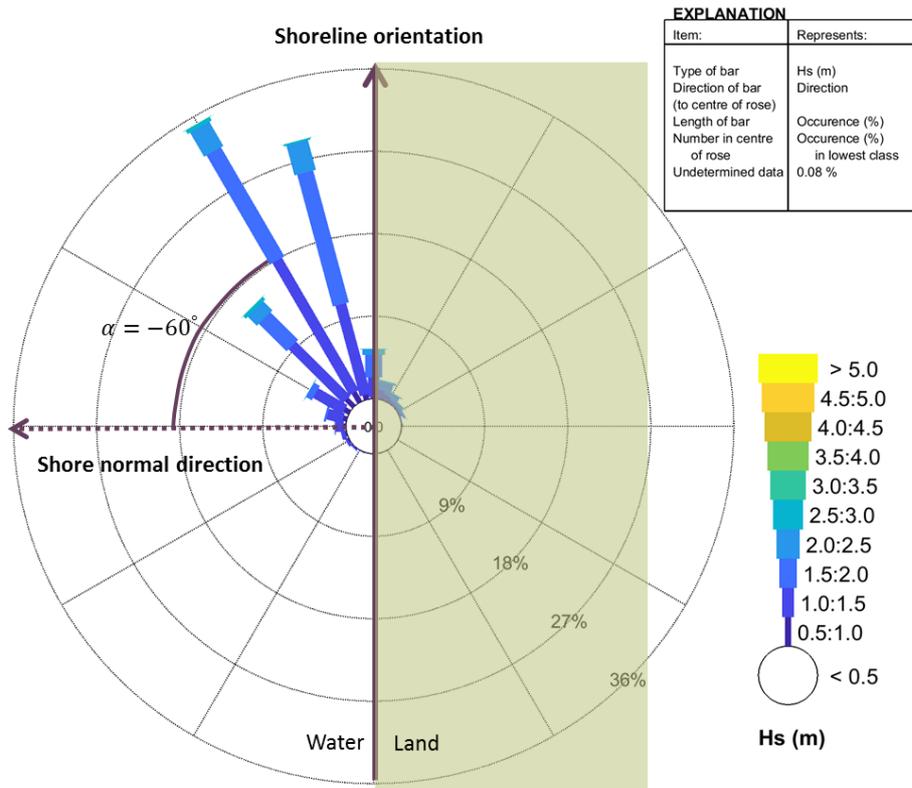

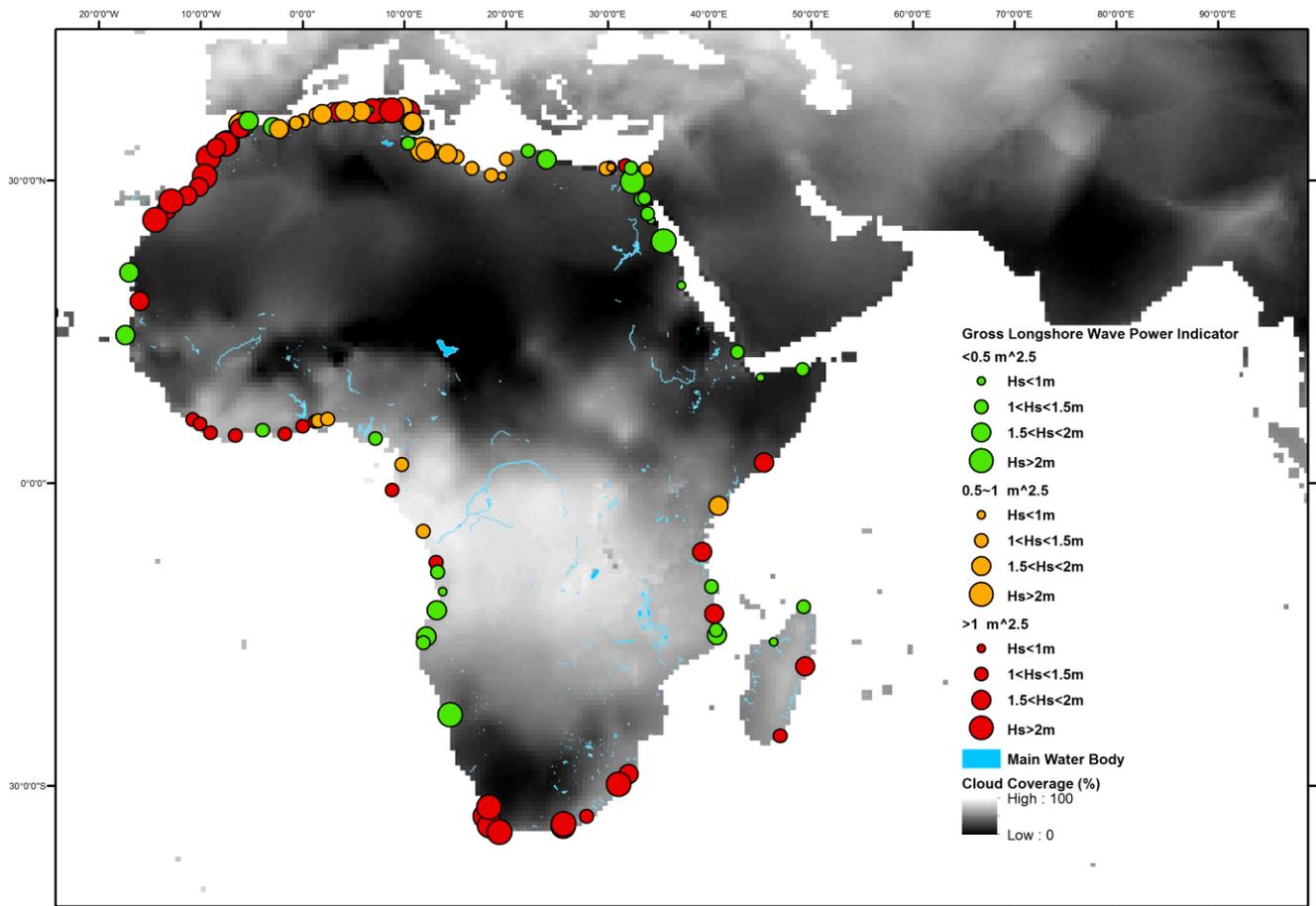*Figure 3-12 Schematic sketch of wave data processing for Nouakchott coast*

Figure 3-13 Significant wave height from dominant wave direction (with respect to $H_s^{2.5} sin2\alpha$) and gross longshore wave power indicator for African seaports (filtered)

Natural shelter conditions

Some ports are naturally sheltered by headlands or spits. The natural sheltering condition determines the difference between offshore and local wave climate around ports. In this thesis, ports are classified into three categories with respect to the different level of exposure to waves, including (1) ports at open coastlines, (2) ports at headland-bay systems and (3) ports sheltered by spits, barrier islands or in estuaries. For the first category, offshore waves experience refraction, shoaling but limited diffraction when propagating from offshore to nearshore, the difference between nearshore and offshore wave climate is less significant. For the second category, curved bathymetry contour makes the refraction process more prominent and offshore waves from certain directions can be blocked by headlands, making offshore wave climate less applicable to nearshore research. For the third category, diffraction process becomes important; wave direction changes significantly and wave power is undermined when it reaches the port. For this category, offshore wave climate cannot reflect nearshore wave condition adequately. These three types of natural conditions can be judged by visual inspection on coastal geometry from present satellite and aerial imagery in Google Earth. Examples for different categories are shown in Figure 3-14

Figure 3-14 Examples of Ports with different sheltering conditions. Left: Port on open coast (Port of Nouakchott, Mauritania); Middle: Port in headland-bay system (Port of Amboim, Angola); Right: Port behind spit (Port of Luanda, Angola)

Type of sources and sinks

As it is described in the literature review, a wide range of morphological elements are defined as sources/sinks. However, most of them are difficult to be defined, which requires additional morphological change analysis. In this thesis, only rivers and tidal inlets are considered as sources and/or sinks. The existence of these two morphological elements is judged based on the coastal geometry from the present satellite image.

Construction date of ports

There is no database for construction date of all African seaports. For ports constructed after 1984, construction date is determined by looking through timelapse of satellite imagery available in Google Earth. The acquisition time of satellite image where ports construction is completed is used as construction date. However, for ports constructed before 1984, construction date is difficult to be derived. Hence the construction date of this group of ports is simply described qualitatively as before 1984.

Length of port breakwaters

For port breakwaters, the projected length of up-drift breakwater in meter in the shore-normal direction is used as the indicator. Although this simplification cannot reflect wave and fluid condition in the shelter zone accurately, it shows breakwater's potential to block longshore sediment transport. This projected length is measured from Google Earth based on the present satellite image, with the beginning of construction as the reference point for measurement.

Types of other human interventions

Besides breakwater of ports, types of human interventions are defined based on their primary aim and structure forms, including LST interruption structures such as groynes and detached breakwaters and shore protection structures such as seawalls and revetments. The existence of these structures is judged based on their visualisation in the satellite image. Examples of different structures are shown in Figure 3-15.

Figure 3-15 LST interruption structures (a) and shore protection structures (b) around Port of Tangier, Morocco

3.4.3   Influences of environmental/port characteristics on coastline evolution

To derive lessons for future port development, it is crucial to understand the influences of environmental and port characteristics on coastline evolution. Amongst parameters in Table 2-1, port construction date, LST parameters, sink/source parameters and human intervention parameters are focused. Among these parameters, non-quantifiable and quantifiable ones are treated differently.

Influences of non-quantifiable parameters

Non-quantifiable parameters including natural shelters, visible sediment sources and sinks (River and inlet) as well as artificial structures have been divided into sub-categories. Construction date before 1984 is non-quantifiable while construction date after 1984 is quantifiable. In this research, construction date is treated as a non-quantifiable parameter with two categories as before 1984 and after 1984.

Influences of these parameters on coastline evolution are reflected from statistics of hindcast and forecast indicators for ports with different characteristics. For each sub-category of ports, sum, mean value and standard deviation of gross and net coastal area change (cumulative magnitude and present rate) are calculated and compared. In addition to the magnitude of coastline evolution, the percentage of ports with net erosion/accretion of each sub-category is also calculated to indicate the probability of different forms of coastline evolution.

Influences of quantifiable parameters

Quantifiable parameters including the indicator for gross longshore wave power and breakwater length can be plotted against present coastal area erosion/siltation rates directly since they are continuous parameters. Forecast instead of hindcast indicators are used for this correlation analysis in order to eliminate the influence of monitoring duration. Influences of these quantifiable parameters can be reflected from trends of scattered points.

If apparent separation of trends of scattered points is identified for gross longshore wave power, this separation point is applied as a threshold to classify ports into two categories as large longshore wave power and low longshore wave power. Similarly, ports can also be classified with respect to the breakwater length as

long breakwater and short breakwater. Then these two quantifiable parameters can also be treated as non-quantifiable parameters introduced above.

3.4.4   Identification of ports with high siltation/erosion hazards

Besides magnitude and probability of coastline evolution of all African seaports, extreme cases also reflect the significance of ports on coastal morphological change. Therefore, methods to identify these extreme cases are introduced in this section.

Firstly, two hindcast indicators including cumulative erosion area and relative shoreline position to breakwater length are selected to identify ports with prominent erosion and siltation history. After ranking African ports with respect to these two indicators from high to low, hazard levels are assigned to all ports based on their relative positions in these two ranks. Criteria of the hazard level assignment are shown in Table 3-2. Ports with hazard level 2~6 are identified as ports with high erosion and/or siltation potentials. Following a similar process, two forecast indicators including present rates of coastal area erosion and shoreline advance at the up-drift boundary are applied to identify ports with prominent erosion and/or siltation potentials.

Table 3-2 Criteria of hazard level assignment for African Ports

Siltation / Erosion	Top 100% in rank	Top 20% in rank	Top 10% in rank	Top 5% in rank
Top 100% in rank	0	1	2	3
Top 20% in rank	1	2	3	4
Top 10% in rank	2	3	4	5
Top 5% in rank	3	4	5	6

4

Results

In this chapter sub-question 3, 4 and 5 in Section 1.2 are answered in Section 4.1, Section 4.2 and Section 4.3 respectively. Then these results are summarized in Section 4.4 to answer the main research question. The structure of this chapter is shown in Figure 4-1.
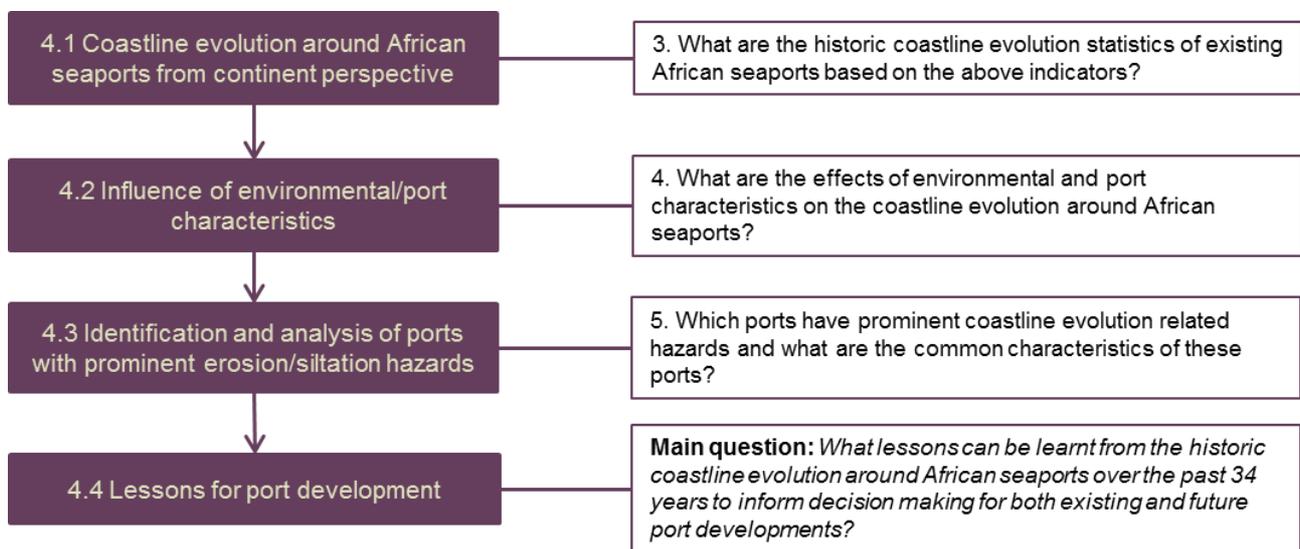
4.1 Coastline evolution around African seaports from continent perspective	3. What are the historic coastline evolution statistics of existing African seaports based on the above indicators?
4.2 Influence of environmental/port characteristics	4. What are the effects of environmental and port characteristics on the coastline evolution around African seaports?
4.3 Identification and analysis of ports with prominent erosion/siltation hazards	5. Which ports have prominent coastline evolution related hazards and what are the common characteristics of these ports?
4.4 Lessons for port development	**Main question:** *What lessons can be learnt from the historic coastline evolution around African seaports over the past 34 years to inform decision making for both existing and future port developments?*

Figure 4-1 Structure of Chapter 4

4.1   Coastline evolution around African seaports from the continental perspective

In this section, coastline evolution indicators are used to analyse the probability and magnitude of coastline evolution from a continent perspective. Firstly in Section 4.1.1, two hindcast indicators including cumulative erosion and accretion area are applied to calculate gross and net coastal area change, which are indicators for the historic coastline evolution magnitude around African seaports. Then in Section 4.1.2, two forecast indicators including present coastal area erosion and accretion rates are used to classify coasts around African seaports into dynamic and stable ones following the criteria introduced in Section 3.4.1. Based on the classification, the portion of the dynamic coasts is used as the indicator for the probability of coastline evolution around ports.

4.1.1   The magnitude of coastline evolution around African seaports

To understand magnitude of the coastline evolution around seaports in Africa, the coastal area change of all of the incorporated 125 African seaports is analysed. The gross coastal area change around all African seaports is 55 km^2, including 29 km^2 accretion and 26 km^2 erosion. As the total coastline length scoped in this research is

2600 km, the average shoreline change is 21m. Compared with the 30m satellite image pixel resolution, this shoreline change magnitude is not significant.

The top 10% of ports resulting in 27 km^2 coastal area change, sharing approximately 50% of total area change. Distribution of gross and net coastal area change of these ports is shown in Figure 4-2. It can be seen that, although the mean gross value is only 0.44 km^2, the gross coastal area change for an individual port can be up to 7 km^2. This suggests that extreme cases dominate the coastal impacts and indicates the necessity for Section 4.3.

The mean value of accretion is larger than that of erosion. However, because all artificial structures extending to the sea are detected as land and added to the coastal area accretion, accretion area is overestimated. Considering the difference between the mean value of coastal area erosion and accretion is only 0.04 km^2, sediment budget around seaports in Africa is approaching a balance from a continental perspective. Additionally, more African seaports have net accretion area (78 ports) than erosion (47 ports). This is due to the reality that African coast has limited sediment supply from rivers, resulting in a so-called Afro-trailing edge coast with narrow beach and correspondingly low erodibility (Bosboom and Stive, 2015). Once LST, although with small magnitude due to limited sediment quantity, is blocked by port breakwater, down-drift coast is eroded but slows down as the erosion reaches rocky substratum while up-drift accretion is still developing, leading to net accretion.

From Figure 4-2, it can be observed that there are still some African seaports that have significant net coastal erosion. For these ports, it is possible that certain amount of sediment deposited in the harbour and then dredged and moved offshore.
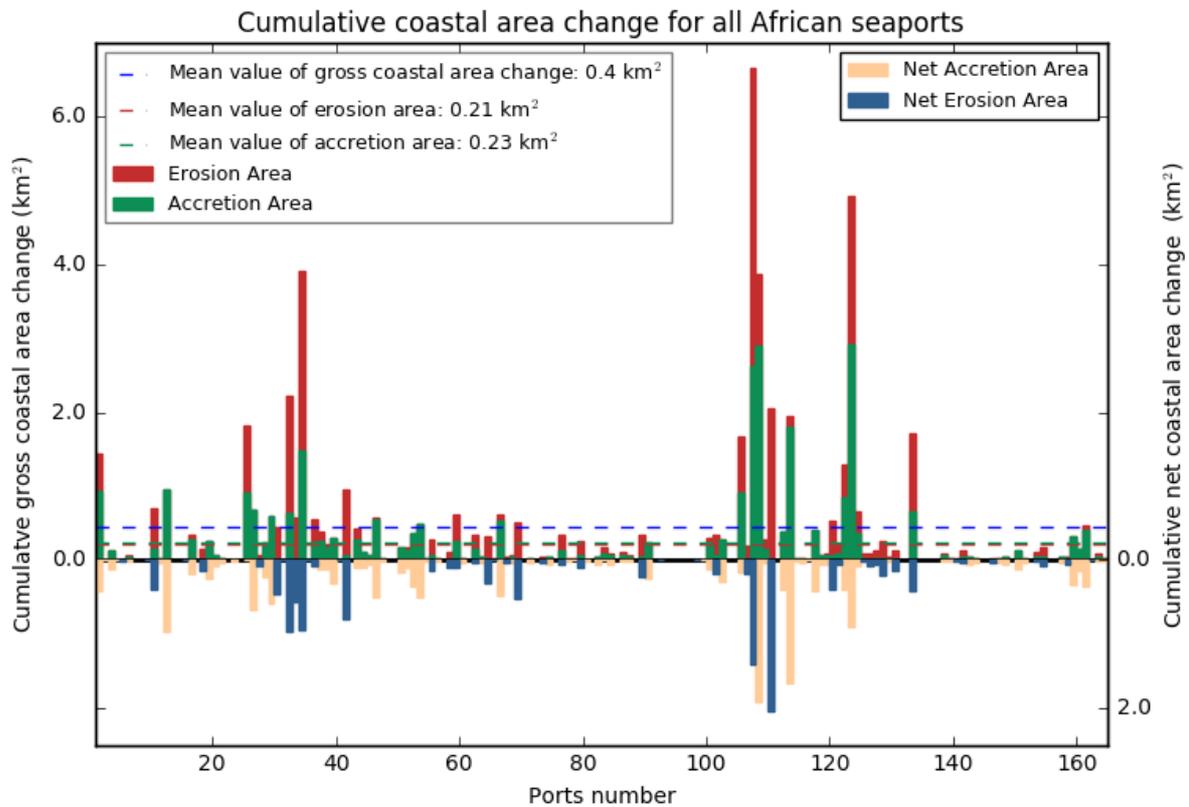
Figure 4-2 Gross and net coastal area change for all African seaports at sandy coastlines

4.1.2 The probability of coastline evolution around African seaports

To understand the present coastline stability around African seaports, 125 African ports at sandy coastlines are classified with respect to coastline evolution (see Figure 4-3). It can be seen that majority of ports are located at unstable coastlines, suggesting a high possibility of coastline evolution around ports. A larger portion of ports shows coastline instability concerning accretion at the up-drift side than erosion at the down-drift side. This can be explained by the property of Afro-trailing coast introduced in 4.1.1.

Examples of a dynamic and stable coast are shown in Figure 4-3. From B1), it can be seen that the most recent SDS outside the port is almost overlapped with the baseline (1st post-construction SDS). Hence it is reasonable to classify the coast of this port as stable. As an example for the dynamic coast, it is apparent in Figure 4-3 B2) that the most recent SDS changes significant from baseline. These two examples reflect the applicability of classification criteria.
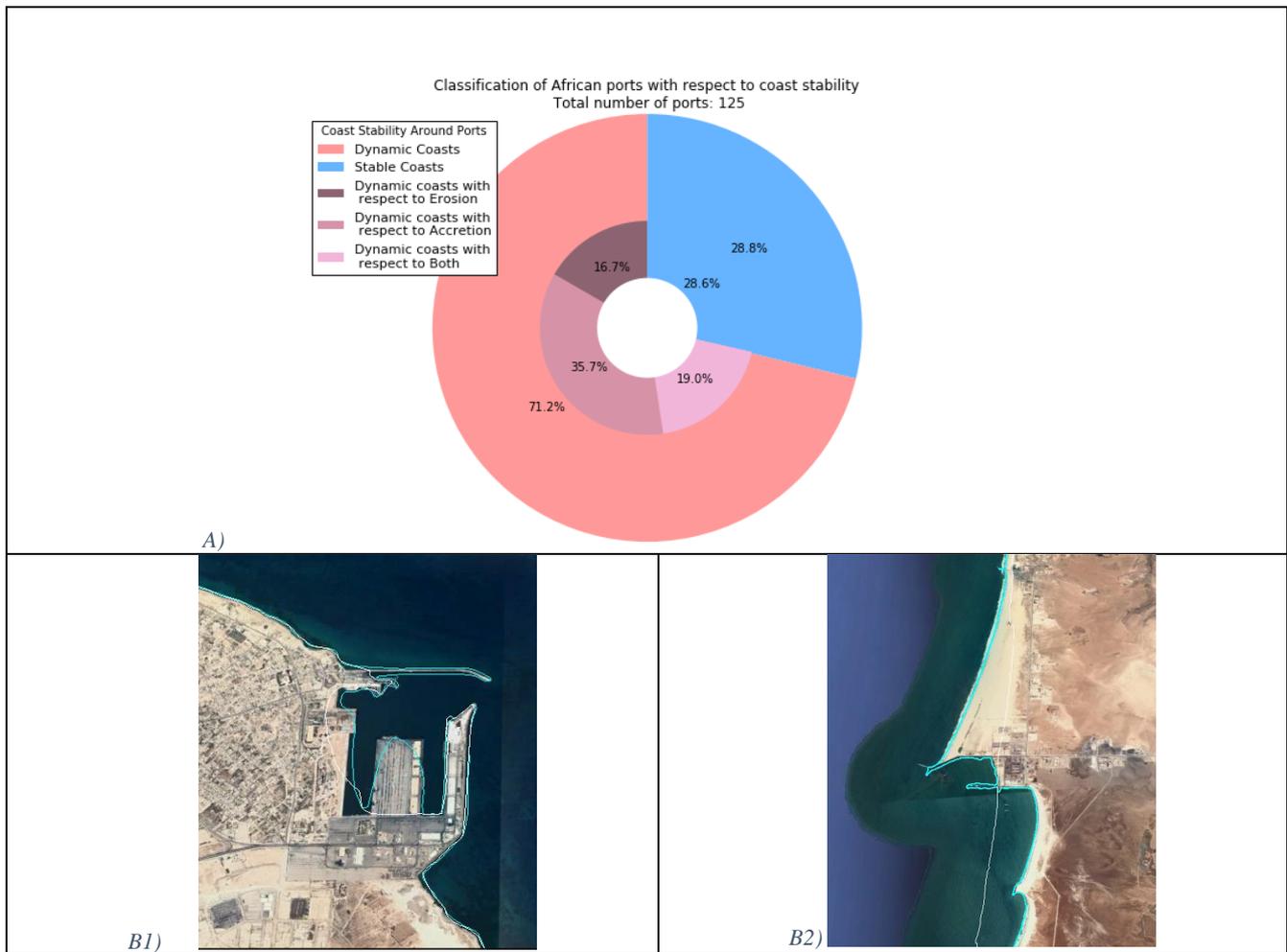
Figure 4-3 Classification of African seaports with respect to coast stability and examples for each category. A) Pie chart of coast stability for filtered African seaports; B1) Satellite image for coast around Port Misurate, an example for stable coasts; B2) Satellite image for coast around Port Nouakchott, an example for dynamic coasts; In B1) and B2) white line is the 1st post construction SDS (Baseline) and blue line is the SDS acquired most recently

4.1.3 Conclusion

Regarding historical coastline evolution, the sum of accretion and erosion area over all 125 African seaports at sandy coastlines is found to be 55 km^2 including 29 km^2 accretion and 26 km^2 erosion since 1984. The 55 km^2 coastal area change is distributed along the 2600km coastline, indicating an average shoreline change of 21m. Compared with the 30m satellite image resolution, the coastline evolution is not significant from a continental perspective. This situation is due to that most ports are located at Afro-trailing coastlines, where a small quantity of sediment is available for longshore sediment transport and coastline evolution. However, when looking at hotspots, the top 10% of ports is responsible for 50% (27 km^2) of the total coastal area change. The gross coastal area change around a single port (Port of Nouakchott) can be up to 7 km^2 including 4.5 km^2 erosion. With the population density of 960/km^2 for the corresponding port city, about 4,000 people can be directly affected by the coastal area erosion. If the increased flood risk due to shoreline erosion is considered, the number of people under influence can be even larger. Regarding present coastline evolution rates, 125 African seaports at sandy coasts are classified concerning coastline stability. 90 ports are found to be located at dynamic coastlines where coastal area erosion (45 ports) or accretion rate (68 ports) is larger than SDS detection accuracy. This means the majority of African ports still have erosion and siltation risks in the future.

Both hindcast and forecast indicators suggest that accretion is more prominent than erosion for African seaports, which can be due to the restriction of rocky substratum on coastal area erosion and human activities to stimulate accretion.

4.2   Influence of environmental/port characteristics

In Section 4.1, statistics of coastline evolution indicators of African seaports are analysed solely while in this section these indicators are related to environmental/port characteristics. Methodology to analyse the influence of non-quantifiable and quantifiable parameters is introduced in Section 3.4.3. Firstly, statistics of hindcast and forecast indicators for all African seaports with different characteristics are summarized in Section 4.2.1, based on which, influences of environmental (gross longshore wave power, natural shelter condition, presence of sources/sinks and presence of human interventions) and port parameters (construction date and port breakwater length) on coastline evolution are analysed in following sections.

4.2.1   Statistics of hindcast and forecast indicators for ports with different characteristics

In this section, 125 African seaports at sandy coasts are firstly classified into different sub-categories based on identified environmental and port parameters. For non-quantifiable parameters including natural shelter condition, the presence of sources and sinks, the presence of human interventions and construction date, classification criteria have been introduced in Section 3.4.2. For quantifiable parameters including gross longshore wave power indicator and breakwater length, thresholds for classification are determined in Section 4.2.2 and 4.2.7 respectively.

For each sub-category, regarding gross coastal area change (cumulative magnitude/present rate), the percentage in total value, the mean value and standard deviation (STD) are calculated. In terms of net coastal area change (cumulative magnitude/present rate), the mean value and absolute mean value are calculated. Beside statistics of coastline evolution magnitude, the percentage of ports with net erosion/accretion is also included. Statistics of hindcast and forecast indicators for ports with different characteristics are summarized in Table 4-1 and Table 4-2 respectively.

By comparing highlighted cells in these two tables, it can be observed that hindcast and forecast indicators show similar trends of statistics and the only difference happens for the presence of sources/sinks concerning net coastal area change, which is discussed in Section 4.2.4. From the mean value of gross coastal area change, it can be seen that ports with larger longshore wave power, at open coasts, with sources/sinks, with LST interruption structures, constructed more recently, with longer breakwaters have larger magnitudes of coastline evolution. From the mean value of net coastal area change, it can be seen that ports in all sub-categories have net accretion. In most cases, ports with larger gross coastal area change also have larger net accretion, except ports with sources/sinks and ports constructed after 1984. These two exceptions will be discussed in Section 4.2.4 and Section 4.2.6 respectively. The STD has the same order of mean value which means ports under each sub-category are also affected by other characteristics.

By comparing coastline evolution statistics of different sub-categories under each classification criteria, influences of environmental and port characteristics are analysed successively.

Table 4-1 Statistics of gross and net coastal area changes (hindcast indicators) for each subcategory of all African seaports. Cells highlighted with blue indicate largest percentage and mean value of gross coastal area change as well as largest absolute mean value of net coastal area change; cells highlighted with green indicate largest net accretion. Colour bar in last two columns indicate the magnitude of parameters

Characteristics	Percentage of ports	Gross coastal area change (km^2)			Net coastal area change (km^2)		Percentage of ports with net erosion	Percentage of ports with net accretion
		Percentage	Mean	STD	Mean	Abs Mean		
Gross longshore wave power indicator (m^2.5)								
<0.55	36%	10%	0,12	0,14	0,02	0,07	33%	67%
>=0.55	64%	90%	0,59	1,07	0,06	0,28	40%	60%
Natuaral shelter condition								
Open Coast	50%	84%	0,71	1,17	0,08	0,31	46%	54%
Headland-Bay	27%	11%	0,17	0,22	0,01	0,12	18%	82%
Spits/Barrier islands/Estuary	22%	5%	0,09	0,10	0,00	0,05	43%	57%
Presence of Sources/sinks								
Yes	38%	56%	0,62	0,96	0,01	0,31	50%	50%
No	62%	44%	0,30	0,81	0,06	0,14	30%	70%
Presence of Shore protection structures and LST interruotion structures								
No structure	73%	60%	0,35	0,77	0,02	0,16	40%	60%
Shore Protection	9%	3%	0,14	0,18	0,05	0,13	36%	64%
LST Interruption	18%	37%	0,86	1,28	0,11	0,42	30%	70%
Construction date								
Before 1984	61%	46%	0,32	0,59	0,06	0,19	37%	63%
After 1984	39%	54%	0,58	1,19	0,01	0,23	39%	61%
Breakwater length (m)								
<400	17%	4%	0,11	0,14	0,00	0,08	33%	67%
>=400	83%	96%	0,49	0,96	0,05	0,23	38%	62%

Table 4-2 Statistics of gross and net coastal area change rate (forecast indicators) of 2018 for each subcategory of all African seaports

Characteristics	Percentage of ports	Gross coastal area change rate (km^2/yr)			Net coastal area change rate (km^2/yr)		Percentage of ports with net erosion	Percentage of ports with net accretion
		Percentage	Mean	STD	Mean	Abs Mean		
Gross longshore wave power indicator (m^2.5)								
<0.55	36%	15%	0,01	0,01	0,001	0,005	37%	63%
>=0.55	64%	85%	0,02	0,03	0,004	0,010	31%	69%
Natuaral shelter condition								
Open Coast	50%	83%	0,02	0,04	0,004	0,012	38%	62%
Headland-Bay	27%	11%	0,00	0,01	0,003	0,004	23%	77%
Spits/Barrier islands/Estuary	22%	6%	0,00	0,01	0,000	0,003	35%	65%
Presence of Sources/sinks								
Yes	40%	52%	0,02	0,03	0,004	0,010	41%	59%
No	60%	48%	0,01	0,03	0,002	0,007	29%	71%
Presence of Shore protection structures and LST interruotion structures								
No structure	73%	61%	0,01	0,02	0,002	0,006	36%	64%
Shore Protection	9%	4%	0,01	0,01	0,005	0,005	25%	75%
LST Interruption	18%	35%	0,02	0,04	0,006	0,015	27%	73%
Construction date								
Before 1984	62%	44%	0,01	0,02	0,004	0,006	29%	71%
After 1984	38%	56%	0,02	0,03	0,002	0,011	40%	60%
Breakwater length (m)								
<400	17%	4%	0,00	0,00	0,001	0,003	39%	61%
>=400	83%	96%	0,01	0,03	0,003	0,009	32%	68%

4.2.2   Influence of gross longshore wave power

Longshore wave power is used as an indicator for longshore sediment transport, which is the parameter that directly affects coastline evolution. However, since offshore wave data used in this research is less applicable to sheltered coasts, the calculated longshore wave power is more valid for open coasts. Therefore, the relationship between gross longshore wave power and coastline evolution trends is only analysed for African seaports at open coasts. As longshore wave power indicator, $H_s^{2.5} sin2\alpha$ is plotted against present erosion and accretion rates. Results are shown in Figure 4-4.

Firstly, it can be seen that most ports with $H_s^{2.5} sin2\alpha < 0.55\ m^{2.5}$ do not have significant coastline evolution around them. It happens for both present coastal area erosion and accretion rates. Secondly, for ports with large wave power indicator say $H_s^{2.5} sin2\alpha \geq 0.55\ m^{2.5}$, it is still possible to have small erosion and accretion rates around them. This is because that LST is determined not only by wave power, but also by sediment properties such as grain size. Additionally, sediment availability also affects the magnitude of coastline evolutions. Due to limited sediment supply from rivers, most African seaports are located on Afro-trailing coasts with narrow beach and low evolution potential. Thirdly, although larger wave energy does not always correspond to large coastline evolution magnitude, it can be seen that as gross longshore wave power increases, coasts have probability to achieve larger evolution rates. In other words, gross longshore wave power determines up limits of coastline evolution rates around ports. Finally, for ports with large longshore wave power indicator ($H_s^{2.5} sin2\alpha \geq 0.55\ m^{2.5}$), mean coastal area erosion rates of those with sources/sinks are larger than those without sources/sinks. This suggests that, if large longshore wave power is coupled with large amount of sediment supply or loss, coastline evolution can be more prominent.

In conclusion, there is a threshold of longshore wave power indicator for prominent coastline evolution trends, which is $H_s^{2.5} sin2\alpha = 0.55\ m^{2.5}$ for coasts around African seaports. This threshold classifies African seaports into two groups in Table 4-1 and Table 4-2. Although affected by other factors, longshore wave power has a positive influence on coastline evolution trends around ports.
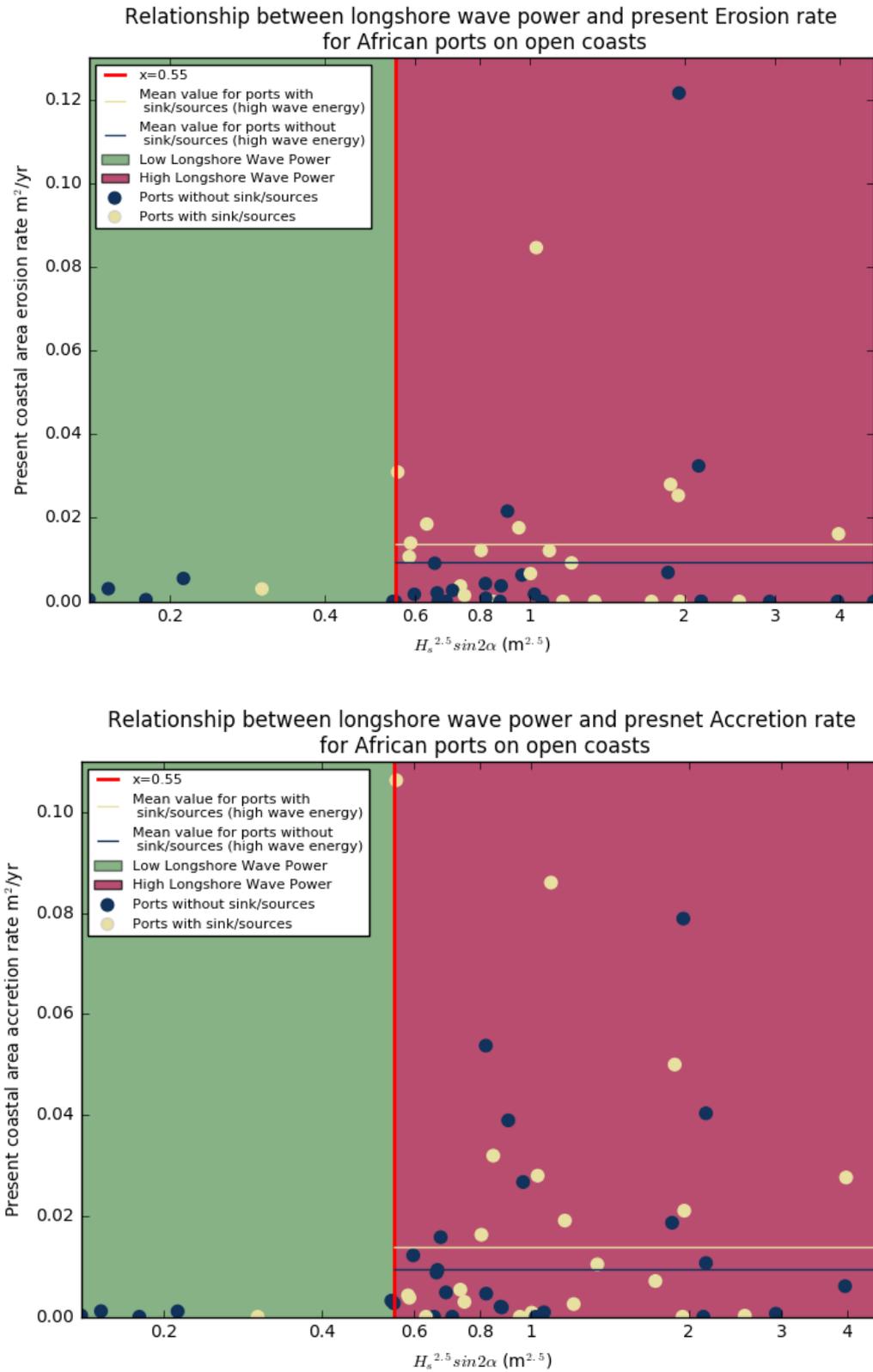
Figure 4-4 Influence of longshore wave power on the present coastal area erosion (top) and accretion (bottom) rate

4.2.3   Influence of natural shelter condition

From Table 4-1 and Table 4-2, it can be seen that hindcast and forecast indicators show the same trend for the influence of natural shelter conditions. Firstly, ports at open coasts, which are directly exposed to waves, has the largest magnitude of coastline evolution regarding both gross and net coastal area change, while ports with the highest level of sheltering have the least coastline evolution magnitude. Secondly, ports between headlands although not with the highest level of sheltering, have the smallest portion of net erosion. This is because most ports between headlands have narrow sandy beaches with rocky substratum, which limits the capability of coast erosion. Thirdly, although some ports are sheltered by spit/barrier islands, they are still possible to have dynamic coasts around them. This indicates that these barriers can shelter ports from direct wave impact, but not able to prevent coastline evolution completely.

4.2.4   Influence of sediment sources and sinks

Both Table 4-1 and Table 4-2 show that ports with sources and sinks have larger magnitude of coastline evolution regarding gross coastal area change, which indicates that besides longshore sediment transport, the existence of source/sink is another potential cause to coastal morphological change around ports. However, in terms of net coastal area change, the smaller mean value and the larger portion of ports with net erosion in Table 4-1 show that the presence of rivers actually contributes to more erosion than accretion. This can be explained by the following reason. Historically, sediment supply from rivers results in a wide beach, which is more erodible than other Afro-trailing coasts. Furthermore, the coastline evolution trend is not affected by the absolute magnitude of sediment supply from rivers, instead, the temporal change of sediment supply is more critical. Since river damming is common in Africa, most rivers have decreasing sediment supply and correspondingly coastline around them is retreating.

Regarding forecast indicators in Table 4-2, although ports with sinks/sources still have larger portion of net erosion, the mean value of net accretion is larger than that for ports without sinks/sources, which is different from hindcast indicators. This difference suggests that coastal area change around rivers and inlets is gradually changing from erosion dominated to accretion dominated since the mean value of the present accretion rate is larger than erosion rate. This trend towards accretion can be due to the awareness of negative effects of river damming and implementation of methods to maintain or increase river sediment supply.

4.2.5   Influence of human intervention

Hindcast indicators in Table 4-1 and forecast indicators in Table 4-2 show the same trend of human intervention influence. Firstly, based on the larger magnitudes and portions of net accretion, both shore protection structures and LST interruption structures are found to stimulate local accretion. However, for LST interruption structure, the mean value of gross coastline area change also increases significantly, indicating that these artificial structures also cause additional erosion. Shore protection structures, on the other hand, increase net accretion, although with smaller magnitude, without inducing extra coastal area erosion. This does not mean erosion problem is completely mitigated by shore protection structures since they are possible to move coastal erosion risks to down-drift regions out of AOI. Additionally, although these structures seem to be reliable within the monitoring period, the interruption of sediment supply from coasts can lead to the development of scour at the feet of structures, which will undermine the reliability of these shore protections in the future.

4.2.6   Influence of construction date

Hindcast indicators in Table 4-1 and forecast indicators in Table 4-2 show the same influence of construction date. In terms of gross coastal area change, ports constructed after 1984 have larger mean value than those constructed before 1984. This is due to that coastline evolution show equilibrium trends within 30 years and correspondingly, the coastline evolution rate for ports constructed before 1984 is smaller than those constructed more recently. Additionally, a significant portion of ports constructed after but close to 1984, making the difference in evolution duration less prominent.

However, in terms of net coastal area change, net accretion is more prominent for ports constructed before 1984, which is contrary to the trend for gross coastal area change. The reason can be that for most African seaports, down-drift erosion slows down or even stops as it approaches the rocky substratum. As this process takes time, ports constructed before 1984 are more possible to have such limitation for down-drift erosion and hence have larger magnitude of net accretion.

4.2.7   Influence of breakwater length

Theoretically, a longer breakwater is able to block larger quantity of LST and induces more significant coastline evolution. In this section, evidence based data of African seaports are used to judge this argument. In this section, ports with the potential of coastline evolution are focused and only ports on dynamic coasts are scoped in research. Relationships between breakwater length and present coastal area erosion and accretion rates are shown in Figure 4-5.

Firstly, no matter how long the breakwater is, there is significant number of ports having coastlines with limited evolution rates, which indicates that a long breakwater does not always lead to significant coastline evolution. Secondly, trend line for ports on both open and sheltered coasts show that breakwater has positive effect on both accretion and erosion rates. Thirdly, different slopes of trend lines for open coasts and sheltered coasts suggest that influence of breakwaters is more prominent for open coasts. However, it is worth to notice that long breakwaters can also be results of adjustment to high siltation potential. This can be another explanation for why long breakwater corresponds to high siltation risk.

From Figure 4-5, it can also be seen that coastline evolution starts to become significant as the port breakwater length becomes larger than 400m, which is then selected as the threshold for the classification in Table 4-1 and Table 4-2.
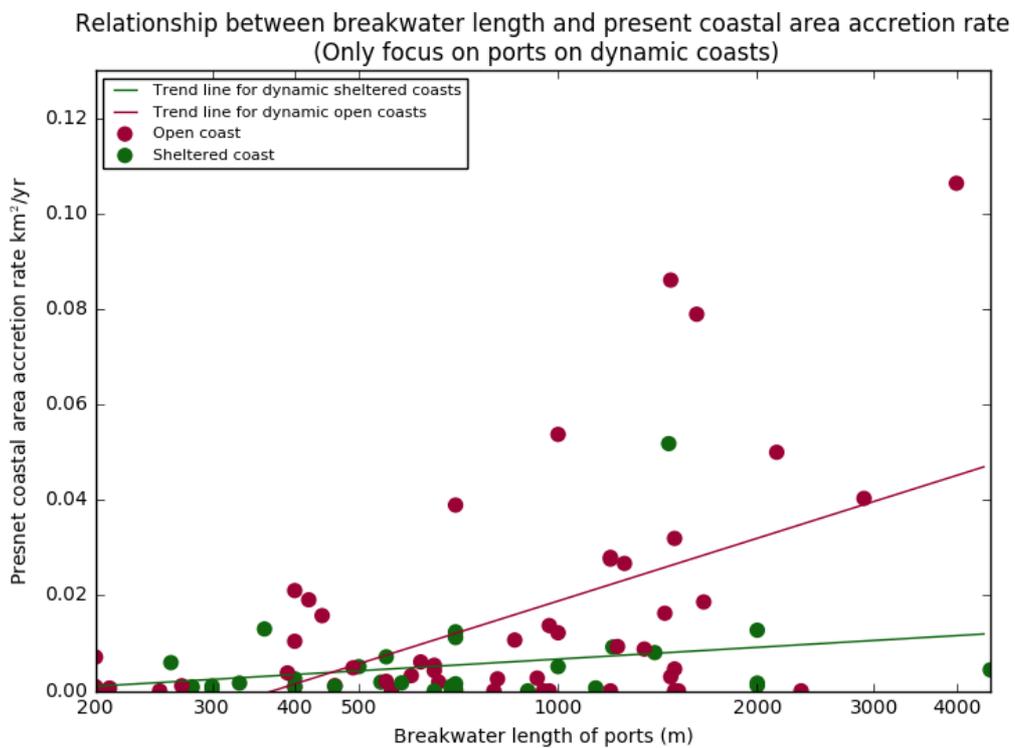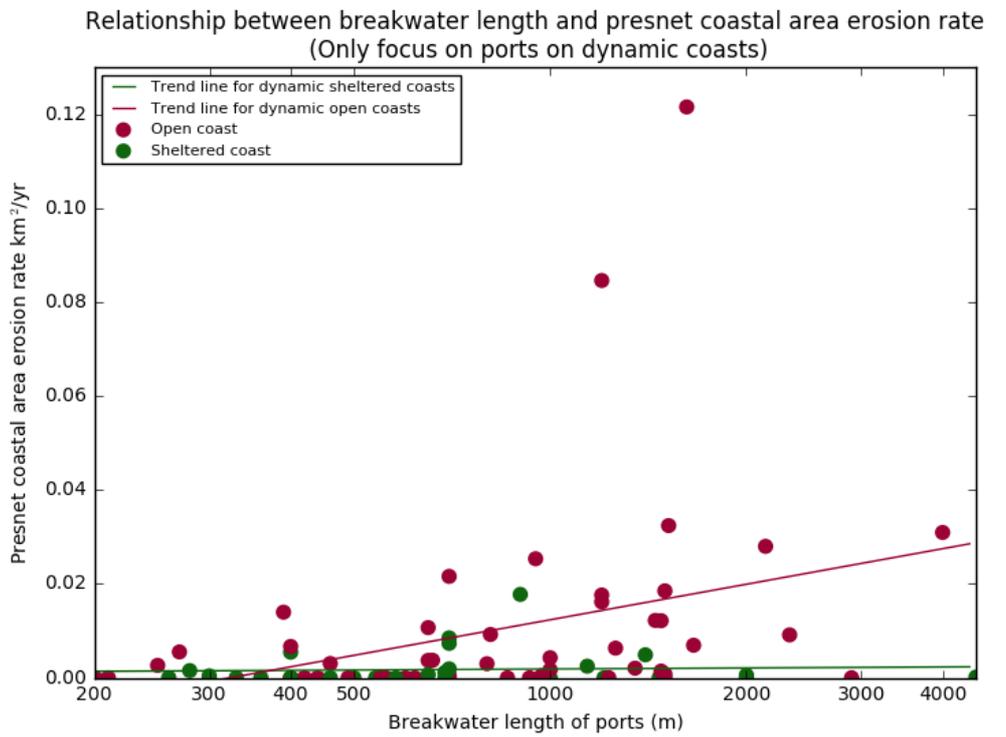
Figure 4-5 Influence of breakwater length on present coastal area erosion (top) and accretion (down) rate

4.2.8   Conclusion

By relating coastline evolution trends of existing African seaports to their environmental and port characteristics, it is found that ports at open coasts with $H_s^{2.5} sin2\alpha \geq 0.55 \ m^{2.5}$ have larger magnitude of coastline evolution especially coastal area accretion. Presence of rivers and/or inlets around ports also contributes to larger magnitude of coastline evolution. However, due to human activities such as river damming, the increase in coastal area erosion is more common than accretion for ports around river and inlets. In terms of ports construction date, ports constructed after 1984 have larger mean value for both hindcast and forecast indicators of gross coastal area change. On the other hand, net accretion is more significant for ports constructed before 1984, which is due to that down-drift erosion of these ports is more likely to reach and limited by rocky substratum after a longer period of development. In terms of human interventions, shore protection structures are able to mitigate coastal area erosion efficiently in 30 years temporal scale. LST interruption structures are useful to stimulate local accretion, but it is found to increase erosion at the mean time. As a quantifiable parameter, breakwater length correlates to coastline evolution rates positively, which is more apparent for ports at open coasts.

4.3   Identification and analysis of ports with prominent erosion/siltation hazards

In previous sections, coastline evolution indicators are analysed from the continental perspective, however, as it is shown in Section 4.1.1, extreme cases are also helpful to reflect significance of coastline evolution. Hence, in this Section, hotspots of African seaports with respect to erosion/siltation hazards are identified and common characteristics of these extreme cases are analysed.

4.3.1   Common characteristics of all identified ports

In this section, two hindcast indicators including cumulative erosion area and relative shoreline position to breakwater length are used to identify ports with significant erosion and/or siltation history. Two forecast indicators including present coastal area erosion rate and present shoreline advance rate are used to identify ports with high erosion and/or siltation potentials in the future.

Rankings of African seaports based on hindcast and forecast indicators are shown in Figure 4-6 and Figure 4-7 respectively. 27 African ports are identified with high erosion/siltation hazards. From Figure 4-6, it can be found that ports with significant erosion problems (rank top 10%) have larger port city size in general which indicates the conflict between coastal area erosion and population growth. In terms of environmental characteristics, it can be found that most identified ports have sources and/or sinks around them and have $H_s^{2.5} sin2\alpha \geq 0.55 \ m^{2.5}$. This corresponds to the findings from the continental perspective. Due to trends to achieve equilibrium, some ports are found to have different positions in rankings of erosion history and erosion potential. For example, Port of Cotonou appears to have more prominent erosion history although with less prominent erosion potentials.

To understand this difference, hindcast and forecast indicators for erosion are plotted against each other in Figure 4-8. It can be seen that although for some cases, coastal area erosion rate decreases within 34 years, there are still a significant number of ports, such as port of Nouakchott, having experienced significant coastal area erosion problems without any signals of mitigation in the future. In terms of ports showing equilibrium trends, the mean longshore wave power indicator for ports with equilibrium is larger than those without such

trend. This suggests that after ports construction, coasts with larger longshore wave power not only evolves faster but also more likely to achieve new equilibrium than those with smaller longshore wave power.
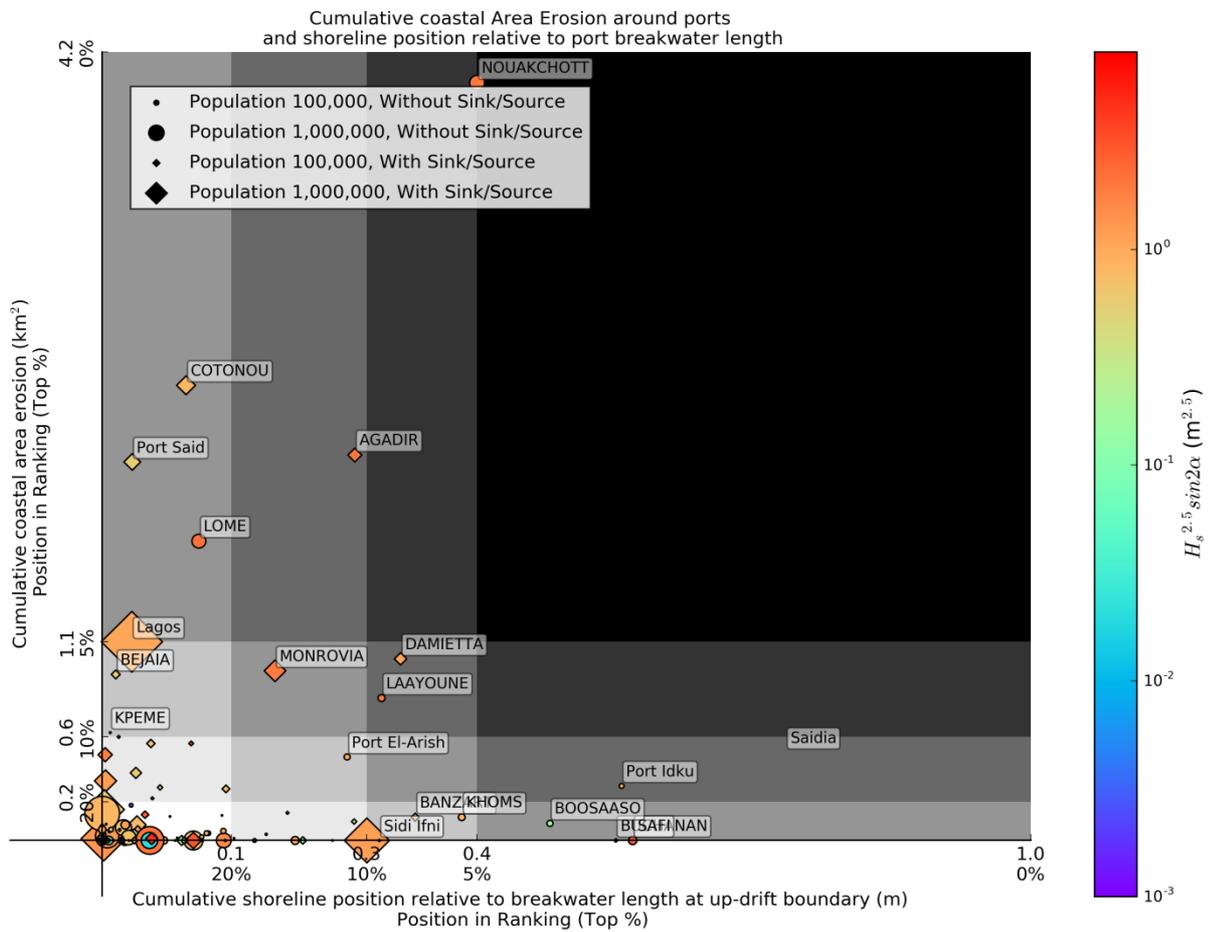

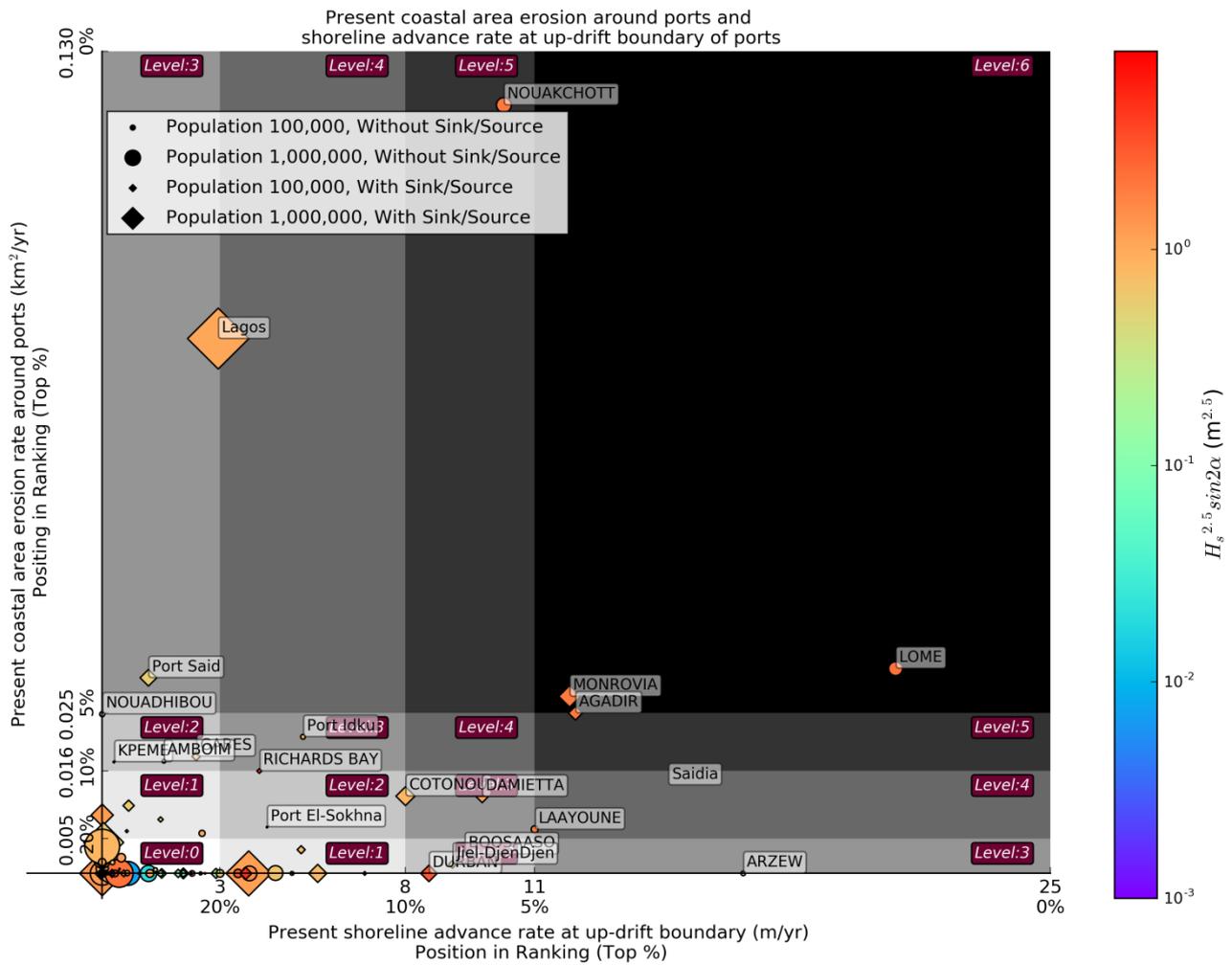*Figure 4-6 African seaports with prominent erosion and/or siltation history*

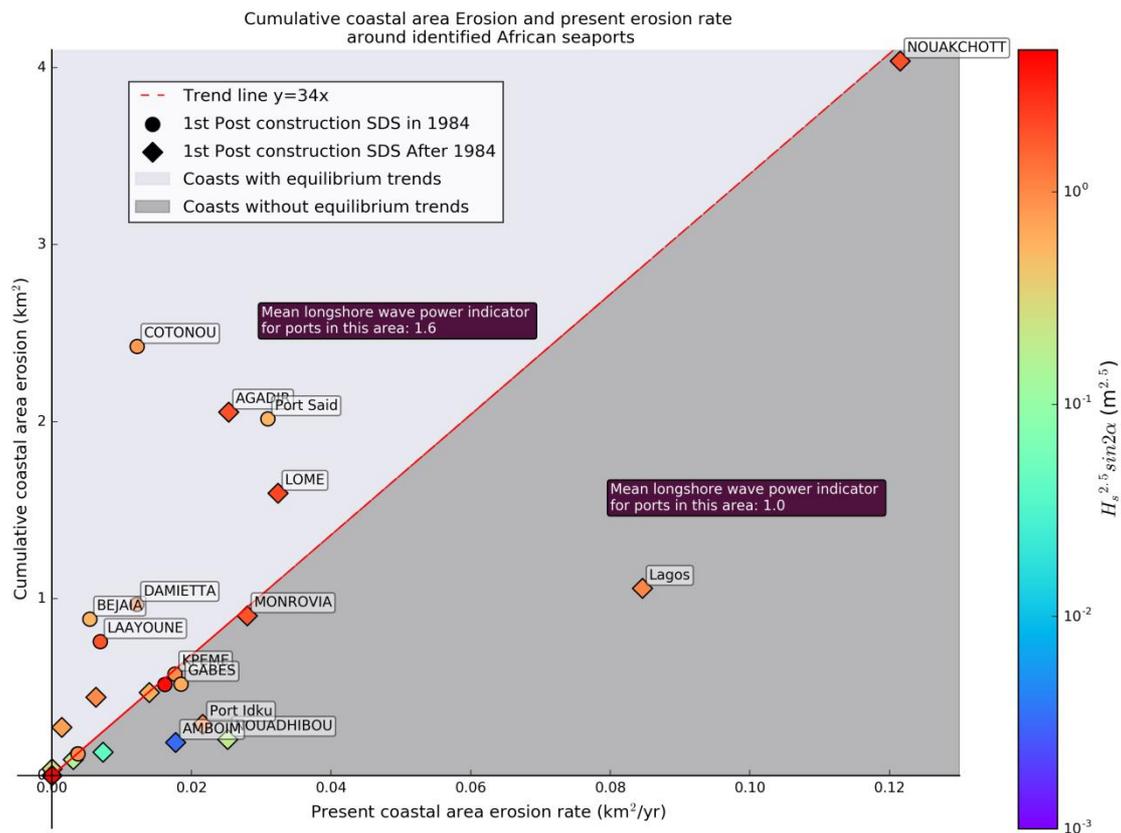*Figure 4-7 African seaports with prominent erosion and siltation risks in the future*

Figure 4-8 Relationship between coastal area erosion history and erosion potential of African port. If 1st post construction SDS of a port is in 1984 and its coastal area erosion follows a linear trend, this port will lie on the red dash line

Statistics of gross and net coastal area change (hindcast) for each subcategory of identified African seaports are summarized in Table 4-3. In terms of the mean value of gross coastal area change, the results found for all African ports are also applicable to these identified extreme cases. However, in terms of net coastal area change, since these extreme cases are mostly located at sediment-rich coasts, down-drift erosion is not limited by rocky substratum and net erosion becomes more common due to sediment deposition in harbour channels and basins. In most cases, ports with massive gross coastal area change also have a larger magnitude of net erosion, except ports at head-bay system, ports without shore protection structures and ports with small short breakwater. For the first exception, ports at a headland-bay system with significant coastline evolution always have rivers around them. The net erosion at down-drift side, in most cases, are not determined by ports but by river damming. For the second exception, both shore protection and LST interruption structures tend to stimulate local accretion and this is the reason for the smaller magnitude of net erosion. For the third exception, similar to the ports at headland-bay system, significant coastline evolution around ports with short breakwater is also not determined by port construction. Hence it is insufficient to make judgements about breakwater length and net coastal area change.

Table 4-3 Statistics of gross and net coastal area change (hindcast indicators) for each subcategory of identified African seaport. Cells highlighted with blue indicate largest percentage and mean value of gross coastal area change as well as largest absolute mean value of net coastal area change; cells highlighted with red indicate largest net erosion. Colour bar in last two columns indicate the magnitude of parameters

Characteristics	Percentage of ports	Gross coastal area change (km^2)			Net coastal area change (km^2)		Percentage of ports with net erosion	Percentage of ports with net accretion
		Percentage	Mean	STD	Mean	Abs Mean		
Gross longshore wave power indicator (m^2.5)								
<0.55	22%	5%	0,35	0,15	-0,05	0,25	67%	33%
>=0.55	78%	95%	1,73	1,70	-0,12	0,62	43%	57%
Natuaral shelter condition								
Open Coast	81%	94%	1,65	1,70	-0,10	0,58	41%	59%
Headland-Bay	11%	5%	0,58	0,32	-0,16	0,50	67%	33%
Spits/Barrier islands/Estuary	7%	1%	0,24	0,03	-0,10	0,10	100%	0%
Presence of Sources/sinks								
Yes	52%	62%	1,69	1,45	-0,13	0,71	57%	43%
No	48%	38%	1,14	1,71	-0,08	0,35	38%	62%
Presence of Shore protection structures and LST interruotion structures								
No structure	74%	56%	1,08	1,41	-0,11	0,41	45%	55%
Shore Protection	0%	0%	0,00	0,00	0,00	0,00	0%	0%
LST Interruption	26%	44%	2,42	1,72	-0,08	0,90	57%	43%
Construction date								
Before 1984	44%	50%	1,60	1,60	0,12	0,59	33%	67%
After 1984	56%	50%	1,29	1,60	-0,29	0,49	60%	40%
Breakwater length (m)								
<400	7%	1%	0,28	0,26	-0,19	0,21	50%	50%
>=400	93%	99%	1,52	1,63	-0,10	0,56	48%	52%

4.3.2   Common characteristics of identified ports in different regions

In this section, based on the distribution of ports with high erosion/siltation hazards (Figure 4-9), sensitive African regions to coastline evolution are identified. The common characteristics of seaports in each region are analysed respectively.
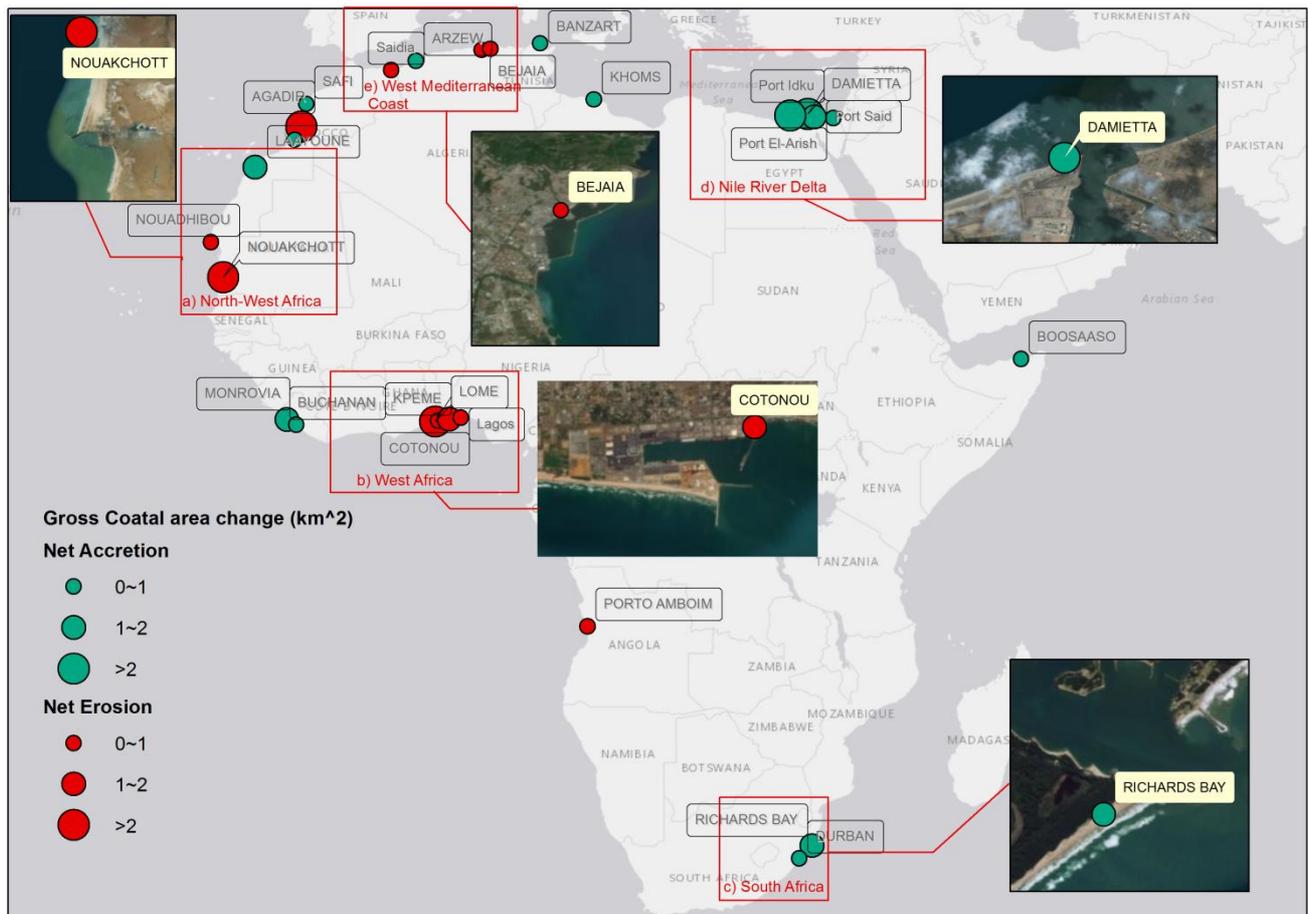
Figure 4-9 Distribution of ports with high siltation/erosion hazards

It can be seen that existing seaports with high erosion/siltation hazards are concentrated on five regions, which are North West Africa, West Africa, East coast of South Africa, Nile River Delta and West Mediterranean Sea.

<u>*a) North West African coast*</u>

This region includes coasts of Morocco, Western Sahara and Mauritania. Coasts in this region have abundant sand and wide sandy beach, although without massive river sediment supply. An example of Nouakchott coast is shown in Figure 4-9. Characteristics of coasts around these ports are shown in Table 4-4. This sedimentary condition makes the beach more erodible, once waves happen to be high and unidirectional, significant amount of sediment will be moved and transported alongshore. The magnitude of net LST on Nouakchott coast is about 1,000,000 m^3/yr (Schoonees, 2000). LST interruption structure has been constructed to mitigate down-drift erosion problem, but the effect is limited and the present coastal area erosion rate remains large (Figure 4-8).

Port of Nouadhibou, although is sheltered by spit, still has coastline evolution around it. This coastline evolution is because the spit itself is evolving even without the port construction which is shown in Figure 4-10. This coastline evolution is not attached but approaching to the boundary of the port, which is a potential problem for ports operation in the future. Hence for ports construction in this region, coastline evolution history of the proposed site should be understood beforehand.

Table 4-4 Characteristics of coasts around identified ports in North West Africa

Name	Region	Country	River/Inlets	Natural shelter	Human intervention	Port-affected evolution*
NOUAKCHOTT	North West Africa	Mauritania	No	Open coast	LST interruption down-drift	Yes
NOUADHIBOU	North West Africa	Mauritania	No	Spit	No	No
LAAYOUNE	North West Africa	Morocco	No	Open coast	No	Yes

* Whether coastline evolution is directly affected by ports or not is indicated by the position of coastline evolution. If coastline evolution is connected to ports boundary, then it is classified as ports induced evolution.

Figure 4-10 Satellite image of coast around Port of Nouadhibou.The white line is the SDS acquired on 1984-06-02 and the blue line is SDS acquired in 2017-12-22.

b) West African coast

This region includes coasts of Côte d'Ivoire, Ghana, Togo, Benin and west coast of Nigeria. Port of Lome, Kpeme, Cotonou and Lagos are located in this region. Characteristics of these ports are shown in Table 4-5.

The magnitude of LST in this region is estimated to be approximately 500,000 m³/yr (Giardino et al., 2017), which is smaller than what is found in Nouakchott. However, coast of this region is interrupted by several rivers and inlets. An example of Cotonou coast is shown in Figure 4-9. Different from ports on North West African coast, besides LST, change of river sediment supply also contributes to coastline evolution (Giardino et al., 2017). Due to river damming, coast of this area is retreating in most sections and construction of ports accelerates down-drift erosion. LST interruption structures in the down-drift are constructed for most of ports in this area, however, except port of Cotonou and Lome, where coastal area erosion rate seems to decrease

with exponential trend (Figure 4-8), erosion problem for other ports have no signal of mitigation. All ports in this region have net erosion.

Table 4-5 Characteristics of coasts around identified ports in West Africa

Name	Region	Country	River/Inlets	Natural shelter	Human intervention	Port-affected evolution*
LOME	West Africa	Togo	No	Open coast	No	Yes
KPEME	West Africa	Togo	No	Open coast	LST interruption down-drift	Yes
COTONOU	West Africa	Benin	At River	Open coast	LST interruption down-drift	Yes
LAGOS	West Africa	Nigeria	At Inlet	Open coast	LST interruption down-drift	Yes

* Whether coastline evolution is directly affected by ports or not is indicated by the position of coastline evolution. If coastline evolution is connected to ports boundary, then it is classified as ports induced evolution.

c) *East coast of South Africa*

In this region, large wave energy is coupled with large tidal influence and creates several tidal inlets, resulting in a large quantity of LST and dynamic coasts. The net LST is estimated to be 500,000 m^3/yr for Port of Durban and 850,000 m^3/yr for Port of Richards Bay (Schoonees, 2000). Although the LST in this region has the same order as West Africa and North-West Africa, the magnitude of coastline evolution is less significant. The reason is that ports in this region including Port of Richards Bay, Durban, East London and Ngqura all have by-pass systems in the form of maintenance dredging or embedded jet pumping (Boswood and Murray, 2001). Due to the implementation of by-pass systems, erosion and siltation hazards around Port of Ngqura and East London are successfully mitigated. Port of Durban also has stable coasts before widening the harbour channel in 2009. Although sediment starts to accrete at up-drift boundary after the channel extension, no significant erosion is found in the down-drift. All these evidences indicate the positive effect of the by-pass system on mitigating erosion and siltation hazards.

In terms of Port of Richards Bay, despite diligent efforts to supply sand to the down-drift beaches, an enormous deficit in sand supply has resulted in 6 million m^3 erosion in the down-drift (Rossouw and Theron, 2009). The existence of inlet in the up-drift can explain the deficiency of by-pass system for this port. Due to the large tidal range in this region, this inlet increases the quantity of trapped sediment in the up-drift dramatically. Hence for ports constructed in this region, wave force is important but not the only consideration for morphological change; the existence of tidal inlets can make coastline evolution more significant than expected.

Table 4-6 Characteristics of coasts around identified ports in East coast of South Africa

Name	Region	Country	River/Inlets	Natural shelter	Human intervention	Port-affected evolution*
RICHARDS BAY	East coast of South Africa	South Africa	At Inlet and inlet up-drift	Open coast	Maintenance dredging of trap	Yes
DURBAN	East coast of South Africa	South Africa	At Inlet	Open coast	LST interruption down-drift; Embedded jet pump system	Yes

* Whether coastline evolution is directly affected by ports or not is indicated by the position of coastline evolution. If coastline evolution is connected to ports boundary, then it is classified as ports induced evolution.

d) <u>Nile River Delta</u>

Port of Idku, Said, Damietta and El-Arish in this region are all found to cause severe coastline evolution, which is also reported in (Bruun, 1995). Historically, due to the sediment supply from Nile River and its branches, coast in this region have wide sandy beaches, which makes massive LST possible. In this region, even ports with short breakwaters such as Idku and ports with long history such as Said are confronted with high siltation/erosion risks. Coasts around these ports have net accretion because a large quantity of artificial structures is constructed to stimulate accretion. For coasts out of AOI and not covered by shore protections and groynes, significant coastal area erosion is found in Luijendijk et al. (2018).

Table 4-7 Characteristics of coasts around identified ports in Nile River Delta

Name	Region	Country	River/Inlets	Breakwater length (m)	Human intervention	Port-affected evolution*
DAMIETTA	Nile River Delta	Egypt	River in down-drift	1480 m	LST interruption downstream	Yes
PORT EL-ARISH	Nile River Delta	Egypt	No	1260 m	LST interruption on both sides	Yes
PORT SAID	Nile River Delta	Egypt	At river mouth	4000 m	LST interruption upstream	Yes
PORT IDKU	Nile River Delta	Egypt	River in down-drift	700 m	No	Yes

* Whether coastline evolution is directly affected by ports or not is indicated by the position of coastline evolution. If coastline evolution is connected to ports boundary, then it is classified as ports induced evolution.

e) West Mediterranean coast

Considering a large number of ports in this region, the ratio of ports with high erosion/siltation hazards is smaller than the other four regions. This region is mentioned here because it shows that ports on rocky substratum, if have sediment source around them, are still able to cause severe coastline evolution. Another lesson can be derived from Table 4-8 is that, since river sediment supply is a precondition for coastline evolution in this region, the relative position of river and port becomes important. For ports constructed in up-drift of river, the sediment redistribution around river mouth is not interrupted by port structure. In this case, morphological change is not connected to the port, which indicates influence of port on coastline evolution is less important than river. Port of Bejaia in Figure 4-11 is an example for this case. However, if port structure is located in the down-drift of river mouth, the sediment from river is blocked by and deposited at up-drift breakwater. Correspondingly, less sediment from river is able to achieve down-drift and the beach in down-drift, if there is any, is eroded. Hence, to reduce potential coastline evolution, ports can be constructed in the up-drift of river. This lesson is also applicable to North West coast of Morocco, where ports have similar characteristics as ports in Table 4-8.

Table 4-8 Characteristics of coasts around identified ports in East coast of South Africa

Name	Region	Country	River/Inlets	Natural Shelter	Human intervention	Port-affected evolution*
SAIDIA	West Mediterranean	Morocco	River in up-drift	Open coast	No	Yes
BEJAIA	West Mediterranean	Algeria	River in down-drift	Headland	LST interruption down-drift	No
ARZEW	West Mediterranean	Algeria	River in up-drift	Headland	No	Yes
JIEL-DJENDJEN	West Mediterranean	Algeria	River on both sides	Headland	No	Yes

* Whether coastline evolution is directly affected by ports or not is indicated by the position of coastline evolution. If coastline evolution is connected to ports boundary, then it is classified as ports induced evolution.

Figure 4-11 Satellite image around Port of Bejaia. While line is SDS acquired on 2004-07-30, when the last extension of port finished. Blue line is SDS acquired in SDS acquired on 2017-12-26

4.3.3   Conclusion

27 ports are identified to have prominent erosion and/or siltation hazards, which rank either top 10% for erosion indicators or top 10% for siltation indicators. Some of these high-hazard ports also have large port city population, resulting in larger coastline erosion impacts. Amongst these ports, those with large longshore wave power are more likely to show equilibrium trends, but the majority of them have erosion rates that are currently still high. In terms of statistics of hindcast indicators, net coastal area erosion becomes more common for these identified ports. The reason is that most ports with significant erosion/siltation hazards are located in sediment-rich regions with less restriction of rocky substratum on down-drift erosion.

These identified hotspots of African seaports are found to mainly distribute in five regions, which are North West Africa, West Africa, East coast of South Africa, Nile River Delta and West Mediterranean Sea. Coast of West Africa is very sandy with large wave energy. It can be dynamic even without port structures. Port developments in this region should not only focus on potential ports influence but also natural coastline evolution history of the coastline itself. West African coastlines tend to retreat due to river damming and existing ports construction. All ports on the East coast of South Africa have by-pass systems which are proved efficient to mitigate coastline evolution around most ports. The deficiency of by-pass in Richards Bay is due to the existence of a sink in the up-drift. In the region of Nile River Delta, sediment supply from Nile River and its branches make the coast very sandy. Ports construction history suggests that coastline in this region is very sensitive to artificial structures. Although net coastal area accretion is found for all ports in this region due to widely distributed artificial structures, coastal area erosion is reported for coasts distant from ports which are less maintained by human. Ports on the West Mediterranean coast are located on the rocky substratum. However, due to the existence of sediment supply from rivers, coastline evolution is still expected. To reduce the influence on coastal morphological change, ports should be constructed in the up-drift of rivers.

4.4   Lessons for port development
4.4.1   Site selection

Firstly, in terms of shelter condition, it should be avoided to construct ports on open coasts. These ports are directly exposed to waves, leading to larger LST than sheltered coasts with the same offshore wave condition. Additionally, to protect harbours from wave influence, longer breakwaters are always required for ports on open coasts, which then block more LST. Therefore, according to both theories and evidence, ports at open coast should be more carefully designed. However, this does not mean ports on sheltered coasts are always safe in terms of coastline evolution. Evidence shows that there is still a portion of ports behind spits and barrier islands experiencing severe coastline evolution around them, although some of these trends are not due to ports construction.

Secondly, in general, ports around rivers/inlets are more likely to have dynamic especially retreating coasts around them. River mouth and tidal inlet themselves are able to interrupt LST and result in coastline evolution, while construction of ports amplifies these trends by disturbing sediment redistribution around river or inlets. Constructing ports away from river/inlets is helpful to reduce erosion/siltation hazards, but in terms of ports function, rivers and estuaries are preferred because they are important nodes to connect inland and coastal area. Hence influence of rivers/inlets cannot be avoided entirely. For a port which is close but not located at a river mouth or inlet, to reduce ports influence on sediment redistribution, it can be constructed in up-drift instead of down-drift of river mouth/inlet. Additionally, since river damming is an important contribution to coastal area eroding, methods to maintain or increase river sediment supply should be coupled with shoreline management plan.

Thirdly, since waves are the most significant environmental force for coastline evolution, construction site of ports should be carefully selected to reduce wave influence on LST and coastline evolution. This evidence database suggests a threshold of 0.55 $m^{2.5}$ for $H_s^{2.5}sin2\alpha$ to justify whether wave climate is able to cause significant morphological change. For the African coast, sites with $H_s^{2.5}sin2\alpha < 0.55\ m^{2.5}$ are more suitable for ports construction with respect to coastline evolution.

4.4.2   Mitigation methods for negative coastline evolution impacts

Firstly, this evidence database validates the influence of breakwater on coastline evolution that the more extended breakwater corresponds to the higher coastline evolution rate. This trend suggests that the extension of breakwater is not the final solution for mitigating harbour siltation problem since it can accelerate the coastline evolution rate at the same time. To mitigate siltation/erosion problems, sediment by-pass systems, which have been proved successful in South Africa, should be considered.

Secondly, longshore sediment transport (LST) interruption structure increases erosion magnitude as it stimulates local accretion, which corresponds to the theory of sediment balance. Shore protection structures are found to reduce coastal area erosion significantly within the monitoring temporal (34 years) and spatial (30km) scales. However, their effects in larger scales are still doubtable since the sediment deficiency in the down-drift is still unsolved.

5

Discussion

This chapter reflects the results presented in previous chapters, establishing a link with results found in the literature. Additionally, influences of the exclusion of ESA Sentinel 2 and the limitation of the spatial research scale are discussed, followed by an introduction to other limitations. Finally, the significance of this research is presented.

5.1   Verification of the detected coastline evolution results with respect to literature

SDS detection has been validated for Sand Engine (The Netherlands), Long Beach, WA (West Coast, USA), Narrabeen (Australia) and Hatteras Island (East Coast, USA) by Hagenaars et al. (2018) and Luijendijk et al. (2018) with in-situ data, however, this validation is based on shoreline positions at shore-normal transects and different SDS detection parameters from this research are used. To understand the accuracy of SDS detection and spatial aggregation, especially coastal area change calculation in this research, erosion and accretion area obtained from this research are validated. Due to the lack of ground truth data in Africa, this validation is conducted with respect to previous research.

Wu (2007) used accretion/erosion area to analyse coastline evolution around Port of Nouakchott, results of which are applied to validate spatial aggregation methods in this thesis. In his research, four Satellite pour l'Observation de la Terre (SPOT) images acquired in 1989, 1995, 1999 and 2001 are used to calculate up-drift accretion and down-drift erosion in different periods. After selecting satellite images with similar date and defining the same research scale, accretion and erosion area are then calculated with spatial aggregation method used in this thesis. Comparison of research conditions is shown in Table 5-1 and comparison of results is shown in Table 5-2. It can be seen that results from this thesis, which are based on Landsat 5 images, are close to the results from Wu (2007). Difference between these two research is within detection error identified in Wu (2007).

Table 5-1 Research conditions of this thesis and Wu (2007)

	Up-drift distance(km)	Down-drift distance (km)	Satellite mission	Date of 1st Image	Date of 2nd Image	Date of 3rd Image	Date of 4th Image
Wu (2007)	3	6	SPOT	1989-11-03	1995-02-04	1999-11-11	2001-01-22
This thesis	3	6	Landsat 5	1989-12-02	1994-04-04	1999-10-03	2001-01-09

Table 5-2 Erosion and accretion area around Port of Nouakchott from this thesis and Wu (2007)

		1989~1995	1995~1999	1999~2001	Total	Error*
Up-drift Accretion(km^2)	Wu (2007)	0.411	0.334	0.170	0.916	
	This thesis	0.431	0.316	0.154	0.901	0.023
	Difference	0.02	0.018	0.016	0.015	
Down-drift Erosion(km^2)	Wu (2007)	0.632	0.639	0.067	1.338	
	This thesis	0.651	0.613	0.094	1.358	0.041
	Difference	0.021	0.026	0.027	0.02	

* The error represents the possible difference between the detected results and true changes and estimated based on the geometric correction RMS error (Wu, 2007)

5.2   Comparison of coastline evolution statistics with literature

The average shoreline change rate is estimated to be -0.07m/yr for the entire African coast (Luijendijk et al., 2018), while the average shoreline change rate around African seaports is estimated to be +0.03m/yr, based on 3 km^2 net accretion, 2600km coastline length and 34 years monitoring found in this research. This suggests that compared with other African coasts, coasts around seaports tend to have more net accretion area.

In an ideal case where only the gradient of LST determines coastline evolution, if port breakwater completely blocks LST, up-drift accretion equals to down-drift erosion due to the balance of mass (Bosboom and Stive, 2015). If LST cannot be completely blocked, a portion of sediment will deposit in port channels and basins, resulting in more down-drift erosion than up-drift accretion. This shows a different conclusion from the results found in this research. The following physical and technical reasons can expalin this difference.

Physical reasons

Firstly, a significant portion of ports is constructed around coasts of Algeria, Morocco, Angola and South Africa with narrow beach and rocky substratum, which limit the potential of down-drift erosion and lead to net accretion. Secondly, coasts around seaports are focused in this research, which are also coasts around cities with larger population and higher flood risks. Hence more activities to protect the shoreline, such as nourishment and construction of shore protection and LST interruption structures, happen at these coasts. These human interventions tend to increase net accretion locally, although they can cause net erosion at coasts out of AOI.

Technical reasons

LST interruption structures, which are more frequently constructed for coasts around seaports and port cities, increase local accretion also due to a technical reason. These structures, if constructed or extended after the start of monitoring, are counted as land when performing SDS detection. Since all of these structures are extended to the sea, additional area is added to net accretion. In the future research, to avoid this uncertainty, artificial structures can be scoped out from the AOI by reshaping the boundary of the polygon.

Due to the above physical and technical reasons, although more net coastal area accretion is found around African seaports, it does not mean that construction of ports will cause more coastal area accretion than erosion. In fact, among 27 identified ports, where sediment availability does not limit coastline evolution, the net coastal area is more common, which corresponds to the knowledge of coastal engineering.

5.3   The sensitivity of coastline stability with respect to threshold selection

In this thesis, part of the analysis is based on the classification of ports with respect to coastline stability. Hence thresholds for this classification are essential. In this research, the threshold for shoreline advance rate is defined following Luijendijk et al. (2018) as:

$$Threshold\ for\ shoreline\ advance\ rate = \frac{Mean\ SDS\ offsets}{Research\ temporal\ scale}$$

Mean offsets of SDS detection, which are calculated from a limited number of sites by Hagenaars et al. (2018), have uncertainties and potentially undermining the reliability of these thresholds. To understand how significant these uncertainties are, the sensitivity of coastline stability classification with respect to threshold selection is analysed. With 15m mean SDS offsets (corresponding to 192 days composite window) and 33 years' time scale, Luijendijk et al. (2018) adopted a threshold of 0.5m/yr. In this research, since 360 days composite window is applied, the mean SDS offsets is expected to be 5m (Hagenaars et al. 2018) and correspondingly the threshold of 0.15m/yr is applied.

The relationship between thresholds for shoreline advance rate and the number of dynamic coasts is shown in Figure 5-1. It can be seen that as thresholds vary from 0.1 to 1, the number of dynamic ports changes from 95 to 38, in other words, 57 extra ports are classified as stable coasts. If replacing the threshold applied in this thesis with that used in Luijendijk et al. (2018), 27 ports will be classified to different categories, leading to a reduction of 21% for the portion of ports with dynamic coasts. Hence the number of ports classified to be at dynamic coasts is very sensitive to the threshold used for the classification, which is determined by the mean SDS offsets. To make the threshold more reliable, SDS detection, with the same parameters as this research, should be compared with in-situ data in multi-sites to obtain the mean SDS offsets. In this research, the number of dynamic coasts is applied to indicate significance of coastline evolution around African seaports from the continental perspective. The threshold of 0.15m/yr identifies more dynamic coasts and leads to the conservative side. Additionally, this threshold and the corresponding classification criterion are not applied to analyse influence of environmental and port characteristics, which means the above uncertainties only affect part of the answer to sub-question 3 about coastline evolution statistics of all African seaports.
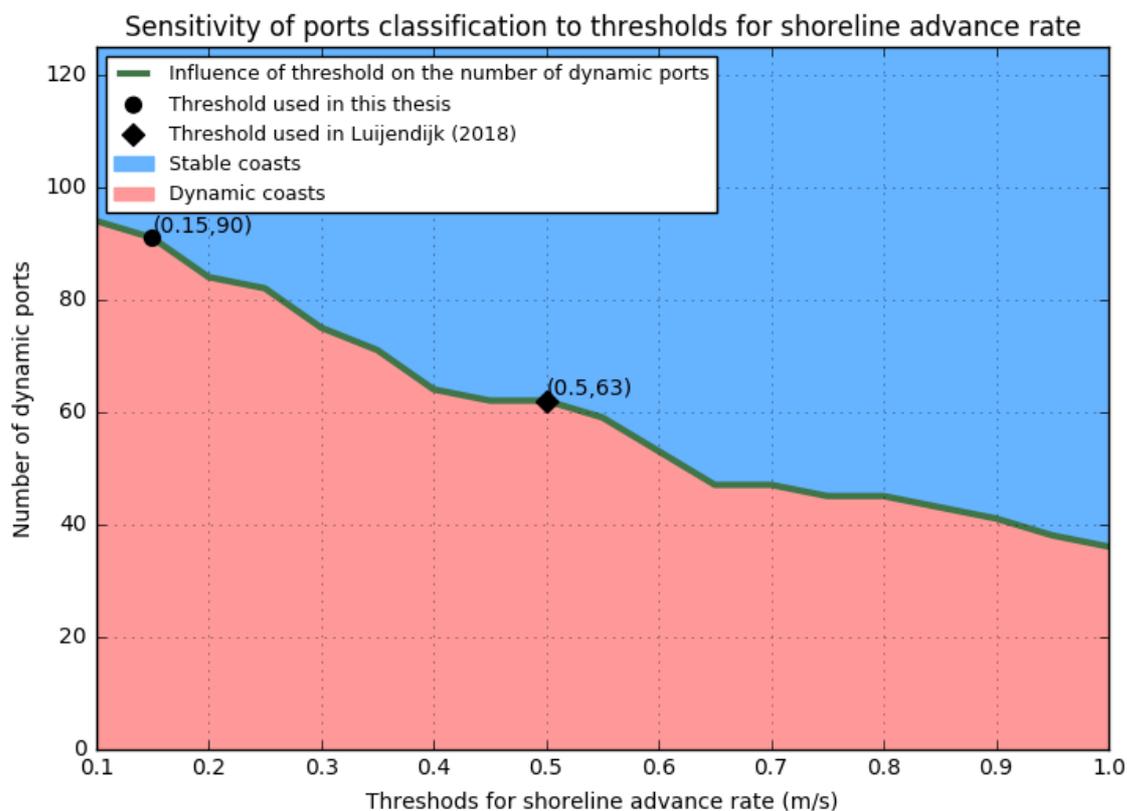
Figure 5-1 The relationship between thresholds for shoreline advance rate and the number of dynamic coasts

5.4   The potential influence of Sentinel 2 images

To improve computational efficiency, Sentinel 2 images are excluded from this research. Sentinel 2 mission has smaller revisit time and higher image resolution, which is found to result in more accurate SDS by Hagenaars et al. (2018). A case of Port of Nouakchott is used to reflect the influence of excluding Sentinel 2 mission. Figure 5-2 shows accretion area curve fittings for image collection with and without Sentinel 2 images. It can be seen that after including Sentinel 2 image, the number of imagery in composite windows increases for scatter points after 2015, which can be reflected from the point size. Although Sentinel 2 images also increase the density of scatter points after 2015, this difference is not prominent because this period has already been well covered by Landsat 7 and 8. In terms of curve-fitting results, both coefficients of fitting formulas and R-squared remain similar with or without Sentinel 2 images. The change of the average coastal area accretion rate, caused by the inclusion of Sentinel 2, is only 4%.

Therefore, for this selected case, although Sentinel 2 images have higher resolution and can increase the temporal density of scatter points, its influence is limited to the most recent three years. Exclusion of Sentinel 2 images has limited influence on indicator calculation.
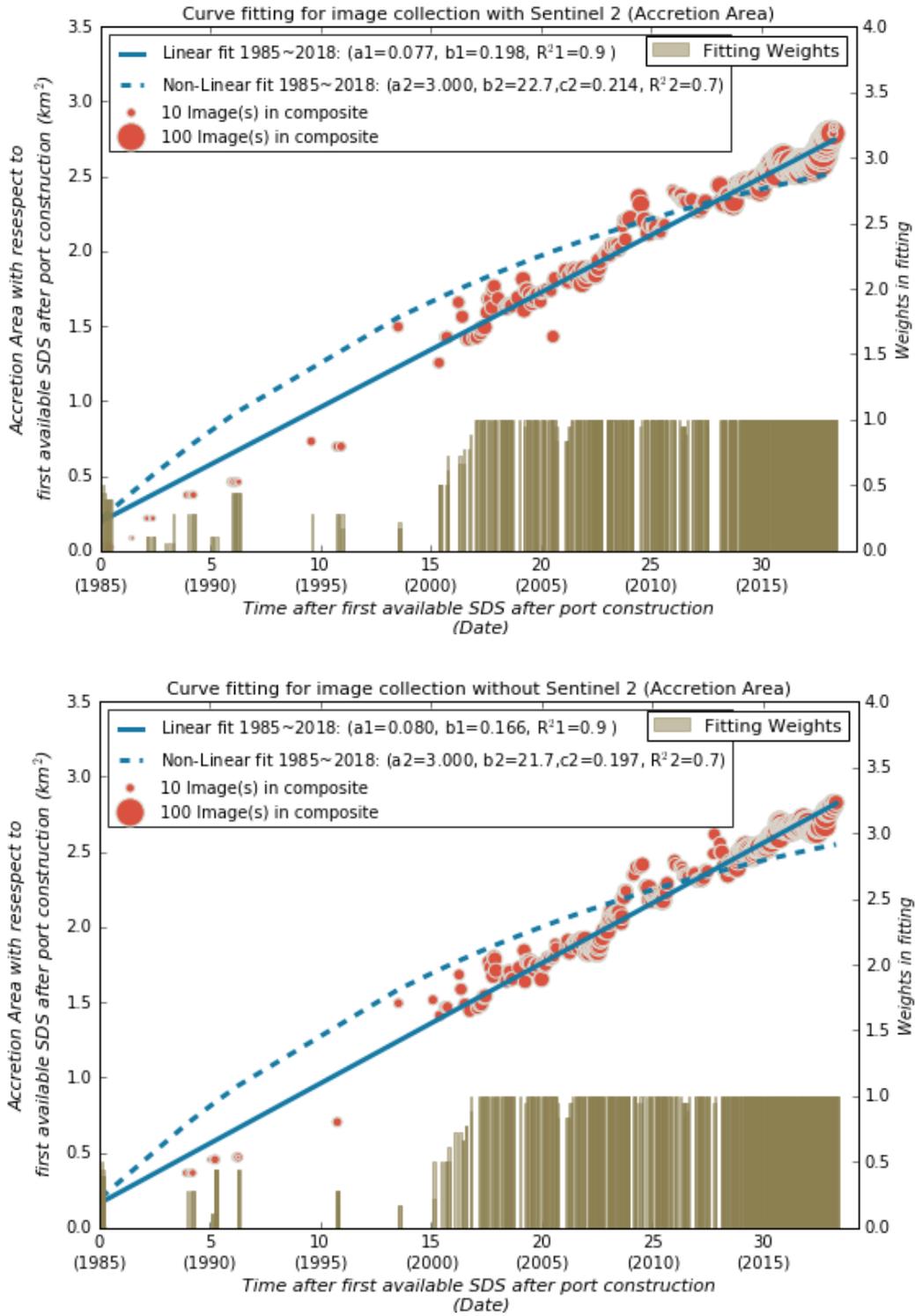
Figure 5-2 Accretion area curve fitting for image collection with (top) and without (bottom) Sentinel images for Port of Nouakchott

However, for cases with shorter monitoring duration, the influence of Sentinel 2 images can be more prominent. For example, if the curve fitting is only applied to the period after 1st available Sentinel 2 image, the scattered points and trend lines for image collection with and without Sentinel 2 are shown in Figure 5-3. It can be seen that, with a shorter monitoring duration, the average coastal area accretion rate doubles by including Sentinel 2 images. Considering the higher pixel resolution and shorter revisit time of Sentinel 2 images, the trend line obtained from Sentinel 2 included collection should be more accurate. Hence for shorter and more recent shoreline monitoring, the inclusion of Sentinel 2 images can be necessary.
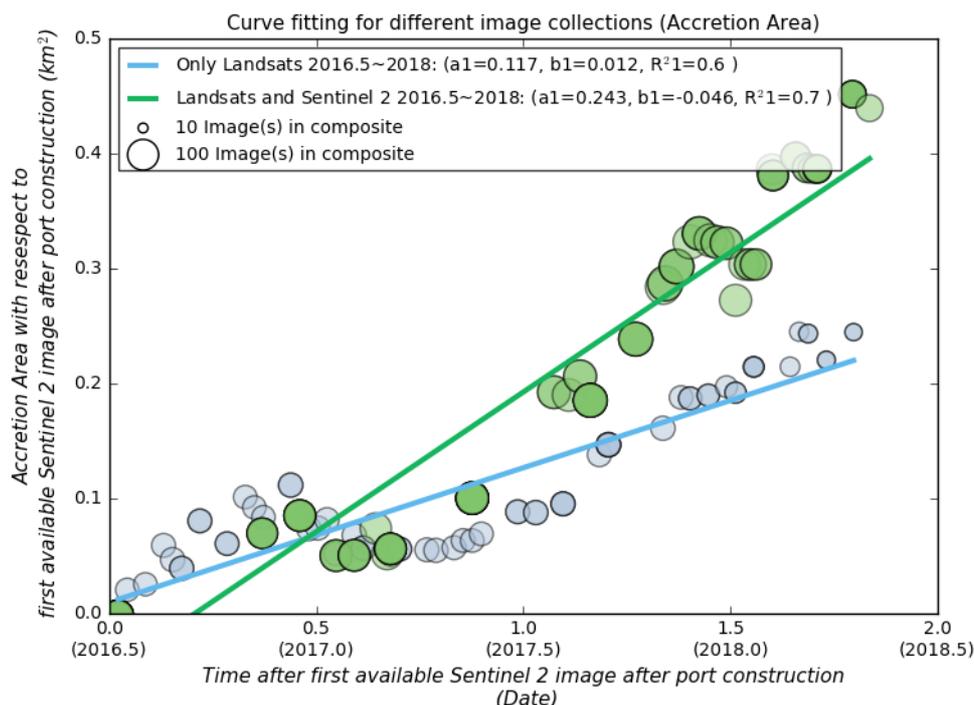
Figure 5-3 Accretion area curve fitting for image collection with and without Sentinel images for Port of Nouakchott after 1st available Sentinel 2 images

Additionally, as time passes, Sentinel 2 images will cover a longer period, which indicates higher potential influence of Sentinel images in the future. Therefore, it is worth to consider the inclusion of Sentinel 2 images in future research.

5.5   The potential influence of SDS detection scale

In this thesis, areas of interest (AOI) extending 15km from both sides of ports are used to define the scope of SDS detection. However, it is reported that coastline evolution around ports, especially down-drift erosion, is able to extend more than 15 km (Bruun, 1995). In this thesis, after comparing the most recent SDS with baseline (1st post construction SDS), down-drift erosion of Port of Lome, Cotonou and Monrovia is found to extend outside the defined AOI. An example for Port of Lome is shown in Figure 5-4. To understand the influence of a larger SDS detection scale, a polygon extends 35 km down-drift is applied. Erosion area curve fittings for polygons of different sizes are shown in Figure 5-5. It can be seen that, as a larger AOI polygon is used, coastal area erosion rate increases significantly. The result indicates that 15km down-drift is not an appropriate scale for this port. The same problem happens for Port of Cotonou and Monrovia and all of them

are located on the coast of West Africa, which is reported to retreat significantly not only due to ports construction but also due to river damming (Giardino et al., 2017). For these three ports, AOIs extending 30km instead of 15km down-drift are applied.

In conclusion, the SDS detection scale (15km down-drift and 15km up-drift) applied in this thesis is suitable for most African ports, but for ports with coastline evolution due to multi causes, this polygon size can be insufficient and erosion/accretion rates around ports can be underestimated. Hence in the future research, a larger polygon should be used for ports where significant coastline evolution has been reported.

Figure 5-4 Spatial aggregation results for the SDS acquired on 2017-11-18 around Port of Lome
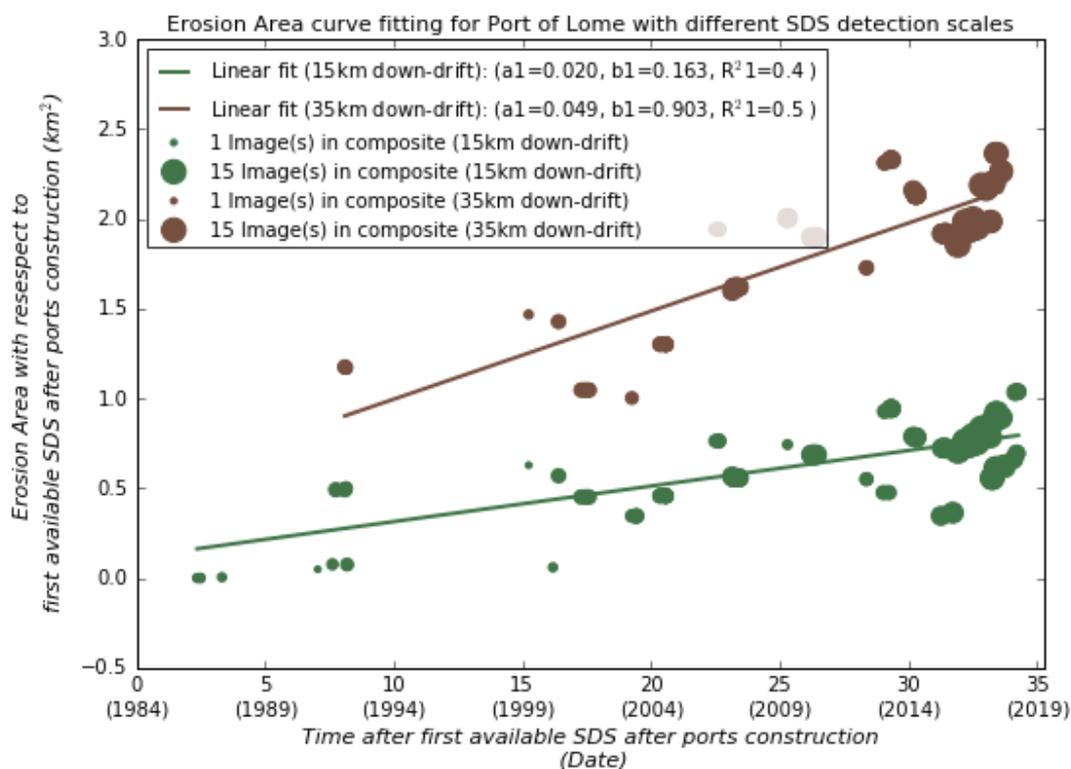
Figure 5-5 Erosion area curve fitting for Port of Lome with different SDS detection scales

5.6   Other limitations

1. In this thesis, shoreline orientation is determined based on the start point and the end point of the coast within AOI. This provides a good description for straight coasts. However, for curved coasts such as bays, the single parameter is not enough to describe shoreline orientation as well as the longshore component of wave power. In this research, when analysing the influence of longshore wave power, only ports at open coasts, where curved coastlines are less common, are included. By doing so, uncertainties of shoreline orientation are reduced.

2. Offshore wave data are applied in this thesis, however, due to the low resolution of ERA-I grids (0.75 latitude/longitude degrees), distance between ports and their closest offshore wave data grid varies from 3 km (width of nearshore zone assumed in this thesis) to 85 km (ERA-I grid size) depends on the relative position of ports and ERA-I grid points. The further offshore where wave data are collected, the worse nearshore wave data is estimated. It imposes more uncertainties on longshore wave power that wave data are collected from different offshore distances. In the future research, the offshore distance of wave data collection point should be included as an indicator for the reliability of gross longshore wave power. If necessary, ports with wave grid points too far from coasts can be filtered out from analysing influence of gross longshore wave power.

3. Although this research investigates coastline evolution trends around African seaports, it cannot always reflect impacts of port on coastal morphological change properly due to the presence of other contributions to coastline evolution such as river damming. For a portion of ports, coastline evolution is found to be significant even without ports construction. In this research, only the presence of rivers and inlets are included in the

database to indicate potential influence from sources and sinks. However, without historical data for the magnitude of these sources and sinks, the potential influence of rivers and inlets cannot be quantified and separated from ports influence. In addition to the presence of rivers and inlets, other environmental and human contributions to coastline evolution such as sea level rise and sand mining can also be significant. The database does not cover these parameters. Therefore, with the existing data, the contribution of ports construction to coastline evolution cannot be separated from other environmental and human contributions. For the 27 ports identified to have significant erosion and/or siltation, by investigating the relative position of erosion/accretion area and the port boundary, coastline evolution which is not directly affected by ports construction is distinguished preliminarily despite the data deficiency introduced above (port-affected evolution from Table 4-4 to Table 4-8). This process is implemented in a supervised way and more efforts are necessary to make it unsupervised and applicable to all African seaports.

5.7   Significance and opportunities

Before this research, coastline evolution trends around African seaports are rarely studied systemically due to the limitation on shoreline data. Although satellite imagery has been used to detect and analyse shoreline change for some cases such as Wu (2007), the temporal and spatial scales of such research are constrained by computational efficiency.

With the help of Google Earth Engine, this research successfully creates an evidence database of coastline evolution around African seaports. Statistics of coastline evolution indicators in this database reflects the significance of coastline evolution around African seaports. This research also identifies existing ports which have prominent erosion and/or hazards. This is helpful to raise awareness of local authorities to design coastal management plans and implement mitigation methods. By relating coastline evolution indicators to environmental and port characteristics, some knowledge of coastal engineering is validated by this evidence database and this knowledge can then be applied to future port development.

Additionally, with the development of remote sensing and implementation of accuracy assessment for sediment compositions other than sand in the future, this methodology has the potential to be utilized for all seaports on a global scale. The enriched database facilitates more quantitative analysis of coastline evolution indicators and environmental and port characteristics, supporting engineers and decision makers to understand coastline evolution around ports worldwide.

Furthermore, the success of this research is a proof for the applicability of SDS detection to obtain historic shoreline data in the large temporal and spatial scales, which make it possible to implement post-construction shoreline monitoring and model validation even in data poor environments, where historical shoreline data are absent. This new source of historical shoreline data is promising to study coastline trends also at locations without ports.

6

Conclusion and recommendation

This chapter provides the conclusions of this research by answering the research questions presented in Chapter1. Based on the discussion from Chapter 5 and these conclusions, Section 6.2 establishes a link with future developments and provides suggestions for improvements of this research.

6.1   Conclusion

The objective of this research is to create an evidence database, combining coastline evolution trends around existing African seaports with environmental and human intervention characteristics. This objective leads to the main research question:

What lessons can be learnt from the historic coastline evolution around African seaports over the past 34 years to inform decision making for both existing and future port developments?

Answers to this main research question and other sub-questions in Section 1.2 are formulated below:

1&2. Environmental and port characteristics in this database include gross longshore wave power, natural shelter condition, the presence of rivers and/or inlets nearby, the presence of LST interruption and shore protection structures, length of the breakwater and construction date. Coastline evolution indicators in this database include cumulative magnitudes and present rates of coastal area erosion/accretion and shoreline position advance at the up-drift boundary of the port. According to World Port Index, 165 African seaports are identified (after excluding river ports, offshore platforms and anchorages) and included in the database while only 125 African seaports at sandy coastlines where SDS detection has been validated are involved in sub-question 3, 4 and 5.

3.   Regarding historical coastline evolution, the sum of accretion and erosion area over all 125 African seaports at sandy coastlines is found to be 55 km^2 including 29 km^2 accretion and 26 km^2 erosion since 1984, with a mean value of 0.44 km^2 for every port, indicating a net accretion. The 55 km^2 coastal area change is distributed along 2600 km coastline, suggesting an average gross shoreline change of 21m. Compared with the 30m image pixel resolution, this coastline evolution is not significant. A similar trend is also found in Luijendijk et al. (2018), where the average shoreline change magnitude of Africa is smallest among all continents. The relative stable coast of Africa can be due to the wide distribution of Afro-trailing coast, where limited sandy beaches are available for evolution. However, when looking at hotspots, the top 10% of ports share about 50% (27 km^2) of the total coastal area change. The gross coastal area change around a single port (Port of Nouakchott) can be up to 7 km^2 including 4.5 km^2 erosion. With the population density of 960/km^2 for the corresponding port city, about 4,000 people are directly affected. If the increased flood risk due to shoreline erosion is considered, the number of people under influence of coastal erosion can be larger. Regarding present coastline evolution rates, 90 ports are found to locate at dynamic coastlines where coastal

area erosion (45 ports) or accretion (68 ports) rate is larger than SDS detection accuracy. This suggests that erosion/siltation risks remain high for majority of African seaports in the future. Both hindcast and forecast indicators suggest that accretion is more prominent than erosion for African seaports, which is different from the coastline evolution trend around a port in an ideal case where net erosion is expected. This difference can be due to the restriction of rocky substratum on erosion and the human activities to increase accretion.

4. By analysing coastline evolution statistics for ports with different environmental and port characteristics, it is found that trends reflected in hindcast and forecast indicators are similar. Net coastal area accretion is found for African seaports in all sub-categories, while the presence of rivers undermines such accretion trend due to decreasing sediment supply from rivers. Ports with prominent coastline evolution are found to be mainly located at open coasts with large longshore wave power ($H_s^{2.5}sin2\alpha \geq 0.55\ m^{2.5}$) and presence of nearby rivers and/or inlets. On the contrary, most ports with limited coastline evolution are located on sheltered coasts with limited longshore wave power and poor sediment supply. After relating coastline evolution indicators to ports characteristics and human interventions, it is found that ports constructed more recently tend to have more substantial present coastline evolution rate because coasts around them are less likely to approach the new equilibrium. Regarding human intervention, breakwater length correlates to present erosion/accretion rates positively. Longshore sediment transport (LST) interruption structure increases erosion magnitude as it stimulates local accretion, which corresponds to the theory of sediment balance. Shore protection structures are found to reduce coastal area erosion significantly within the monitoring temporal (34 years) and spatial (30km) scales, while their effects in larger scales are still doubtable since the sediment deficiency in the down-drift is still unsolved.

5. After analysing coastline evolution indicators from the continental perspective, hotspots are focused. 27 ports are identified to have prominent erosion and/or siltation hazards, which rank top 10% either for erosion hazard or siltation hazard. Some of these high-hazard ports also have large port city population, resulting in larger coastline erosion impacts. Ports with large longshore wave power are more likely to show equilibrium trends, but the majority of identified ports have erosion rates that are currently still high. In terms of coastline evolution statistics, as most high-hazard ports are located in sediment-rich environments, different trends are found for net coastal area change. Without the restriction of sediment availability and rocky substratum, net coastal erosion instead of accretion is found for all sub-categories, which corresponds to the knowledge of coastal engineering and suggests the potential of sediment deposition in harbour channels and basins. These identified hotspots of African seaports are found to be mainly located in five regions, which are North West Africa, West Africa, East coast of South Africa, Nile River Delta and West Mediterranean. Coast of West Africa is very sandy with large wave energy. It can be dynamic even without port structures. West African coastlines tend to retreat due to river damming. All ports on the East coast of South Africa have by-pass systems which are proved efficient to mitigate coastline evolution around most ports. In the region of Nile River Delta, sediment supply from Nile River and its branches make the coast very sandy. Ports construction history suggests that coastline in this region is very sensitive to artificial structures. Ports on the West Mediterranean coast are located on the rocky substratum. However, due to the existence of sediment supply from rivers, coastline evolution is still expected. Ports constructed in the up-drift of rivers are found to have less direct impact on coastline evolution.

These influences are then applied to derive lessons for future port design. Firstly, regarding site selection and breakwater design, ports constructed in regions of large sediment supply either by littoral drift or river supplies have larger negative coastal impacts in terms of port siltation and down-drift erosion. Port developments in this region should focus on not only the potential ports influence on coast stability but also

natural coastline evolution history of the coastline itself. For coasts with river sediment supply, it is better not to construct ports at the down-drift side of the river mouth to avoid interruption of river supplied sediment transport. Furthermore, breakwaters at open coastlines should be well designed to achieve smaller shore-normal projected length, especially when the gross longshore wave power is substantial. Regarding mitigation methods for coastline evolution hazards, shoreline protection structures are effective in reducing coastal area erosion in the time scale of 30 years. Extension of breakwater can be a temporary solution to mitigate siltation problem but to reduce erosion problem at the meantime, other measures such as sediment by-pass system can be designed.

6.2 Developments and recommendations

6.2.1 Developments

There are new developments in the field of remote sensing that might enhance the applicability of this study in the near future. Developments in sensor technique increase spatial resolution. Since more missions from NASA and ESA will be launched, a more frequent revisit time of satellite images will increase the number of images in a composite window and increase the temporal density of SDS vectors. These developments will improve the accuracy of indicator calculation in the future.

Additionally, the multi-spectral resolution increases by an increasing number of bands per satellite. Rather than using the NDWI value per pixel, other indicators can be established based on different band combinations. Using different band combinations will make it possible to detect surf zone width or to extract depth contours from the image. More parameters, which are not available in data poor environment, can then be derived from the satellite imagery, included in the database and applied to further research of coastline evolution.

If ground surveys for shoreline position can be gradually implemented in Africa in the future, the database of this research can be validated and updated by those new shoreline position data. Furthermore, if data for other environmental conditions such as sediment properties, nearshore wave conditions are available in the future, better correlation analysis can be performed to understand the influence of environmental characteristics.

6.2.2 Recommendations

1. In the future, Sentinel 2 mission will have a more considerable temporal coverage. Correspondingly, benefits of smaller revisit time and higher resolution of Sentinel 2 images will become increasingly prominent. Hence Sentinel 2 mission should be included in future research. Additionally, although AOI covering 30km coastline is found to be large enough for the majority of African seaports, extreme cases are identified to have coastal area erosion extending outside AOI. Therefore, in the future research, for ports where significant coastline evolution is reported, a larger SDS detection scale should be selected.

2. In this research, a threshold of gross longshore wave power indicator ($H_s^{2.5} sin2\alpha \geq 0.55 \ m^{2.5}$) is identified for significant coastline evolution. This threshold is helpful to preliminarily determine the suitability of a site for ports construction (with respect to coastline evolution) only based on the offshore wave data. However, the process to determine this threshold is still subjective. To validate this threshold, comparison with previous resaerch is necessary. As another threshold related to sediment transport, the threshold of Shields number can be used for this validation. After includig additional assumptions on sediment property and bed roughness, the relationship between these two thresholds can be researched.

3. In this research, only erosion area is used to describe down-drift erosion, which itself is not enough to reflect the hotspots of down-drift erosion. In addition to this indicator, the position of maximum erosion and migration rate of this position are also frequently used to analyse down-drift erosion and suggest coastal management. In future research, shore-normal transects can be defined along the baseline and shoreline changes can be calculated for all transects. Then the maximum shoreline change in the down-drift and its corresponding position will be recorded. The time series of maximum shoreline retreat and its relative position to down-drift boundary of ports will be analysed for all African seaports, especially those identified to have high erosion hazards.

4. This research focuses on African seaports, where the property of the Afro-trailing coast limits coastline evolution. Only a small portion of African seaports are found to have typical coastline evolution trends. This small quantity of typical cases limits the effort to understand coastline evolution around ports in a sedimentary environment quantitatively. To include more ports with significant coastline evolution in the analysis, the methodology in this research can be applied to coasts in other continents, especially those with Amero trailing edges which are expected to have wider sandy beaches.

5. This research analyses coastline evolution trends around African seaports, even though some of those trends are not directly affected by ports construction. Only for the 27 identified ports with prominent morphological change, cases that coastline evolution is unrelated to ports construction are distinguished by manually inspecting the relative position of erosion/accretion area and ports boundary. In the future research, this process can be atomised and applied to all ports. To check whether erosion/accretion area is connected to the port boundary, transects can be defined along the baseline and shoreline change rate along the coast can be calculated. Tracing the shoreline change from the port boundary, if cumulative shoreline change is larger than the detection accuracy continuously, erosion/accretion is judged as connected to the port boundary and can be assumed as directly affected by ports.

6. In this research, presence of rivers and inlets are included as potential contributions to coastline evolution, while the historical magnitude of these sources and sinks, as well as other natural and human causes such as Sea level rise (SLR) and sand mining, are not considered. In the future research, sediment inputs from sources and outputs to sinks should be described quantitatively. Natural causes such as regional SLR, regional climate variation and human causes such as sand mining should also be included in the database. Spectral and regression analysis on shoreline variation signals are possible methods to extract different causes to coastline evolution.

Bibliography

APPEANING ADDO, K., WALKDEN, M. & MILLS, J. P. 2008. Detection, measurement and prediction of shoreline recession in Accra, Ghana. *ISPRS Journal of Photogrammetry and Remote Sensing,* 63**,** 543-558.

ARCHETTI, R. 2009. Quantifying the evolution of a beach protected by low crested structures using video monitoring. *Journal of Coastal Research***,** 884-899.

BOSBOOM, J. & STIVE, M. J. 2015. *Coastal Dynamics I: Lecture Notes CT4305*, VSSD.

BOSWOOD, P. & MURRAY, R. 2001. World-wide sand bypassing systems: data report. *State of Queensland-Coastal Services technical report R20 Conservation technical report No. 15 ISSN 1037-4701*.

BRUUN, P. 1995. The development of downdrift erosion. *Journal of Coastal Research***,** 1242-1257.

CERKOWNIAK, G. R., OSTROWSKI, R. & PRUSZAK, Z. 2017. Application of Dean's curve to investigation of a long-term evolution of the southern Baltic multi-bar shore profile. *Oceanologia,* 59**,** 18-27.

CROARKIN, C., TOBIAS, P. & ZEY, C. 2002. *Engineering statistics handbook*, NIST iTL.

DE SCHIPPER, M. A., DE VRIES, S., RUESSINK, G., DE ZEEUW, R. C., RUTTEN, J., VAN GELDER-MAAS, C. & STIVE, M. J. 2016. Initial spreading of a mega feeder nourishment: Observations of the Sand Engine pilot project. *Coastal Engineering,* 111**,** 23-38.

DEAN, R. G. 1977. *Equilibrium beach profiles: US Atlantic and Gulf coasts*, Department of Civil Engineering and College of Marine Studies, University of Delaware.

DEE, D. P., UPPALA, S., SIMMONS, A., BERRISFORD, P., POLI, P., KOBAYASHI, S., ANDRAE, U., BALMASEDA, M., BALSAMO, G. & BAUER, D. P. 2011. The ERA‐Interim reanalysis: Configuration and performance of the data assimilation system. *Quarterly Journal of the royal meteorological society,* 137**,** 553-597.

DEVORE, J. L. 2011. *Probability and Statistics for Engineering and the Sciences*, Cengage learning.

DICTIONARY, M.-W. 2002. Merriam-Webster. *On-line at http://www. mw. com/home. htm*.

DONCHYTS, G., BAART, F., WINSEMIUS, H., GORELICK, N., KWADIJK, J. & VAN DE GIESEN, N. 2016. Earth's surface water change over the past 30 years. *Nature Climate Change,* 6**,** 810.

EDWARD, J. A. 2006. The muddy tropical coast of West Africa from Sierra Leone to Guinea-Bissau: geological heritage, geomorphology and sediment dynamics. *Africa geoscience review,* 13.

FLEMMING, B. 1981. Factors controlling shelf sediment dispersal along the southeast African continental margin. *Marine Geology,* 42**,** 259-277.

FLEMMING, B. W. 2002. Chapter Six Geographic distribution of muddy coasts. *In:* HEALY, T., WANG, Y. & HEALY, J.-A. (eds.) *Proceedings in Marine Science.* Elsevier.

FURLANI, S., PAPPALARDO, M., GóMEZ-PUJOL, L. & CHELLI, A. 2014. Chapter 7 The rock coast of the Mediterranean and Black seas. *Geological Society, London, Memoirs,* 40**,** 89-123.

GALGANO, F. A. & DOUGLAS, B. C. 2000. Shoreline position prediction: methods and errors. *Environmental Geosciences,* 7**,** 23-31.

GAO, B.-C. 1996. NDWI—A normalized difference water index for remote sensing of vegetation liquid water from space. *Remote sensing of environment,* 58**,** 257-266.

GARCíA-RUBIO, G., HUNTLEY, D. & RUSSELL, P. 2015. Evaluating shoreline identification using optical satellite images. *Marine Geology,* 359**,** 96-105.

GEOSPATIAL-INTELLIGENCE, U. N. 2017. *World Port Index (Pub 150)*, National Geospatial-Intelligence Agency.

GIARDINO, A., SCHRIJVERSHOF, R., NEDERHOFF, C., DE VROEG, H., BRIèRE, C., TONNON, P.-K., CAIRES, S., WALSTRA, D., SOSA, J. & VAN VERSEVELD, W. 2017. A quantitative assessment of human interventions and climate change on the West African sediment budget. *Ocean & Coastal Management*.

GORELICK, N., HANCHER, M., DIXON, M., ILYUSHCHENKO, S., THAU, D. & MOORE, R. 2017. Google Earth Engine: Planetary-scale geospatial analysis for everyone. *Remote Sensing of Environment,* 202**,** 18-27.

HAGENAARS, G., DE VRIES, S., LUIJENDIJK, A. P., DE BOER, W. P. & RENIERS, A. J. H. M. 2018. On the accuracy of automated shoreline detection derived from satellite imagery: A case study of the sand motor mega-scale nourishment. *Coastal Engineering,* 133**,** 113-125.

HARRIS., P.D., J., T.J., O. & D.H., L. 2014. Updated high‐resolution grids of monthly climatic observations – the CRU TS3.10 Dataset. *International Journal of Climatology,* 34**,** 623-642.

JARRETT, J. T. Coastal sediment budget analysis techniques. Coastal Sediments, 1991. ASCE, 2223-2233.

JONAH, F. E., BOATENG, I., OSMAN, A., SHIMBA, M. J., MENSAH, E. A., ADU-BOAHEN, K., CHUKU, E. O. & EFFAH, E. 2016. Shoreline change analysis using end point rate and net shoreline movement statistics: An application to Elmina, Cape Coast and Moree section of Ghana's coast. *Regional Studies in Marine Science,* 7**,** 19-31.

KAJI, A., LUIJENDIJK, A., DE VRIES, J. V. T., DE SCHIPPER, M. & STIVE, M. 2014. Effect of different forcing processes on the longshore sediment transport at the sand motor, the Netherlands. *Coastal Engineering Proceedings,* 1**,** 71.

KAMDI, S. & KRISHNA, R. 2012. Image segmentation and region growing algorithm. *International Journal of Computer Technology and Electronics Engineering (IJCTEE) Volume,* 2.

KAMPHUIS, J. W. 1991. Alongshore sediment transport rate. *Journal of Waterway, Port, Coastal, and Ocean Engineering,* 117**,** 624-640.

KUMAR, V. S. & NASEEF, T. M. 2015. Performance of ERA-Interim Wave Data in the Nearshore Waters around India. *Journal of Atmospheric and Oceanic Technology,* 32**,** 1257-1269.

LUIJENDIJK, A., HAGENAARS, G., RANASINGHE, R., BAART, F., DONCHYTS, G. & AARNINKHOF, S. 2018. The State of the World's Beaches. *Scientific Reports,* 8**,** 6641.

MHAMMDI, N., SNOUSSI, M., MEDINA, F. & JAAïDI, E. B. 2014. Chapter 10 Recent sedimentation in the NW African shelf. *Geological Society, London, Memoirs,* 41**,** 131-146.

OTSU, N. 1979. A threshold selection method from gray-level histograms. *IEEE transactions on systems, man, and cybernetics,* 9**,** 62-66.

PIANCA, C., HOLMAN, R. & SIEGLE, E. 2015. Shoreline variability from days to decades: Results of long‐term video imaging. *Journal of Geophysical Research: Oceans,* 120**,** 2159-2178.

ROSSOUW, M. & THERON, A. 2009. Aspects of potential climate change impacts on ports and maritime operations around the Southern African coast.

RUGGIERO, P., KAMINSKY, G. M., GELFENBAUM, G. & VOIGT, B. 2005. Seasonal to interannual morphodynamics along a high-energy dissipative littoral cell. *Journal of Coastal Research***,** 553-578.

SCHOONEES, J. S. 2000. Annual variation in the net longshore sediment transport rate. *Coastal Engineering,* 40**,** 141-160.

SIMM, J., BRAMPTON, A., BEECH, N. & BROOKE, J. 1996. *Beach management manual*, Construction Industry Research and Information Association.

SP MANUAL, U. A. C. O. E. 1984. Shore protection manual. *Army Engineer Waterways Experiment Station, Vicksburg, MS. 2v***,** 37-53.

STIVE, M. J. F., AARNINKHOF, S. G. J., HAMM, L., HANSON, H., LARSON, M., WIJNBERG, K. M., NICHOLLS, R. J. & CAPOBIANCO, M. 2002. Variability of shore and shoreline evolution. *Coastal Engineering,* 47**,** 211-235.

STOPA, J. E. & CHEUNG, K. F. 2014. Intercomparison of wind and wave data from the ECMWF Reanalysis Interim and the NCEP Climate Forecast System Reanalysis. *Ocean Modelling,* 75**,** 65-83.

THIELER, E. R., HIMMELSTOSS, E. A., ZICHICHI, J. L. & ERGUL, A. 2009. The Digital Shoreline Analysis System (DSAS) version 4.0-an ArcGIS extension for calculating shoreline change. US Geological Survey.

UACOE, U. A. C. O. E. 2002. Coastal engineering manual. *Engineer Manual,* 1110**,** 2-1100.

UNCTAD, U. N. C. O. T. A. D. 2017. *Review of Maritime Transport - Chapter 4 Ports*, United Nations.

WU, W. 2007. Coastline evolution monitoring and estimation—a case study in the region of Nouakchott, Mauritania. *International Journal of Remote Sensing,* 28**,** 5461-5484.

List of Figures

List of Tables

List of formulas

List of Abbreviations

SDS	Satellite Derived Shoreline
GEE	Google Earth Engine
LST	Longshore Sediment Transport
DSAS	Digital Shoreline Analysis System
USGS	United States Geological Survey
NASA	National Aeronautics and Space Administration
ESA	European Space Agency
TOA	Top-Of-Atmosphere
NIR	Near InfraRed
NDWI	Normalized Difference Water Index
SLC	Scan Line Corrector, sensor device to align pixels
OLS	Ordinary Least Squares
WPI	World Port Index
SPOT	Satellite Pour l'Observation de la Terre
RMS	Root Mean Squared
MSL	Mean Sea Level
SLR	Sea Level Rise
AOI	Areas Of Interest

A

Optimisation of SDS detection

As supplementary to Section 3.1.3, this section explains choices on SDS detection parameters. A case study is performed to achieve the standardised indicator calculation process. Two criteria are set for case selection. Firstly, uncertainties in SDS detection determine the variation of scattered points and then affect curve fitting and indicator calculation results. Since case study is applied to understand and minimise the influence of these uncertainties, the case selected should be able to reflect these drivers of uncertainties. Secondly, the indicator calculation is optimised based on curve fitting quality and it is necessary to guarantee achievable good fittings. Hence the case should have prominent coastline evolution patterns.

Based on these two criteria, Port of Lome is selected to standardise indicator calculation process. This site is under the influence of most drivers of SDS offsets. Additionally, according to previous research, Port of Lome is found to induce severe coastline evolution in both up-drift and down-drift.

Methodology

Scenario analysis is applied to decide SDS detection parameters.

Scenario design

As it is described in Section 3.1.2, both environmental and satellite instrument characteristics affect detection accuracy. Environmental drivers for SDS offsets are approached by image composite window technique, which bases its accuracy on the length of the composite window. Hence composite window length is the first parameter to be decided. Regarding uncertainties due to satellite instruments, image resolution has been determined as image collection is selected while the inclusion of SLC-off images needs to be discussed by case study. Besides these two parameters, the choice on AOI size is also validated. Therefore scenarios 1~4 in Table A-1 are designed. SDS detection and linear curve fitting are applied to each scenario to calculate indicators.

Table A-1 Scenarios for testing mitigation methods

Scenario	SLC-off images	Composite window length (days)	Port-centre Coastline length (km)	Fitting Improvements
1	Included	360	10	No
2	Excluded	360	10	No
3	Included	360	30	No
4	Included	720	30	No
5	Included	720	30	Weighted fitting
6	Included	720	30	Outlier Detection

Results assessment

In order to justify the effects of different mitigation methods, manual SDS detection is performed to produce a reference. The quality of the mitigation method is justified based on two criteria. Firstly, it is significant to check whether detection errors are removed or not. This can be reflected from the coefficient of determination R-squared, which is introduced in Section 3.2.2. Secondly, indicators derived from different scenarios are compared with the reference to check under which scenario indicators are better predicted.

Results

Effect of excluding SLC-off images

Scenario 2 which excludes SLC-off images is compared with scenario1. Satellite images included in Scenario 1 and Scenario 2 are shown in Figure A-1. After excluding SLC-off images, there is no satellite image coverage after 2003 until 2013 when Landsat 8 was launched. Additionally, even after 2013, satellite images in scenario2 are not as dense as that in scenario 1.

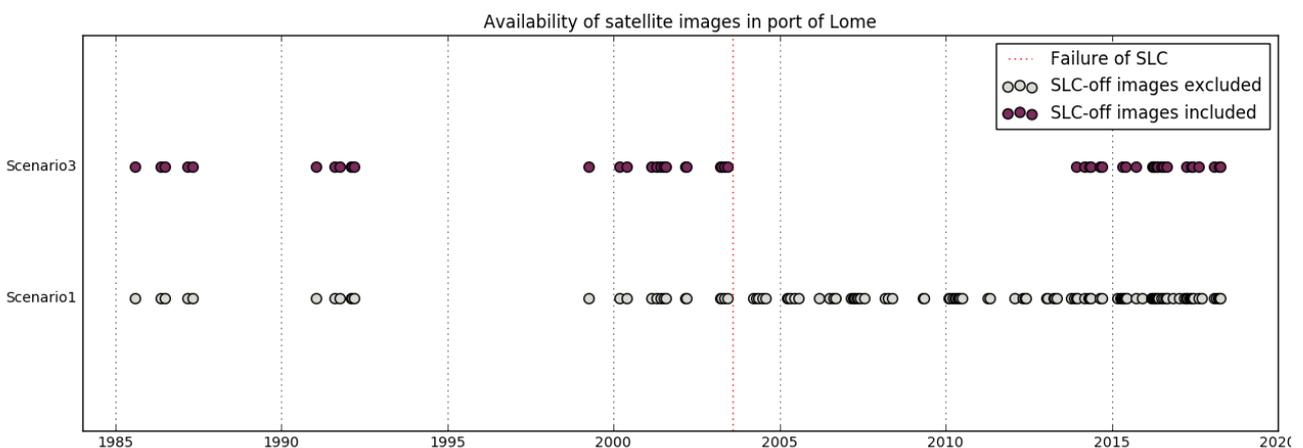*Figure A-1 Availability of satellite images of Scenario 1 and 3 in the port of Lome*

Comparison of curve fitting results is shown in Table A-2. After excluding SLC-off images, a portion of satellite images with poor quality are removed. The R-squared of curve fitting increase for all indicators. However, exclusion of SLC-off images makes scattered points sparser. The absence of satellite images from

2003 to 2013 results in significant errors of shoreline position indicators, which is shown in Figure A-2. It should be noticed that the difference of b1 coefficient among scenarios is due to offsets of baselines, which has no influence on the prediction of indicators.

In conclusion, although excluding SLC-off images can remove some errors, it decreases the number of scatter points significantly, which has adverse effect on indicator prediction.

Table A-2 Curve fitting results for scenario 1 and 2

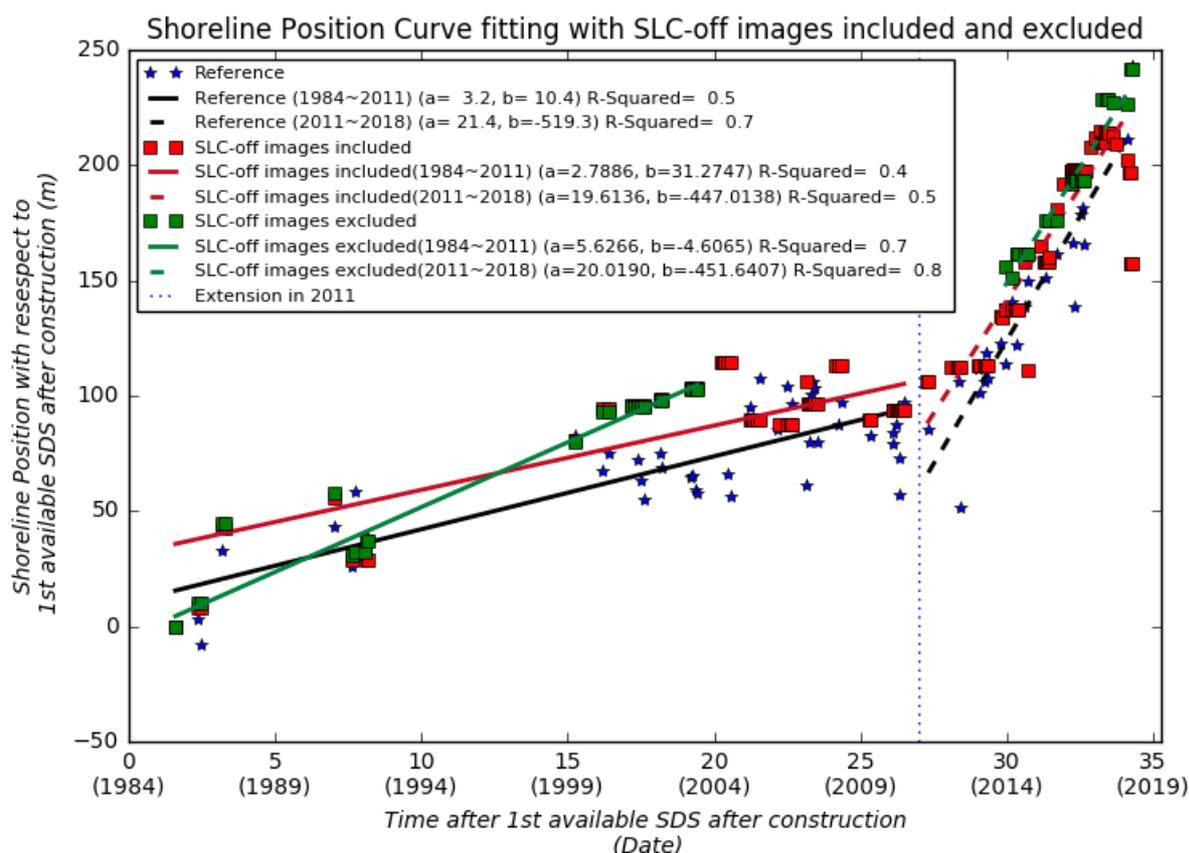| Scenarios	Shoreline position before extension		Shoreline position after extension		Erosion Area		Accretion Area	
	R-squared	Error of a1	R-squared	Error of a1	R-squared	Error of a1	R-squared	Error of a1
Scenario 1	0.446	12%	0.498	3%	0.456	3%	0.668	13%
Scenario 2	0.695	78%	0.766	6%	0.561	7%	0.701	17%

Figure A-2 Time series and trend lines for shoreline position around the up-drift boundary for scenario1 and scenario2

Effects of increased coastline length

Scenario 3 and Scenario 1 in Table A-1 are compared. Since increased coastline length has no influence of shoreline position at up-drift boundary, its effects on erosion/accretion area are focused. It can be seen from Table A-3 that although increased coastline length is not effective on removing SDS offsets based on R-squared value, it gives closer predictions for coastal area gaining/losing trends.

Table A-3 Curve fitting results for scenario 1 and 3

Scenarios	Shoreline position before extension		Shoreline position after extension		Erosion Area		Accretion Area	
	R-squared	Error of a1	R-squared	Error of a1	R-squared	Error of a1	R-squared	Error of a1
Scenario 1	0.446	12%	0.498	3%	0.456	3%	0.668	13%
Scenario 3	0.446	12%	0.498	2%	0.526	2%	0.534	2%

Effects of increased composite window length

Scenario 4 and 3 are compared in this Section; image number per window for these two scenarios is compared in Figure A-3. With a doubled composite window length, the number of imagery in each window increases significantly.
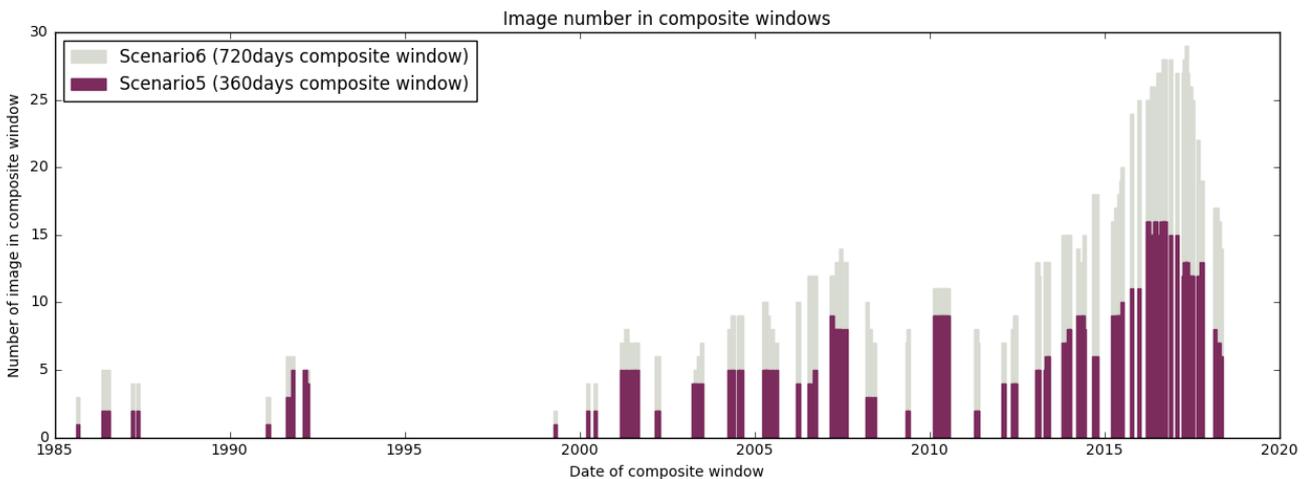
Figure A-3 Image number in composite windows for scenario 5 and scenario 6

The influence of composite window length on indicator predictions is shown in Table A-4. It can be seen that after increasing composite window length, although R-squared value increases significantly, which means less detection error happens, the prediction for coastline evolution trends are not improved a lot. Hence, as composite window length increases, SDS detection for each composite image is more accurate, but a too long composite window sacrifices too many details in morphological change and finally affects the accuracy of indicator prediction.

Table A-4 Curve fitting results for scenario 3 and 4

Scenarios	Shoreline position before extension		Shoreline position after extension		Erosion Area		Accretion Area	
	R-squared	Error of a1	R-squared	Error of a1	R-squared	Error of a1	R-squared	Error of a1
Scenario 3	0.446	12%	0.498	2%	0.526	2%	0.534	2%
Scenario 4	0.454	4.6%	0.731	8%	0.655	7%	0.617	16%

Conclusion

In general indicator predictions based on unsupervised SDS detections are similar to that based on manual SDS detections. Differences between them are within 20% for most scenarios. More images in a composite window do affect accuracy of SDS detection positively. Decisions on SDS parameters are summarized in Table A-5.

Table A-5 Effects and choices of mitigation measures

SDS detection parameters/ Curve fitting methods	Type	Error Remove/damp	Trendline improvement	Decision
SLC-off exclusion	Parameter Selection	No	No	SLC-off inclusion
Polygon longshore stretch increase	Parameter Selection	Yes	Yes	30km applied
Composite window extension	Parameter selection	Yes	No	360 days applied

B

Optimisation of curve fitting

As supplementary to Section 3.2, this section explains curve fitting improvements. Similar to Appendix A, this section is also based on the case study on Port of Lome.

Methodology

In order to improve curve-fitting, the following two methods are designed and tested.

1) Weighted fitting: The quantity of images in a composite window determines the reliability of the SDS detection and then spatial aggregation. In other words, uncertainties of scattered points vary according to the number of images involved. The assumption of constant variance of errors is violated and Weighted Least Square (WLS) fit can be performed. In a weighted fit, less weight is given to less precise measurements and more weight to more precise measurements (Croarkin et al., 2002).

2) Outliner Detection: While weighted fitting is only able to reduce image number related errors, outlier detection targets on all kinds of deviations. A curve fitting is performed first and points with 10%largest variations are detected and removed from fitting.

Design of Weighted fitting

To understand the influence of the number of imagery in a composite window and decide on criteria to assign weights, a sensitivity analysis is performed on error of unsupervised SDS detection (compared with manual SDS detection) with respect to the number of image in composite windows.

Test of curve-fitting methods

Scenario 5 and Scenario 6 in Table A-1 are designed to test effects of above two curve-fitting methods, following the same results assessment criteria as Appendix A.

Results

Weights for weighted fitting

This section aims at analysing the relationship between SDS detection errors and the number of image per composite window. With fittings for manual detection as references, deviation of scattered points of unsupervised scenario can be calculated. These deviations are then correlated to the number of satellite image per composite window. In order to include a broader range of image quantity, 720 days composite window is selected in SDS detection with 30km coastline scoped in research and SLC-off images included. Results for accretion area are shown in Figure B-1. It can be seen that errors of SDS detection and aggregation decrease as the number of image per composite window increases. However, this trend becomes less prominent after the number of image in a composite window reaches 17, after which SDS detection error is reduced to an acceptable level found in Hagenaars et al. (2018) and remains stable. This separation of trends indicates a threshold for the number of image per composite, and the performance of image composite technique is doubtable if the number of image is below this threshold. The value of this threshold is found to be 17 for accretion area, 11 for erosion area and 19 for shoreline position calculation. To be conservative, 20 images in a composite window are set as the threshold for image composite technique to have reliable performance. If the image number is larger than this threshold, corresponding points are assigned weights of 1. For points with less image number than the threshold, weights are normalized between 0 and 1 based on image quantity.

Effect of weighted fitting

Scenario 5 and 4 are compared, and curve fitting results for these two scenarios are shown in Table B-1, it can be seen that except shoreline position before extension where scattered points are too sparse, errors for indicator predictions are reduced, which means weighted fitting does have effect on improving indicator calculation.
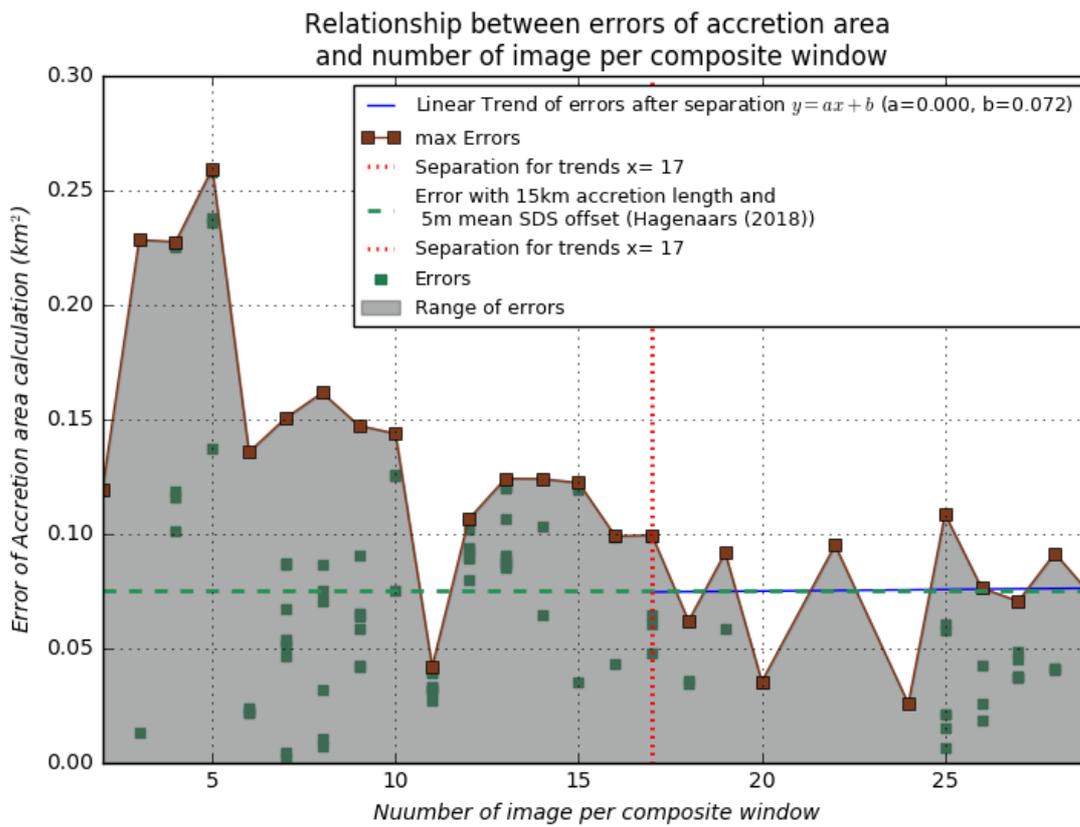
Figure B-1 Relationship between Accretion area calculation and number of image per composite window

Table B-1 Curve fitting results for scenario 4 and 5

Scenarios	Shoreline position before extension		Shoreline position after extension		Erosion Area		Accretion Area	
	R-squared	Error of a1	R-squared	Error of a1	R-squared	Error of a1	R-squared	Error of a1
Scenario 4	0.454	5%	0.731	8%	0.655	7%	0.617	16%
Scenario 5	0.434	13%	0.725	4%	0.654	3%	0.614	10%

Effect of outlier detection

Similar to weighted fitting, Outliner detection is also proved to be useful for improving indicator predictions in most cases. The failure for shoreline position before the extension is because too few points are available for curve fitting after filtration.

Table B-2 Curve fitting results for scenario 4 and 6

Scenarios	Shoreline position before extension		Shoreline position after extension		Erosion Area		Accretion Area	
	R-squared	Error of a1	R-squared	Error of a1	R-squared	Error of a1	R-squared	Error of a1
Scenario 4	0.454	5%	0.731	8%	0.655	7%	0.617	16%
Scenario 6	0.346	44%	0.719	2%	0.655	7%	0.601	2%

C

Sources for environmental/port parameters

Database and methods used in collecting data for environmental/port parameters are summarized in Table C-1

Table C-1 Summary of methodology to prepare data for environmental and human intervention parameters

	Parameters		**Quantification /Classification**	**Data source**	**Indicator/Categories**
Port information	Port location		Quantification	World Port Index (WPI)	Coordinates
	Port construction date		Quantification	Google Earth	Construction years
	Port city size		Quantification	Wikipedia	Population
SDS Detection Accuracy	Sediment type		Classification	Luijendijk et al. (2018), Google Earth	Sandy, Muddy, Rocky
	Cloud cover rate		Quantification	Harris. et al. (2014)	Annual mean cloud cover rate
	Satellite image availability		Quantification	Google Earth	Number of available satellite images after 1984
LST	Gross Longshore Wave power	Wave parameters	Quantification	ERA-Interim reanalysis data (Dee et al., 2011)	$H_s^{2.5} sin2\alpha$ [m$^{2.5}$]
		Shoreline orientation	Quantification	Google Earth	
	Natural shelters		Classification	Google Earth	Open coast, Headland-Bay, Spits/lagoons/estuaries
Sediment sources and sinks	Visible sediment sources and sinks(River and inlet)		Classification	Google Earth	Yes, No
Human intervention	Length of port breakwater		Quantification	Google Earth	Projected length of up-drift breakwater [m]
	LST interruption and shore protection structures		Classification	Google Earth	LST interruption structures, Shore protection structures, No structures